

General Disclaimer

One or more of the Following Statements may affect this Document

- This document has been reproduced from the best copy furnished by the organizational source. It is being released in the interest of making available as much information as possible.
- This document may contain data, which exceeds the sheet parameters. It was furnished in this condition by the organizational source and is the best copy available.
- This document may contain tone-on-tone or color graphs, charts and/or pictures, which have been reproduced in black and white.
- This document is paginated as submitted by the original source.
- Portions of this document are not fully legible due to the historical nature of some of the material. However, it is the best reproduction available from the original submission.

SEPTEMBER 1983

ADVANCED NICKEL-HYDROGEN CELL CONFIGURATION STUDY FINAL REPORT

Contract No. NAS3-22249



Prepared By
Space and Communications Group
Hughes Aircraft Company
El Segundo, California

Prepared For
Lewis Research Center, NASA
Cleveland, Ohio

HUGHES

HUGHES AIRCRAFT COMPANY
SPACE AND COMMUNICATIONS GROUP
EL SEGUNDO, CALIFORNIA



Hughes Ref No. E9787 • SCG 830552R

SEPTEMBER 1983

ADVANCED NICKEL-HYDROGEN CELL CONFIGURATION STUDY FINAL REPORT

Contract No. NAS3-22249

Prepared By
Space and Communications Group
Hughes Aircraft Company
El Segundo, California

E. Adler
Program Manager
F. Perez
Principal Investigator

Prepared For
Lewis Research Center, NASA
Cleveland, Ohio



Hughes Ref No. E9787

ACKNOWLEDGMENTS

This study encompasses broad areas of nickel-hydrogen battery technology and is the product of contributions from many specialists. Hong S. Lim contributed to the evaluation of various electrode design options and the determination of development requirements associated with the implementation of bipolar batteries. Richard P. Bobco initiated thermal and oxygen management analysis. Lowell F. Kamper helped in generating the pressure vessel design concepts for the bipolar battery. Stan Gordon contributed to the definition of manufacturing technologies required to produce bipolar batteries. Finally, the authors wish to acknowledge the technical guidance and support provided by Robert L. Cataldo of NASA's Lewis Research Center.

PRECEDING PAGE BLANK NOT FILMED

CONTENTS

	<u>Page</u>
1. INTRODUCTION AND SUMMARY	
1.1 Background	1
1.2 Objectives	3
1.3 Scope	3
1.4 Summary	4
2. BASELINE NICKEL-HYDROGEN STORAGE DEVICES	
2.1 State of the Art Individual Pressure Vessel Cell	7
2.2 Near Term Common Pressure Vessel Module Configuration	10
2.3 Performance Projections	15
3. ADVANCED BIPOLAR BATTERY DESIGN AND REQUIREMENTS	
3.1 Negative Electrodes	21
3.2 Positive Electrodes	21
3.3 Separator	25
3.4 Bipolar Plate	25
3.5 Cooling Plates	28
3.6 Terminals	28
3.7 Endplate/Weld Ring Assembly	31
3.8 Pressure Vessel	31
3.9 Instrumentation	36
3.10 Electrolyte and Oxygen Management	37
3.11 Oxygen Management	39
3.12 Thermal Management	42
3.13 Performance Projections	44
3.14 Development Requirements	46
4. SPACECRAFT INTEGRATION	
4.1 Baseline Mission	53
4.2 Individual Pressure Vessel Cell Integration	55
4.3 Common Pressure Vessel Module Integration	57
4.4 Bipolar Battery Integration	57
4.5 Systems Comparison	61

PRECEDING PAGE BLANK NOT FILMED

	<u>Page</u>
5. CONCLUSIONS	63
6. REFERENCES	65
APPENDIX	
Technical Paper, "Development of a Large-Scale Bipolar Ni-H ₂ Battery"	67

ILLUSTRATIONS

		<u>Page</u>
1	Individual Pressure Vessel, Common Pressure Vessel, and Bipolar Battery Comparison (150 A-Hr)	2
2	Bipolar Battery	5
3	Ni-H ₂ Individual Pressure Vessel Layout	9
4	Ni-H ₂ Cell Electrochemical Reactions	9
5	CPV Module Design Concept 1	11
6	Projected Individual Pressure Vessel Cell and Common Pressure Vessel Module Specific Energy	17
7	Projected Individual Pressure Vessel Cell and Common Pressure Vessel Module Energy Density	17
8	Cell Stack Assembly	20
9	Stack Subassembly	20
10	Ni-H ₂ Cell Cycle Life History	22
11	Electrode/Frame Geometry	26
12	Bipolar Plate	27
13	Cooling Plate Frame Assembly	29
14	Cooling Plate	29
15	Terminal	30
16	End Plate	32
17	End Plate/Weld Ring Assembly	33
18	Pressure Vessel Weld Design	35
19	Oxygen Recombination Site Model	41
20	Fully Redundant Liquid-Cooled Thermal Management Systems	43
21	Liquid-Cooled Stack Thermal Network Model	44
22	Preliminary Thermal Analysis Results of Liquid-Cooled Subassembly	45
23	Bipolar Battery Specific Energy Versus Cell Capacity Voltage and Positive Electrode Thickness	48
24	Bipolar Battery Specific Energy Density Versus Cell Capacity Voltage and Positive Electrode Thickness	49
25	Effect of Operating Pressure on Energy Density	50
26	Projected Bipolar Battery System Characteristics	51
27	Baseline Satellite Power System	54

	<u>Page</u>
28 Individual Pressure Vessel Cell and Battery Pack Concept	56
29 Two-Phase Fluid Loop Installation	56
30 Two-Phase Fluid Loop Schematic	56
31 Common Pressure Vessel Battery Pack	58
32 Spacecraft/Bipolar Battery Interface Rings	59
33 Thermal Interface Between Bipolar Battery and Spacecraft Heat Rejection Systems	59
34 Cylindrical Spacecraft Radiator Weight Versus Dissipated Power	60

TABLES

	<u>Page</u>
1 CPV Module Design Requirements	13
2 Positive Electrode Comparison	23
3 Recombination Strip Modelling Assumptions	40
4 Recombination Strip Design Modelling Procedure	40
5 Baseline Satellite Nickel-Hydrogen Battery Design Characteristics	55
6 Radar Satellite Nickel-Hydrogen Battery Weight Comparison	61

1. INTRODUCTION AND SUMMARY

1.1 BACKGROUND

Long-term trends in the evolution of space power technology point toward increased payload power demand which in turn translates into both higher battery system charge storage capability and higher operating voltages. State of the art nickel-hydrogen cells of the 50-60 Wh size, packaged in individual pressure vessels, are capable of meeting the required cycle life for a wide range of anticipated operating conditions; however, they provide several drawbacks to battery system integration efforts.

Because of size, high voltage/high power systems require integrating hundreds of cells into the operating system. Packaging related weight and volume inefficiencies degrade the energy density and specific energy of individual cells currently at 30 Wh/dm³ and 40 Wh/kg respectively. In addition, the increased parts count and associated handling significantly affect the overall battery related costs. Spacecraft battery systems designers within industry and Government realize that to reduce weight, volume, and cost will require increases in the capacity of nickel-hydrogen cells. To achieve this objective extensive efforts are being made to double the energy storage capacity of state of the art cells packaged in individual pressure vessels (IPV) and to provide order of capacity magnitude increases by packaging several cell stacks within a common pressure vessel (CPV). With the incorporation of active cooling, additional growth can be projected for these systems.

The bipolar battery concept described in this report extends the advantages realized by the state of the art IPV and near term CPV cell technology by packaging the equivalent several hundred cells into a single pressure vessel. Figure 1 provides a comparison between the relative size of the three devices studied during this contract. The nominal voltage output, associated with the 150 A-hr units shown in IPV, CPV, and bipolar battery configurations, is 1.2, 7.2, and 300 volts respectively. Larger dimensions and 1000 kg weight of the bipolar battery require implementing new technology to meet traditional nickel-hydrogen battery design and manufacturing requirements. This report outlines the objectives, scope of work, background, projected performance development needs, and a possible approach to bipolar battery design that was baselined on this contract. Other design variations are possible without significantly affecting the technical feasibility or anticipated performance.

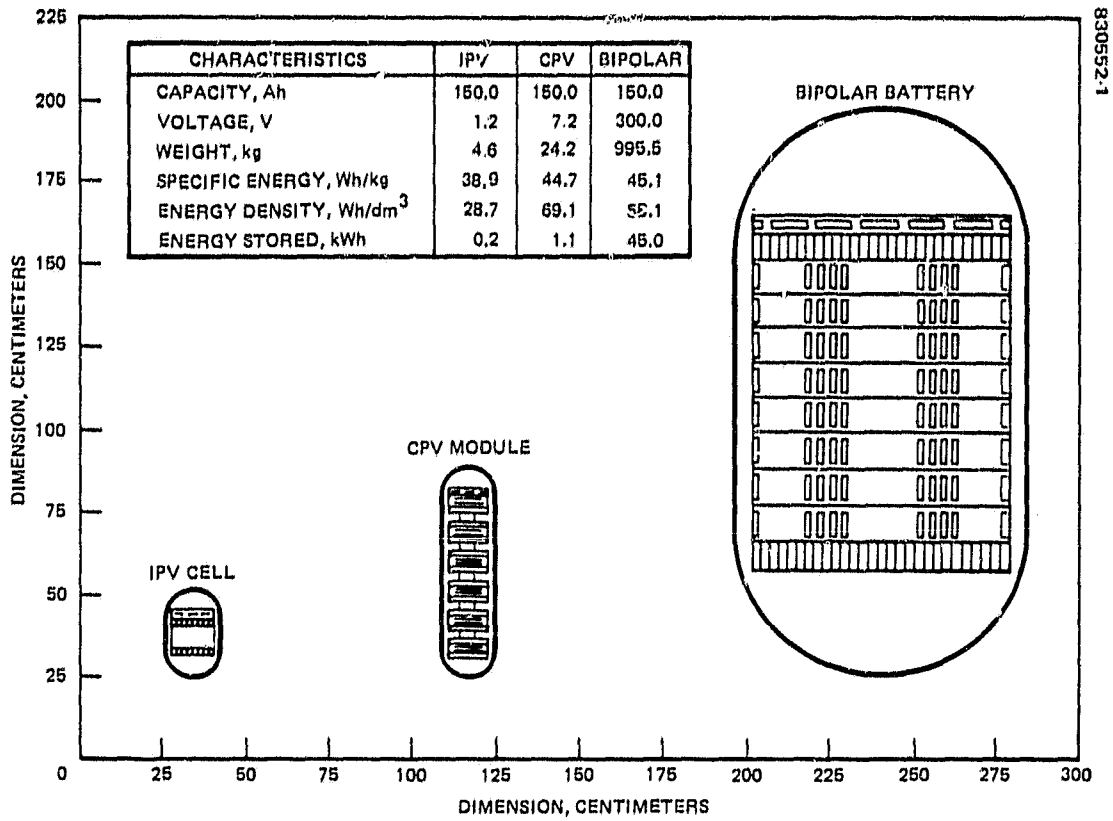


FIGURE 1. INDIVIDUAL PRESSURE VESSEL, COMMON PRESSURE VESSEL, AND BIPOLAR BATTERY COMPARISON (150 A-HR)

1.2 OBJECTIVES

The objective of this study was to provide a comparison of the projected performance of state of the art IPV, near term CPV, and advanced bipolar nickel-hydrogen battery technologies. Emphasis was placed on evaluating weight tradeoffs associated with integrating these technologies into a large spacecraft and in defining the advanced bipolar battery concepts to make the weight projection comparison meaningful.

1.3 SCOPE

This study, funded by NASA's Lewis Research Center, presents the relative weight benefits associated with the implementation of nickel-hydrogen batteries into large spacecraft. It represents a year's effort by one person assigned to the project half-time. To provide a basis for this study, the performance of state of the art IPV cells and near term CPV modules was extrapolated up to the 150 A-hr size. The IPV hardware baselined for these projections was based on configurations that have been successfully demonstrated at Hughes during a series of Air Force funded development programs. The CPV design concepts are to a large extent based on the results of Air Force funded exploratory development efforts at EIC and the relative maturity of the advanced development design effort at Hughes during the early part of 1982. Since that time several major design changes have been implemented into the CPV module design as a result of Air Force funded activities. The cumulative impact of these changes has been to enhance the CPV module peak power capability and reliability and to extend the projected operating life of the CPV system. These changes, however, do not alter significantly the conclusions of this study.

To provide a basis for the performance projections, a liquid-cooled version of the bipolar battery design concept (developed in 1981 at NASA's Lewis Research Center) was studied. This effort identified bipolar battery design requirements and components to allow a computer aided optimization. Weight projections, generated for the bipolar battery system, were specified to the configuration used in this report. Alternative approaches can provide equally viable designs with slight variances in weight. The design requirements and the conditions for optimum performance, however, apply to all large scale bipolar battery configurations.

The emphasis of the bipolar battery conceptual design effort was to integrate mechanical, thermal, electrolyte, and oxygen management functions into the electrochemical stack design to facilitate fabrication, assembly, and activation of the unit. Areas in which the current levels of technological maturity are inadequate to support the design and fabrication efforts were identified and goals were established to create the optimum conditions for future implementation of the design.

1.4 SUMMARY

Evaluation of the projected weight of alternative nickel-hydrogen technologies available for integration in a large 52 kWh space vehicle has shown that bipolar batteries could provide weight savings of 850 and 400 kg at the system level vis-a-vis state of the art IPV and near term CPV battery systems. Seventy-five percent of these weight savings is due to weight reductions in the auxiliary components (i. e., structures, wiring, bipolar electronics instrumentation) required to support the integration of small energy storage modules into the spacecraft. To provide these weight savings the bipolar battery design will have to incorporate spacecraft structural and thermal interface functions into the pressure vessel and stack design respectively. The Hughes design concept that meets these requirements is shown schematically in Figure 2. In it, electrolyte is contained inside each unit cell by integrating cell components in an insulated hydrophobic frame. Oxygen recombination sites are provided behind each nickel electrode to reduce oxygen migration outside the stack and recombination on the adjoining negative electrodes.

A unique feature of any bipolar cell design is the reduced electrode lateral electrical and thermal conductivity requirement which has been a limiting factor to the use of large diameter electrodes in IPV cells. Because of this, positive electrode screen current collector may be eliminated or replaced by a lighter grid. With proper development use of a thicker nickel electrode than currently used may also be considered for reducing overall battery weight without an appreciable increase in resistive loss. Manufacturing of thick sinters and impregnation of the plaque to be used in bipolar cells will require a substantial technical investment to overcome a number of unique technical difficulties. Successful development of this technology will substantially reduce the weight of IPV, CPV, and bipolar nickel-hydrogen storage devices.

In addition, bipolar batteries require eliminating shunt currents through electrolyte bridges, preventing electrolyte maldistribution among unit cells and outside the cell stack, providing new oxygen management techniques, eliminating electrochemical corrosion due to presence of high potential gradients within the cell, and accommodating unmatched capacity among unit cells. Although some of these technical issues are similar to those in fuel cells and CPV modules, innovative design and new fabrication technologies are required for their resolution.

Sections 2 through 5 provide an approach to bipolar battery design, describe key issues related to the development of suitable electrodes, oxygen, and electrolyte management systems, and present a preliminary assessment of the battery performance in a large spacecraft power system. The appendix is a copy of a technical paper on the development of a large-scale bipolar Ni-H₂ battery presented at the IECEC conference in 1983.

830552-2

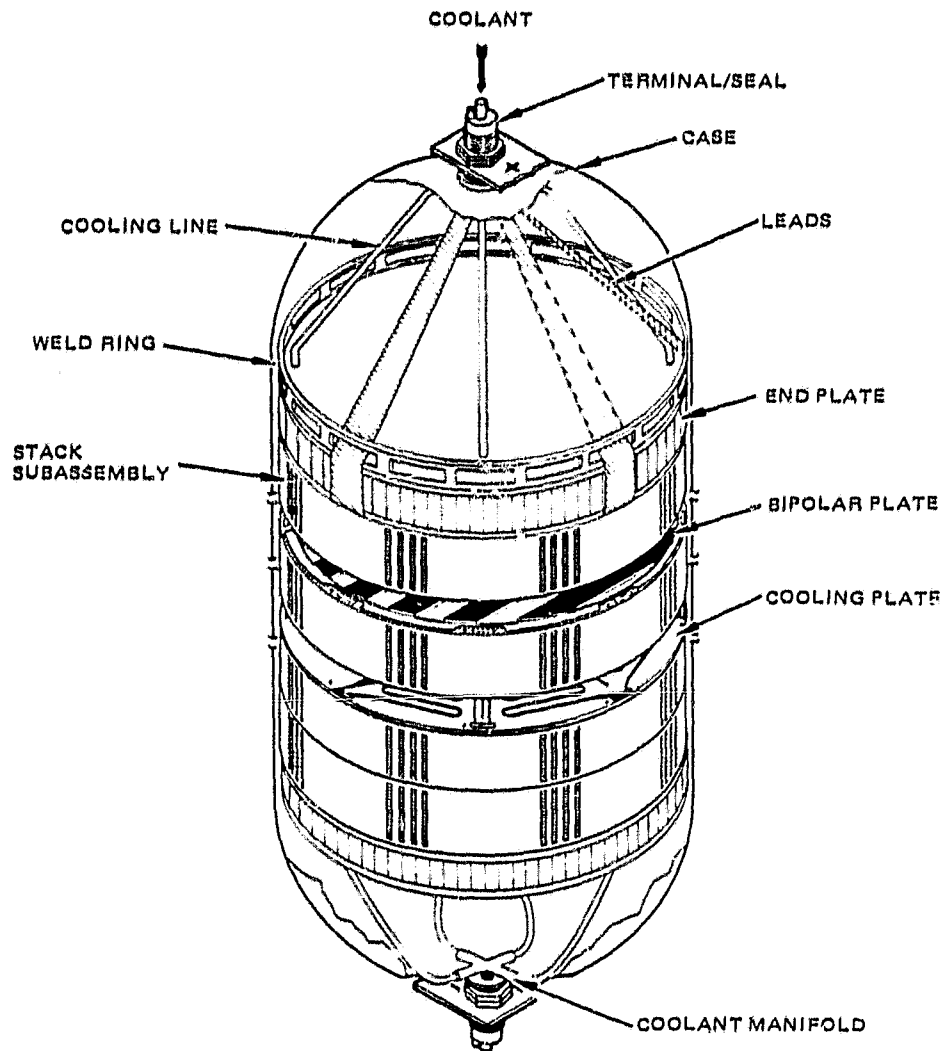


FIGURE 2. BIPOLAR BATTERY

2. BASELINE NICKEL-HYDROGEN STORAGE DEVICES

In comparison with Ni-Cd batteries, nickel-hydrogen batteries offer an overwhelming weight advantage due to the higher depth of discharge at which they can be operated to achieve the same mission life. Battery designers currently have only two options in packaging nickel-hydrogen energy storage modules. The first, which has been flight qualified and is the heavier, packages a group of parallel connected plates into a cell stack that is contained within an individual pressure vessel. An alternative approach, currently being developed by Hughes in partnership with Yardney and EIC, provides the option of packaging a group of series connected cell stacks within a common pressure vessel. This design increases the battery active to dead weight ratios, thus creating potential weight savings of 10 to 20 percent at the battery system level. These technologies are included to provide a yardstick against which the advantages offered by a bipolar battery system can be measured.

2.1 STATE OF THE ART INDIVIDUAL PRESSURE VESSEL CELL

The IPV electrode stack assembly is contained in an 11 cm diameter by 28 cm Inconel pressure vessel. Figure 3 shows a schematic of the baseline IPV configuration developed by Hughes for the U.S. Air Force. This design incorporates the following design features:

- 1) The electrochemical battery stack packaging is separate from the hydrogen containment vessel for ease of battery construction and assembly and to minimize mutual structural loading during battery charging and discharging.
- 2) Electrodes are stacked between rigid end plates. These end plates are preloaded to a specified contact pressure within the cell stack by compressing the assembled stack in a fixture and tightening the nut at the end of the core.
- 3) The stack configuration is designed for structural simplicity.

REPRINTING PAGE BLANK NOT PRINTED

- 4) The central polysulfone core protruding from the baseplate is designed to provide:
 - a) Electrode alignment in assembly
 - b) Position and alignment control between cell stack and pressure vessel
 - c) Cell stack structural support without relying on frictional shear
 - d) Formation of two conduits for positive and negative power leads
- 5) The two pressure vessel sections are joined by a single circumferential weld which also anchors the stack assembly into the pressure vessel.
- 6) The attachment lugs from the weld to the baseplate are configured to provide negligible radial constraint to the pressure vessel for extended cyclic vessel life.
- 7) The single line attachment between the cell stack and case provides unrestrained axial growth in the vessel during cycling; that is, no mutual mechanical loading between the cell stack and case occurs as a result of pressure variation during battery charge discharge cycle.
- 8) Lateral structural loads transmitted to the stack during spacecraft launch are supported by the pressure vessel at the weld seam and the top of the battery cell stack.
- 9) All electrical connections are designed to allow testing prior to final vessel welding.
- 10) The zirconium oxide liner of the case provides a wick for electrolyte return to the stack as a result of either evaporation or recombination differences within the cell. This liner prevents dry-out of cell components and limits gradients in electrolyte concentration.
- 11) The terminal housing is integrally hydroformed into the dome of the cell and contains no weld. The terminal design is such that a central conductor is welded to the electrode leads and is tightened only during final assembly.

A simplified representation of the electrochemical reactions occurring in a Ni-H₂ cell is given in Figure 4. As shown, the hydrogen is generated during charge and consumed during discharge. During overcharge, oxygen is generated at the positive and recombined at the negative electrode.

ORIGINAL PAGE IS
OF POOR QUALITY

830552.3

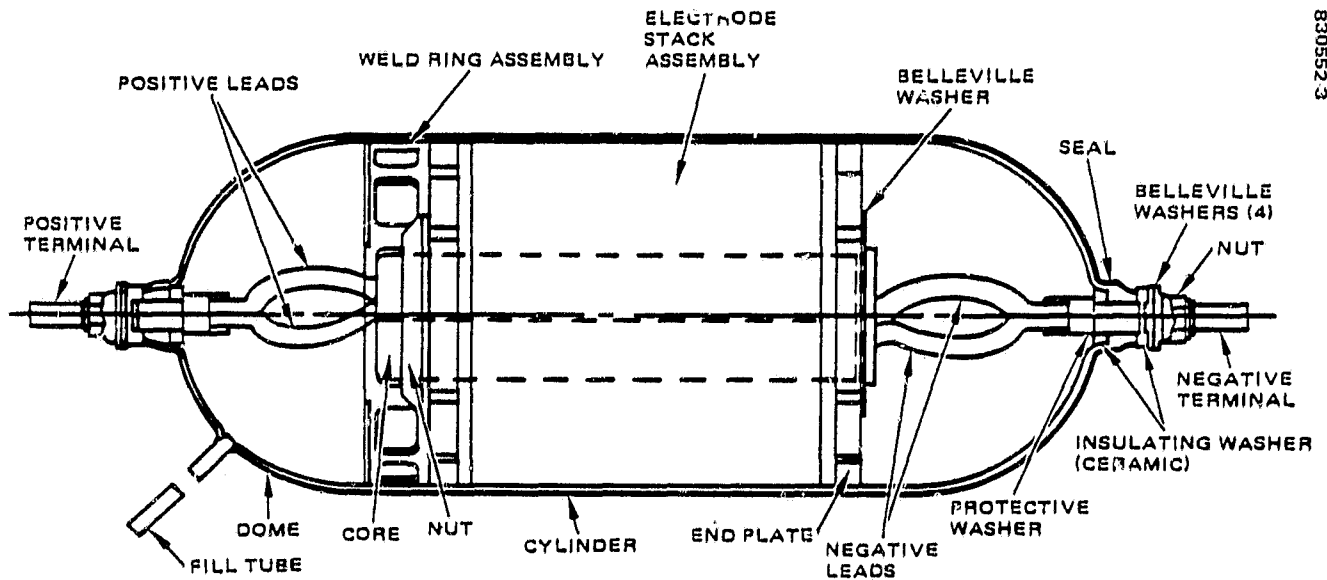


FIGURE 3. Ni-H₂ INDIVIDUAL PRESSURE VESSEL LAYOUT

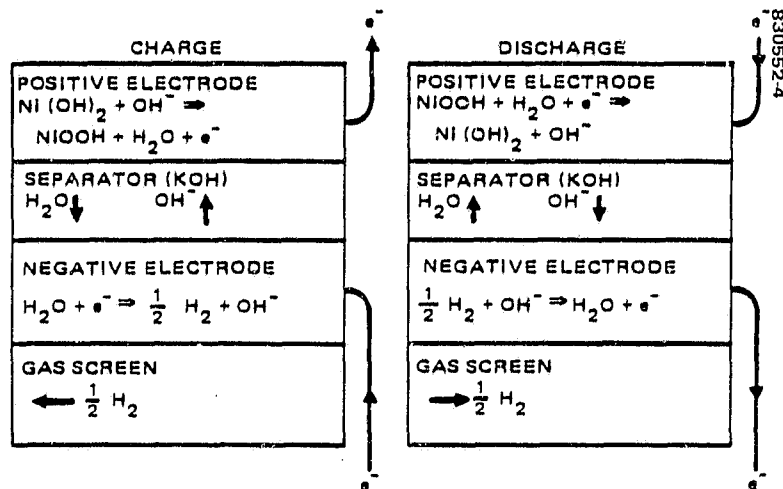


FIGURE 4. Ni-H₂ CELL ELECTROCHEMICAL REACTIONS

The positive electrode is considered to be the key life-limiting component of the electrochemical cell. At end of life its degradation takes the form of electrode swelling and/or active material extrusion from the plate, and is strongly dependent upon the duty cycle and depth of discharge (DOD) levels. These effects have been minimized by improved positive electrode processing techniques that feature dry sintering of the plaque followed by the electrochemical impregnation of active material.

Catalytic negative electrodes used in IPV cells consist of a 10 mg/cm^2 platinum-teflon slurry sintered on to a nickel substrate. Degradation mechanisms associated with this electrode have been characterized in fuel cell work. Due to relatively low temperatures and current densities, negative electrodes are sufficiently active so that the amount of degradation predicted in 10 years of operation is negligible. Negative electrode flooding is prevented by the use of a porous teflon membrane sintered to the gas side of the catalytic surface and a special electrode treatment during fabrication. None of these components is soluble, subject to recrystallization, or other physical changes during cycling. The net result is that the negative electrode life is independent of the DOD of the cell.

Asbestos and zirconium oxide are widely used separator materials in IPV cells. There is no evidence to indicate that the interactions between the electrolyte and separator material will result in loss of separator properties or in cell performance degradation with either of these materials. Asbestos, which is a natural material, requires careful processing control to ensure uniform chemical and mechanical properties. The electrolyte used in IPV cells is 31 percent KOH by weight. An excess of 10 percent is provided to maintain sufficient electrolyte in the separator in the event of positive electrode morphology changes. The IPV cell design has been flight qualified at Hughes and is currently being used on several flight programs.

2.2 NEAR TERM COMMON PRESSURE VESSEL MODULE CONFIGURATION

The CPV module design selected for this study is configured to eliminate potential trouble spots associated with the integration of several stacks into the pressure vessel (Figure 5). The selected concept is consistent with the requirements outlined in Table 1. The environmental constraints on module design (i.e., temperatures, pressures, vibration levels) are similar to those on the IPV nickel-hydrogen cell design developed at Hughes. However, in order to meet similar life and performance requirements, additional considerations unique to CPV module operation were taken into account.

One of the most critical is eliminating conductive electrolyte films between stacks. Called electrolyte bridging, this effect is eliminated by providing stack separation through hydrophobic components between stacks. For example, enclose stacks in teflon cups, teflon coat electrical leads and bus bars, and separate adjoining hydrophylic stack components with teflon seals. A similar effect is obtained between module stacks and the pressure vessel by applying a hydrophobic coating to the pressure vessel and exposing only the heat affected zones to electrolyte.

ORIGINAL PAGE IS
OF POOR QUALITY

LEGEND

- * 240 WH CAPACITY AT 40 AH
- 1 SWAGELOCK FITTING
- 2 FILL TUBE
- 3 TERMINAL ASSEMBLY
- 4 PRESSURE VESSEL (TEFLON COATED)
- 5 INTEGRAL BELLEVILE WELDING ASSEMBLY
- 6 STRAIN RELIEVED LEADS
- 7 THREADED POLYSULTONE CORE
- 8 POLYSULFONE ENDPLATE SLIPRING (CLEARANCE ID)
- 9 TEFLON CUP
- 10 WALL WICK
- 11 TEFLON O R'NG
- 12 TEFLON COATED LEADS
- 13 POLYSULFONE ENPLATE NUT (THREADED ID)
- 14 TEFLON SHEET
- 15 STACK TO STACK LEAD WELD POINT
- 16 THREADED TIE ROD
- 17 POLYSULFONE CORE
- 18 BELLEVILE WASHER
- 19 COMPRESSION FLANGE
- 20 BELLEVILE WASHERS
- 21 NUTS
- 22 INTEGRAL BELLEVILE WELDING ASSEMBLY
- 23 BERYLIUM OXIDE WASHER
- 24 TEFLON SEAL
- 25 WASHER
- 26 BELLEVILE WASHER

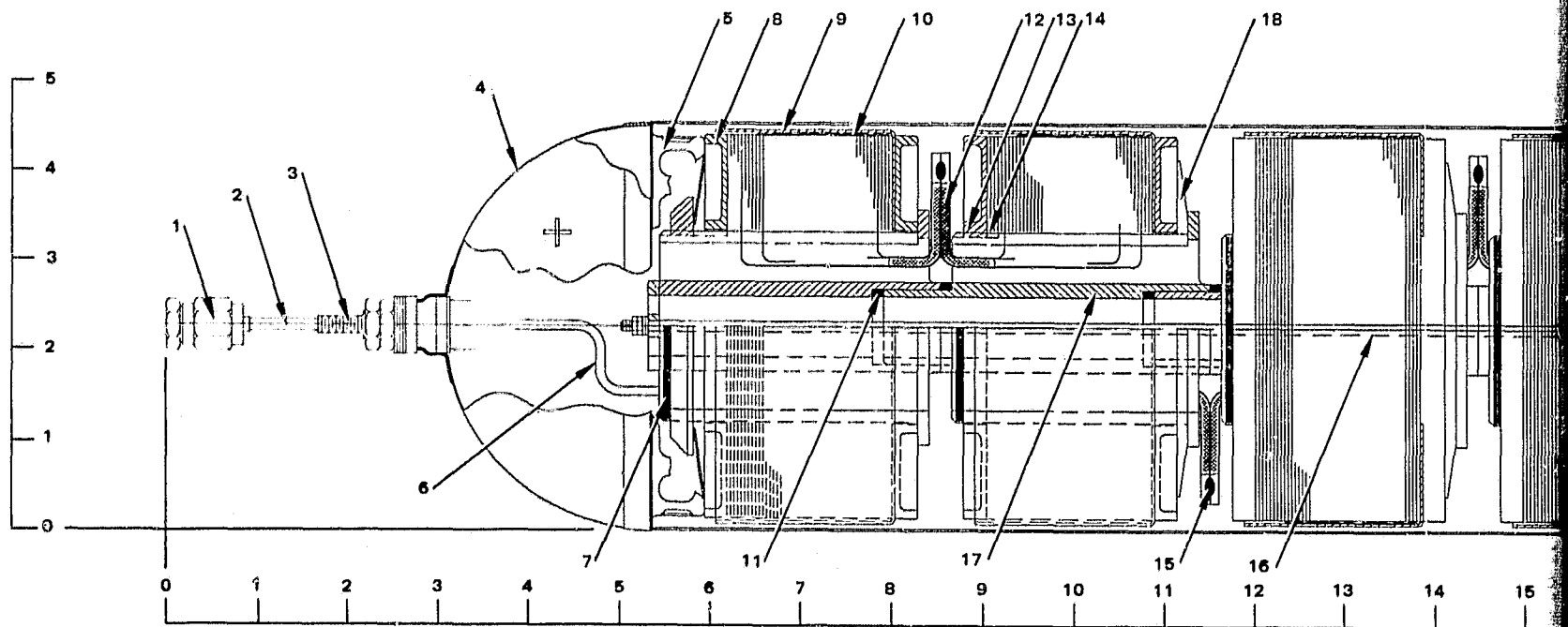
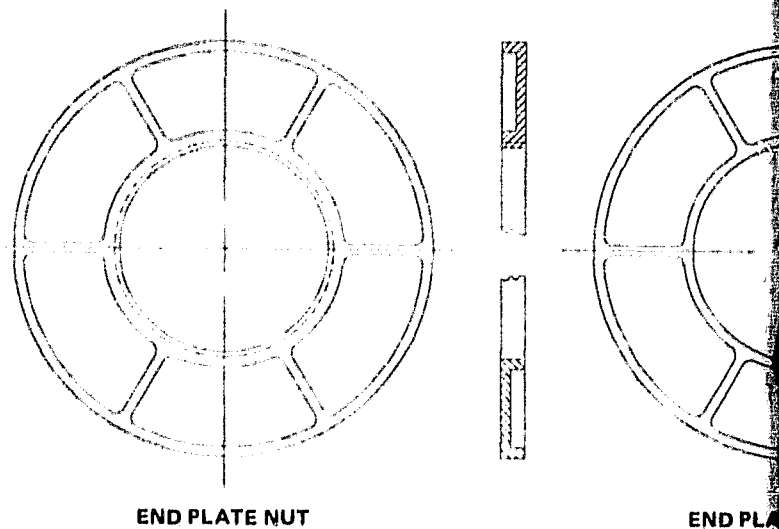
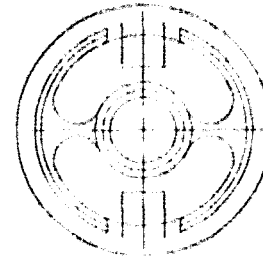
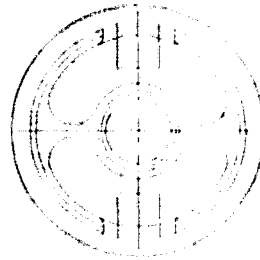
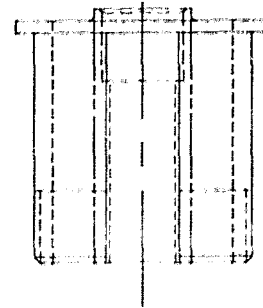
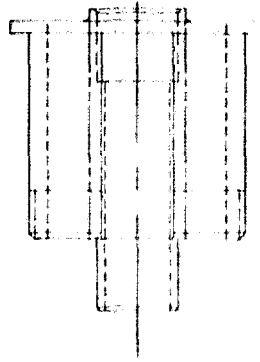


FIGURE 5. CPV MODULE DESIGN CONCEPT 1

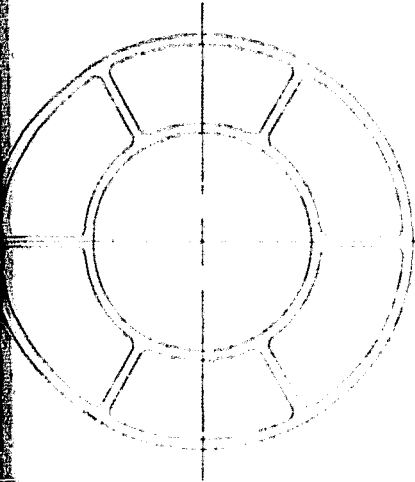
ORIGINAL FIG. 1
OF POOR QUALITY

830552-5

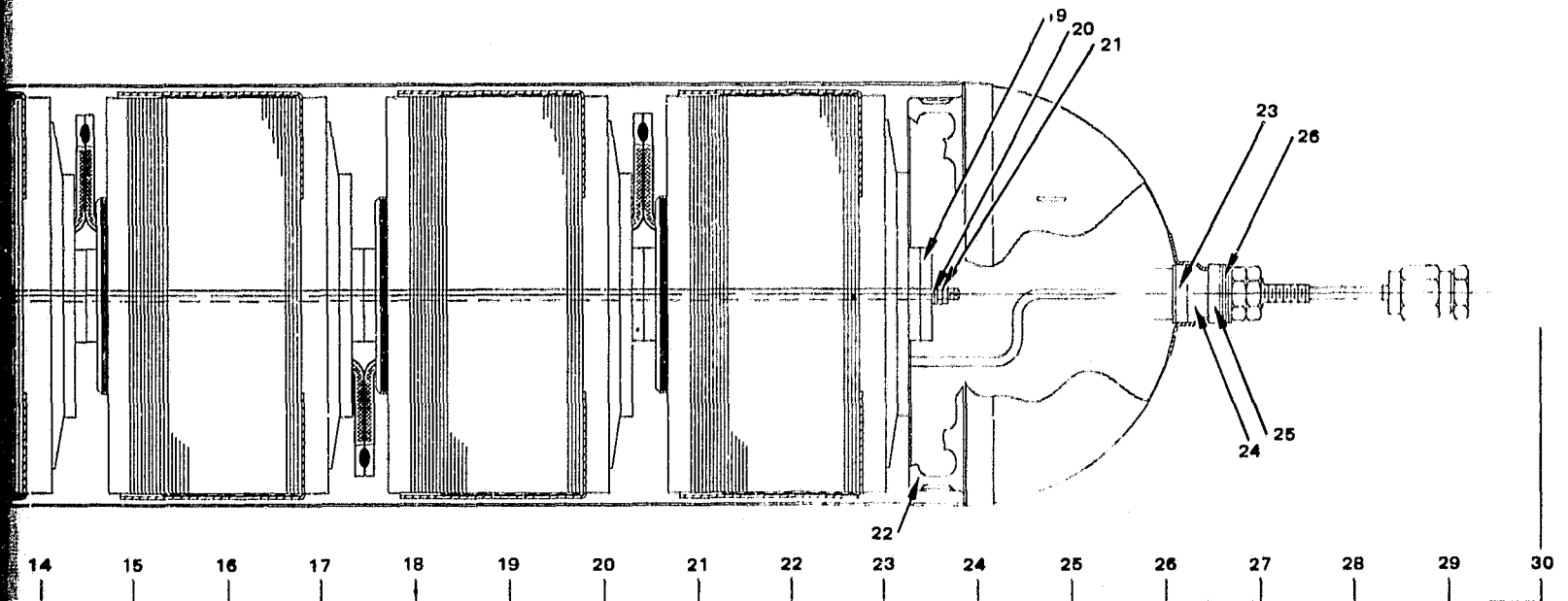


COMMON CORE

POS END CORE



END PLATE SLIP RING



2 FOLDOUT FRAME

TABLE 1. CPV MODULE DESIGN REQUIREMENTS

<u>Item</u>	<u>Requirement</u>	
Capacity	≤150 A-hr	
Orbit	LEO/GEO	
Depth of discharge	80 percent	
Cycle life	10,000 cycles	
Duty cycle	<u>Leo</u>	<u>Geo</u>
Charge	55 min	7 hr
Discharge	35 min	72 min
Nominal temperature	20°C	20°C
Stack EOL EODV	1.0 V	
Wet life	15 yr	
Storage	18 mo at 25°C	
Exposure temperature range	-20°C +30°C	
Humidity tolerance	MIL-STD-810B	
Shock	36 in. drop	
Handling tolerance	MIL-STD-810B	
	30 at 11 ms	
Standby temperature	Ambient	
Acceleration	15 g at 5-min/axis	
Mechanical shock	30 G 1/2 sine 8 ms/axis	
Flight temperatures	-30°C to +30°C	
Flight acceleration	0.16 g	
Seal life	15 yr	
Electrolyte bridging	None	
Vapor transfer	None	
Electrical connections	Adaptable to 6C use	
Pressure vessel life	≥30,000 cycles	
Activation	Uniform electrolyte distribution	
Mechanical support	Consistent with loads	
Ambient pressure	Vacuum to 16 psia	

PRECEDING PAGE BLANK NOT FILMED

An additional aspect of electrolyte management is water vapor transfer between stacks and between stacks and the pressure vessel. The design concept selected for this study minimizes the vapor transport effects by 1) reducing the temperature gradients between the stacks and other module components to 14°F or less, 2) decreasing the vapor pressure of electrolyte through an increase in KOH concentration within 30 to 40 percent, the net result of which will be the enhancement of the required temperature difference to transport water vapor between two surfaces, and 3) increasing the cell precharge.

Mechanical design of IPV cells depends mostly on the transfer of structural loads from the stack through the weld ring to the pressure vessel. Due to the added mass of extra stacks, CPV modules require axial and radial support of the cell stack assemblies. The selected design meets axial support requirement by providing a built-in weld ring support at one end of the module similar to that used in IPV cells and a simply supported preloaded joint at the other weld ring. This technique allows for a small differential displacement in the axial direction due to electrode swelling separator expansion or readjustment in the interstack connections without affecting stack axial support requirements.

Radial stack support is provided through the two weld rings and through mechanical contact between the stack and the pressure vessel along three contact lines. Additional radial support can be provided by the internal cores or by preloading the stack assembly with tie bands to prevent shear deformations.

Providing steady state axial and radial support of the stack assemblies is not a sufficient condition for meeting spacecraft requirements. Dynamic load conditions induced by the launch environment mandate that dynamic coupling between various module components place the resonant frequency response of the module outside the high energy input region of the vibration spectrum. To meet these requirements the recirculating electrode stack used in the CPV module is designed around a central polysulfone core that provides radial and axial support of the individual cell stack components with complete lead strain relief and a uniform stack preload between two polysulfone endplates loaded by Belleville washers. The H-shaped cores intermesh with each other and two hydrophobic teflon seals which prevent the continuity of electrolyte flow along the hydrophylic core assembly. Further isolation of the individual stack is provided by teflon cups that completely enclose each stack and by teflon coated leads.

Each stack is a self-contained separately assembled unit that is connected to the adjoining stacks through intermeshing core joints and a titanium or Inconel 718 tie rod which maintains a constant preload on the overall assembly. Both ends of the stack string assembly are attached to weld rings containing an integral Belleville washer to provide radial and axial support. One stack end is built in through a welding and the opposite one is simply supported through the other welding with additional radial support being provided by the contact line between the teflon cups and the pressure vessel along three contact lines located 120° apart.

Stacks are electrically interconnected through strain relieved TIG welded lead joints. All leads are teflon coated outside the heat affected zone (HAZ). The design concept provides for the isolation of potential failure modes (i.e., overheating due to shorts within one cell stack) and allows for the readjustment of individual stack components with cycling independent of other stacks.

The overall impact of alternate advanced module design concepts on the overall weight performance of CPV modules is in the 10 percent range and therefore does not affect significantly the performance projections outlined in the following section.

2.3 PERFORMANCE PROJECTIONS

To provide accurate IPV and CPV module weight and volume projections, proprietary software simulation packages were modified to allow the energy density and specific energy optimization of the CPV and IPV cell configurations. For any given choice of stack design characteristics, optimization depends on the following conditions:

- 1) Cell capacity
- 2) Number of cells within a pressure vessel
- 3) Cell diameter

At any diameter, as cell capacity is increased, the energy density (Figure 6) decreases. This decrease is caused by the added pressure vessel weight. The free volume available for gas containment increases at constant capacity by increasing the cell diameter into the 4 to 6 inch range. This increase results in a pressure decrease and a corresponding change in the pressure vessel weight. However, as the cell diameter increases, the weight savings associated with the decrease in pressure vessel wall thickness are counterbalanced by the increase in pressure vessel surface area.

For nickel-hydrogen energy storage modules with one or a few stacks within a pressure vessel, practical limitations associated with the manufacturing of very thin walled, large diameter components result in a substantially higher sensitivity of cell weight to the increase in surface area resulting in a finite optimum energy density. Adding more cell stacks to a common pressure vessel allows more effective use of case weight through a better match between the cell operating pressure and the minimum allowable wall thickness. Energy density as expressed by Wh/Kg can be optimized with state of the art technology to approximately 40 Wh/Kg in 15.2 cm diameter IPV cells and up to 46 Wh/Kg in CPV cells having four to six cell stacks within a pressure vessel.

Nickel-hydrogen cell specific energy (Wh/cm^3), as shown in Figure 7, decreases as the diameter increases due to the added volume tied up in the domes. Adding more stacks to a pressure vessel of a given diameter

provides a higher energy density caused by the decrease in the ratio of the dome volume to the cumulative volume of the stacks. Therefore, optimization of nickel-hydrogen cell energy density requires relatively small diameters, less than or equal to 15 cm and more than four stacks.

Based on these analyses, the optimum IPV and CPV module design in the 100 to 250 A-hr range would be packaged in a pressure vessel having a nominal 15 cm diameter while the optimum number of stacks would be six. In this configuration a CPV energy storage module could have a 20 percent weight and 20 to 30 percent volumetric advantage over IPV designs.

COMMONALITY OF OF POOR QUALITY

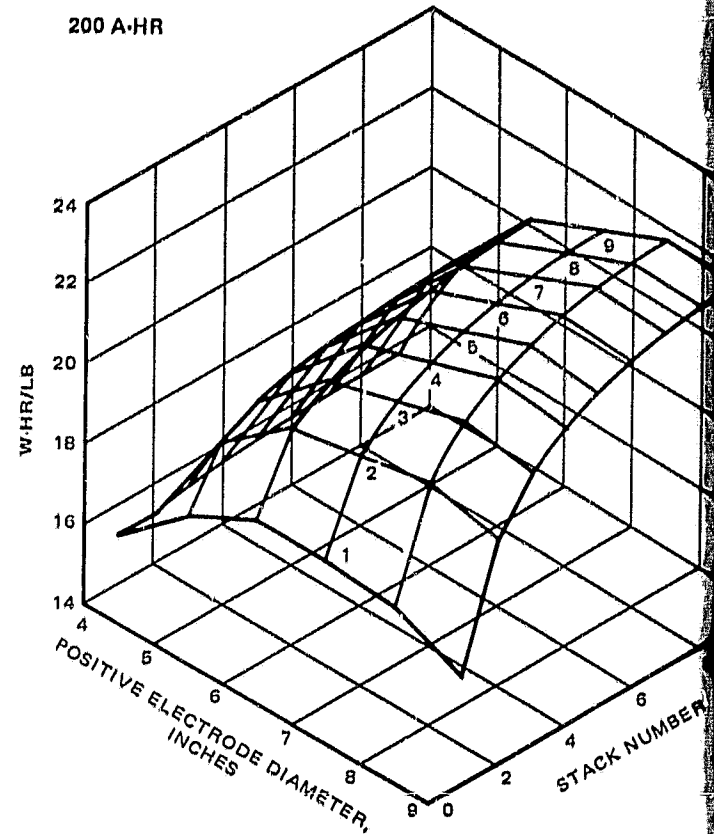
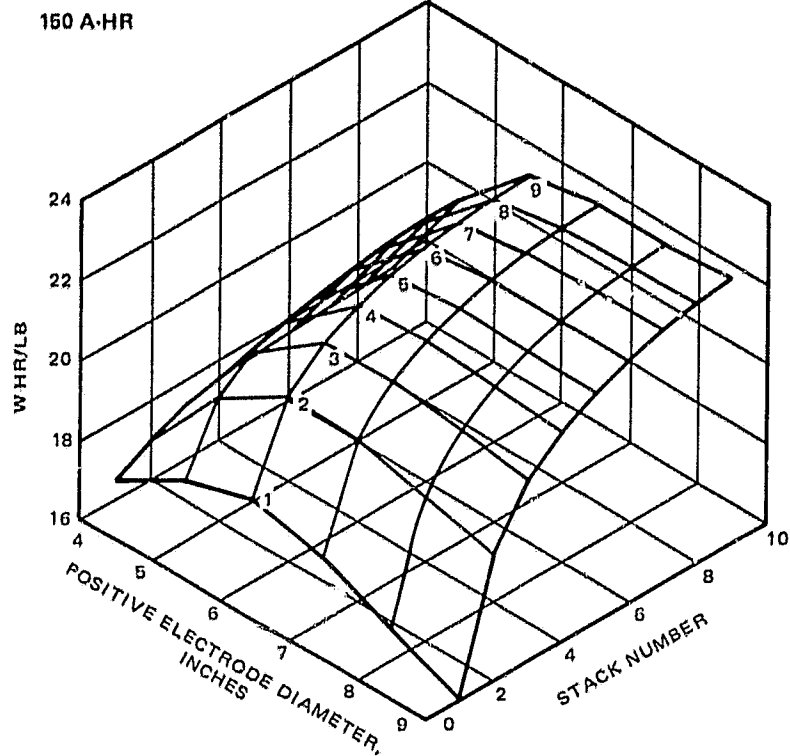


FIGURE 6. PROJECTED INDIVIDUAL PRESSURE VESSEL CELL AND COMMON PRESSURE VESSEL MODULE SPECIFIC ENERGY

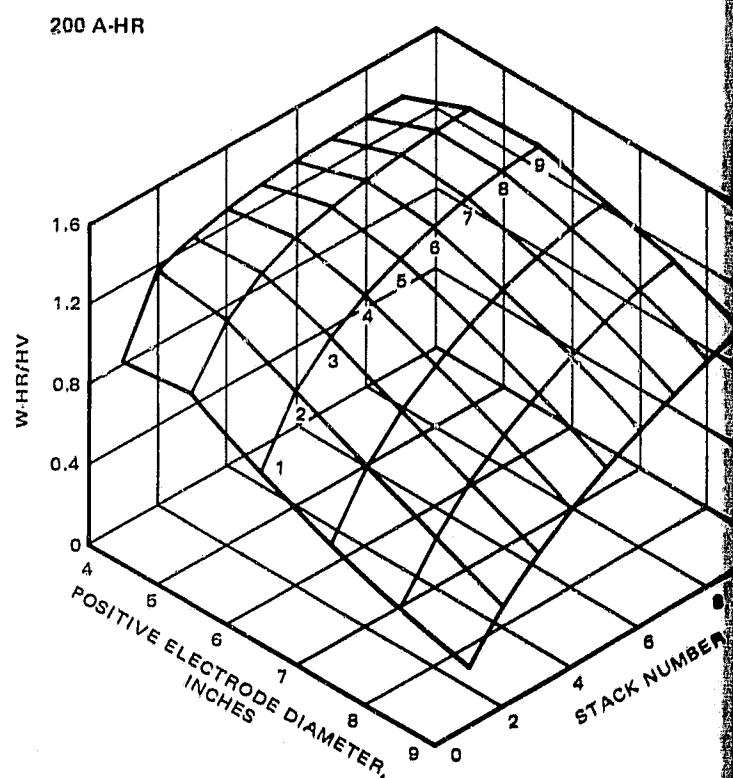
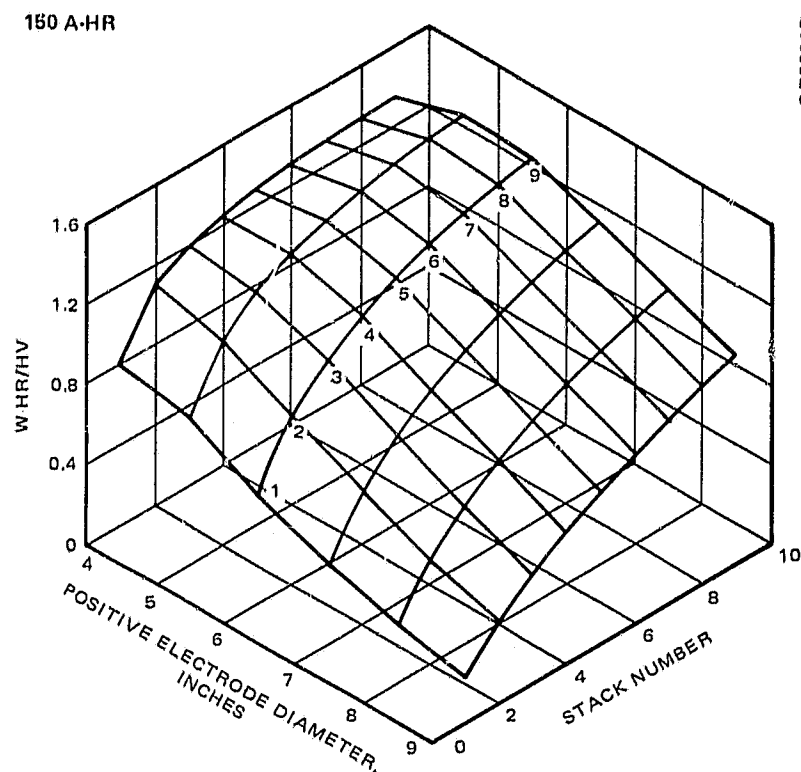
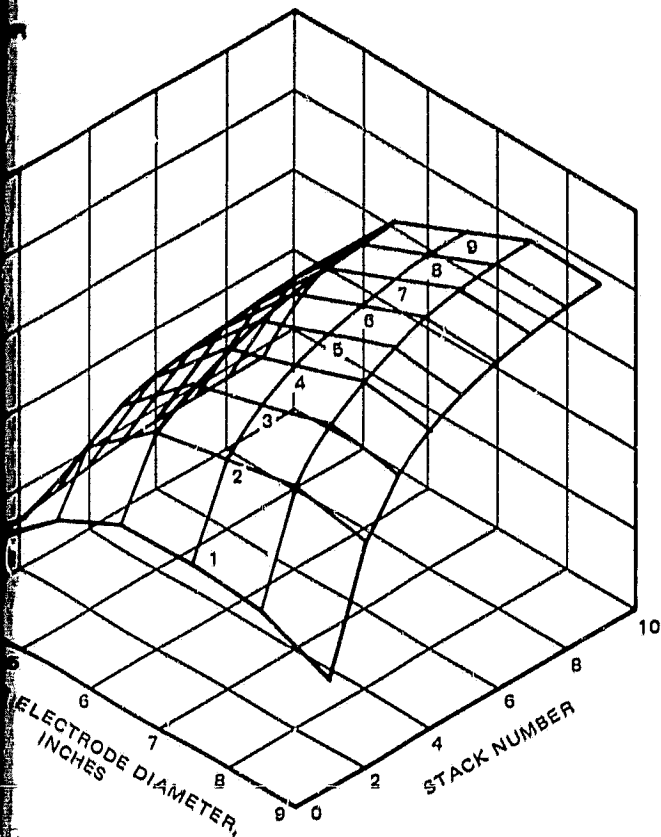


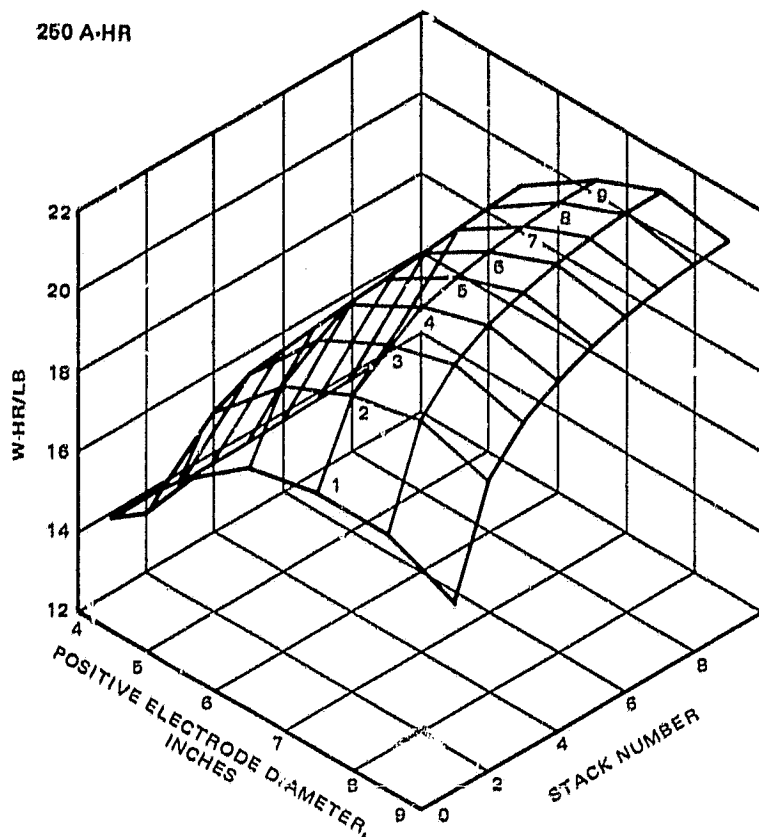
FIGURE 7. PROJECTED INDIVIDUAL PRESSURE VESSEL CELL AND COMMON PRESSURE VESSEL MODULE ENERGY DENSITY

830552-7



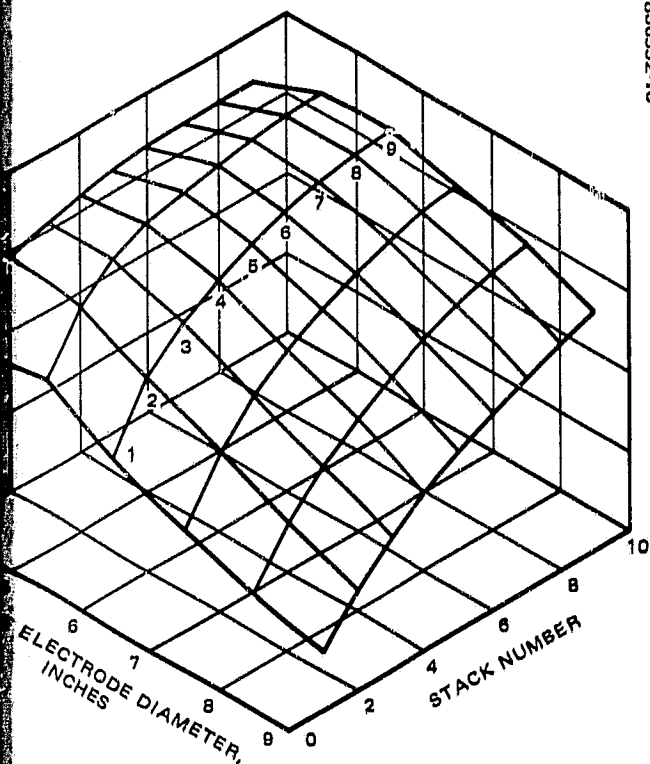
PRESSURE VESSEL MODULE SPECIFIC ENERGY

250 A-HR



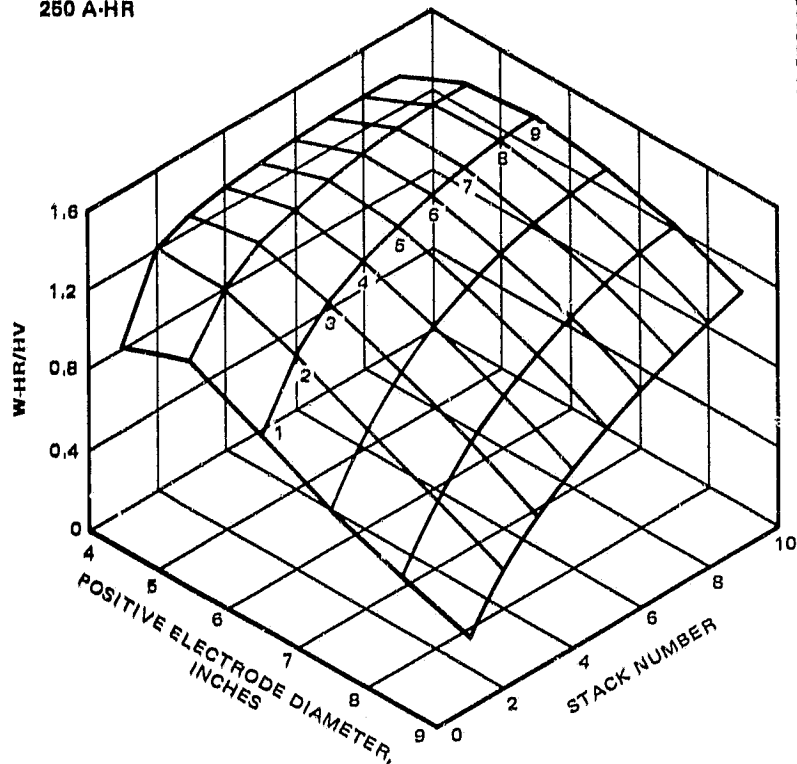
830552-8

830552-10



PRESSURE VESSEL MODULE ENERGY DENSITY

250 A-HR



830552-11

3. ADVANCED BIPOLAR BATTERY DESIGN AND REQUIREMENTS

The bipolar cell stack layout selected for optimization on this contract is illustrated in Figure 8. This configuration is a modified version of a concept originally developed at NASA's Lewis Research Center. ⁽¹⁾ As shown, several electrode pairs are packaged within a common hydrophobic plastic frame and connected in series by a corrugated, conductive bipolar plate. Movement of hydrogen gas to and from the negative electrode is provided through corrugations built into the bipolar plate. Recombinations of evolved O_2 takes place behind the positive electrode on a teflon encapsulated platinum catalyst strip embedded in the bipolar plate corrugation facing the positive electrode. Recombination strips are in turn supported by a layer of Zirconium oxide cloth that acts as an electrolyte reservoir for the positive electrode, and a piece of polypropylene gas screen that allows access of hydrogen gas to the back of the platinum coated recombination strip. A high bubble pressure fuel cell grade asbestos separator is used between the positive and negative electrode to prevent the bulk of evolved oxygen from recombining at the negative electrode.

This stacking concept provides both oxygen and electrolyte management within the cell stacks. As shown in Figure 9, thermal management is provided for a group of 25 series connected electrode pairs through mechanical contact at both ends of the group with liquid-cooled plates. The ratio of cooling plates to electrodes is primarily a function of the cell operating regime, i. e., low earth orbit (LEO) geosynchronous orbit (GEO) or peaking, and the allowable maximum temperature difference within the electrode stack, assumed at $10^\circ C$ in this study to minimize inter cell water vapor transfer.

To complete the cell stack, several cooling plate cell stack sub-assembly pairs are connected in series as shown in Figure 2 to build up the required voltage. They are held together by compression between two rigid honeycomb endplates. Electrical connections and cooling lines brought out from the cell stack are connected to the sealed coaxial cell terminals. The whole assembly is contained within an Inconel 718 pressure vessel designed to sustain 30,000 pressure cycles the device is likely to experience during its useful life.

PRECEDING PAGE BLANK NOT FILMED

830552-12

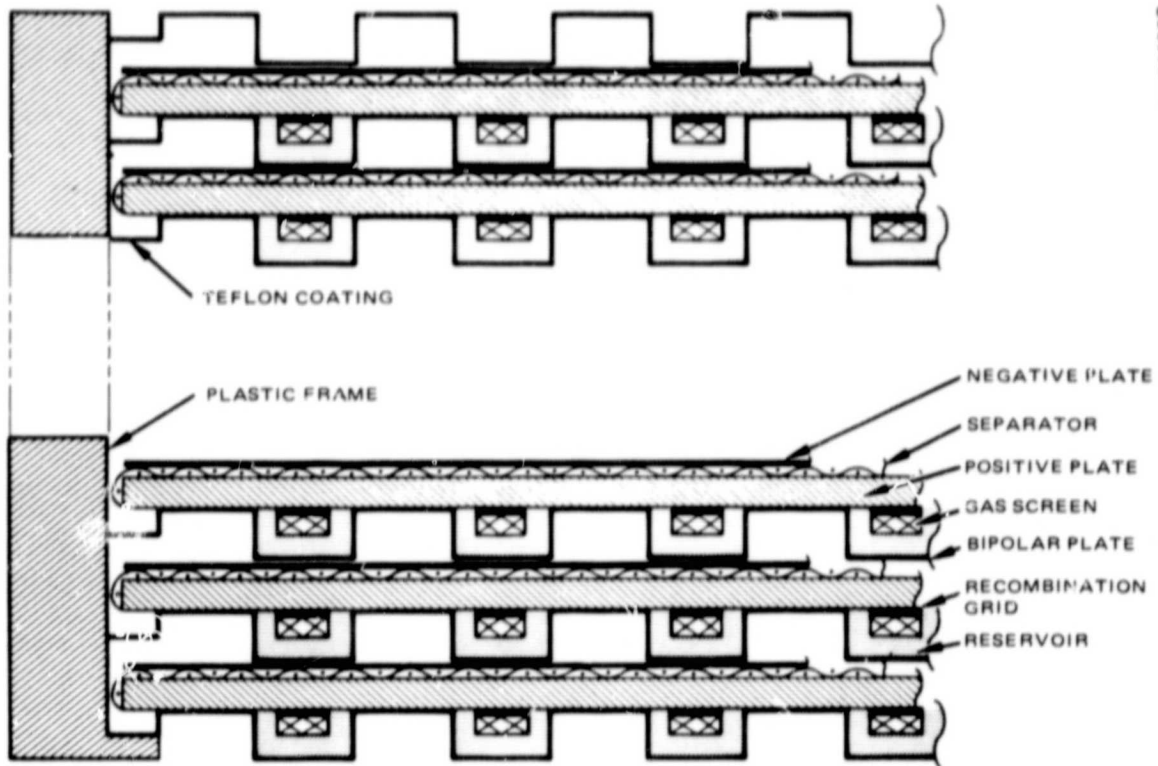
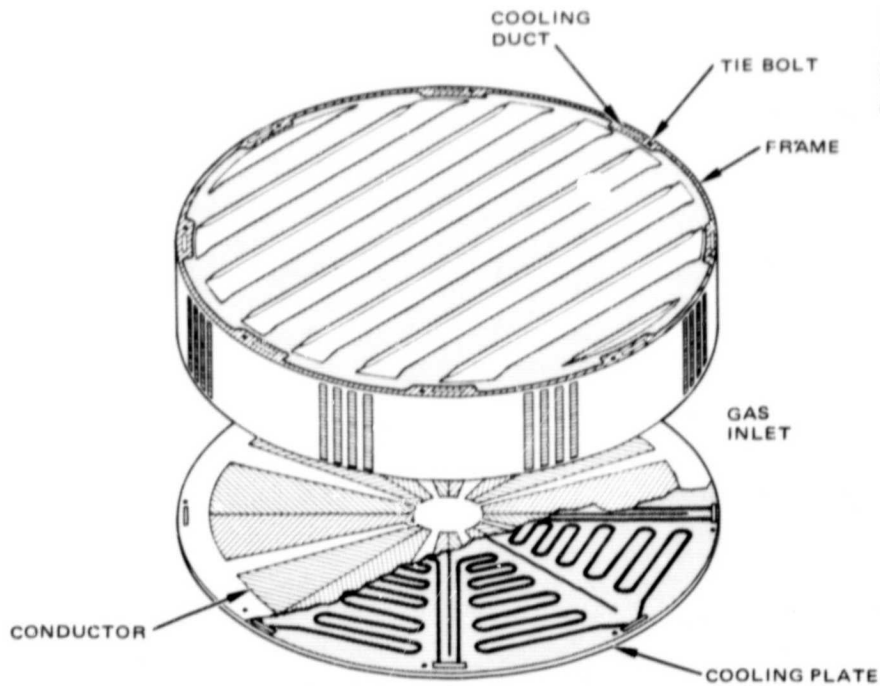


FIGURE 8. CELL STACK ASSEMBLY



830552-13

FIGURE 9. STACK SUBASSEMBLY

3.1 NEGATIVE ELECTRODES

The electrode technology selected for our studies is similar to that currently used in state of the art nickel-hydrogen cells. It relies on a photochemically etched 0.1 mm thick nickel substrate coated with a mixture of platinum powder and TFE30. Platinum loadings substantially less than the currently used 7 to 10 mg/cm² are feasible with the most likely catalyst mixture containing between 3 to 5 mg/cm² for operation at current densities up to 60 or 70 mA/cm². With the use of fuel-cell based electrode technology, in which a carbon based electrode or screen substrate is doped on the surface with platinum coated carbon particles, loading could be reduced to the 1 mg/cm² level, resulting in substantial cost savings in materials.

To prevent dryout of the electrode by H₂ gas entrainment, active portions of the electrode could have a thin Goretex backing that will be permeable to gas flow but will be impervious to liquid transport. The resulting nominal electrode thickness will be approximately 0.2 mm.

To ease oxygen and electrolyte management, a layer of Goretex encapsulated platinum-TFE mix deposited on a screen or photochemically etched nickel sheet is provided at the back of the positive electrode. The major benefit of this approach is the elimination of geometry related uneven O₂ recombination within the cell stack. H₂ gas is provided to the back of the recombination strips by polypropylene gas screen strips placed into the proper bipolar plate corrugations.

By relying on proven technology, the major difference between this and electrodes used in other nickel-hydrogen cells is that of scale. The overall technology is well within the state of the art capability.

3.2 POSITIVE ELECTRODES

Positive electrodes have been considered a critical part of nickel-hydrogen cell operation. As such, they have received considerable attention in the literature. Experience at Hughes and Eagle-Picher, Colorado Springs, has shown that electrochemical impregnation of electrodes using dry sinter attached to a welded nickel screen substrate provides good performance in state of the art Ni-H₂ cells. These electrodes are substantially lighter, provide a longer demonstrated life, and have reached a level of higher demonstrated manufacturing readiness than competing United States or Swiss technologies. The former represents, what we believe is, the best state of the art process. Electrodes of this type were demonstrated in Hughes cells that were cycled from 5000 to almost 9000 cycles under 80 percent depth of discharge (DOD) low earth orbit conditions and for several years in 80 percent DOD real time geosynchronous operation. Figure 10 gives the cycle life history of a typical Hughes-built Ni-H₂ cell.

CRITICAL EVALUATION
OF POWER QUALITY

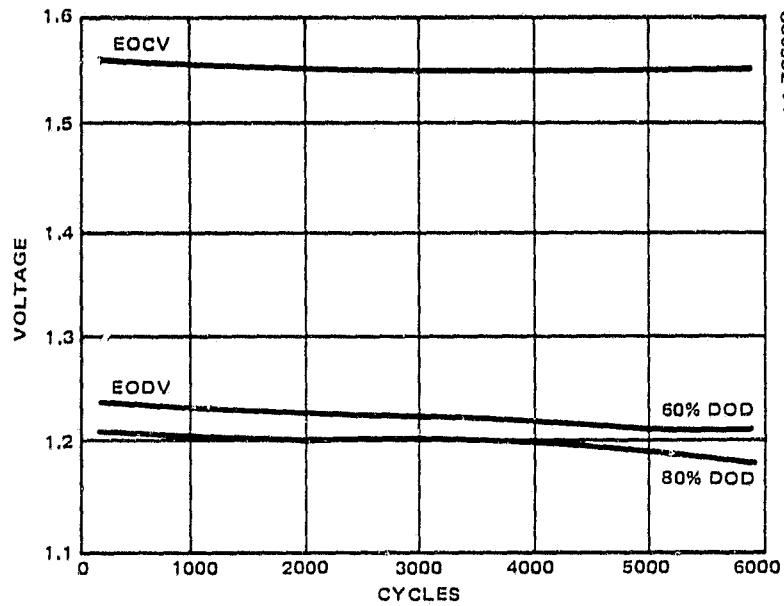
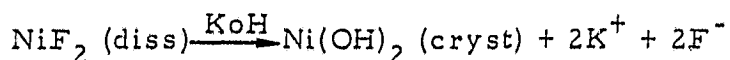
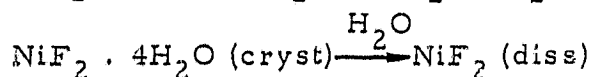
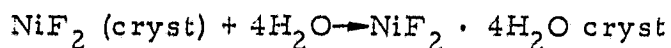


FIGURE 10. NI-H₂ CELL CYCLE LIFE HISTORY

The Swiss process developed at Battelle Geneva consists of sintering the electrode in the presence of Ni and a nickel compound (NiF₂) capable of forming the active material through chemical conversion. Current collection has been provided by a nickel wire screen having a 0.16 mm (6 mil) diameter and 0.5 mm (20 mil) opening. Sintering occurs for four minutes at 550°C (1000°F) and 500 kg/cm² (7200 psi) in either an inert atmosphere (N₂ or Ar) or in a slightly reducing atmosphere (N₂ plus 10 percent H₂).

After sintering NiF₂ is converted into Ni(OH)₂ according to the following reactions:



The time span associated with this conversion is approximately 24 hours with residence times at 25°C and 50°C of 20 and 4 hours respectively. During activation, porosity decreases by 25 percent caused primarily by changes in density associated with the Ni(OH)₂ conversion. Table 2 provides a comparison between the characteristics of state of the art electrodes produced by AFWAL and those produced at Battelle.

Electrodes produced at Battelle were cycled to 100 percent DOD at C/3 rate discharge and C/4 charge for 25 cycles. During these tests electrodes that were heavily loaded (≥45 w% of NiF₂) have shown 15 to 30 percent

TABLE 2. POSITIVE ELECTRODE COMPARISON

Parameter	EPI/AFWAL Electrode	Battelle Electrode
Area, cm ²	47.9	—
Thickness, mm	0.7 to 0.9	1.0 to 1.3
Porosity sinter, %	85	40 to 44
Overall porosity, %	45	29 to 39
Loading, gm/cm ³	1.45 to 1.70	3.4 to 3.8*
Starved capacity, Ah/kg	100 to 110	70 to 130
Sinter bend strength, kPa	3450	4900 to 9800

*Based on Ni-F₂ loading.

swelling. Similar behavior occurs in EPI/AFWAL electrodes only after more than 6000 cycles of C rate charge and 1.4 C rate discharge to 80 percent of actual cell capacity.

Work performed at Hughes shows that electrode expansion and sinter damage are major contributors to cell performance degradation during cycling. During the expansion process, remote active material becomes progressively less accessible for discharge due to the insulating characteristics of the discharged active material in closer vicinity to the current collector matrix.

Based on Battelle test results, it is likely that only electrodes having a Ni-H₂ content of 35 to 40 watt percentage are capable of meeting anticipated NASA low earth orbit life requirements. However, these electrodes yield at best only 80 to 95 A-hr/kg, making their performance inferior to commercially available AFWAL/EPI electrodes. Since a sizable fraction of electrode costs are associated with sinter fabrication, electrode inspection, and testing, it is believed that the Battelle process in its current form could provide only a small cost advantage relative to existing electrode technology.

Therefore, to minimize the risks associated with the implementation of the bipolar cell stack design, we have opted to baseline the EPI Colorado Springs electrode technology. However, due to the unique features of the bipolar battery, changes in electrode design are desirable. Among these, elimination of the screen and doubling of the electrode thickness from the currently used 0.8 mm, while retaining the same active material loading of 1.6 to 1.8 gm/cm³, and the same overall sinter and electrode porosities of 85 and 45 percent respectively are the most important. As discussed in 3.13, these changes are conducive to a 15 percent increase in bipolar cell specific energy.

The impact of the positive electrode thickness on bipolar battery specific energy is shown in Figure 23 where electrodes having twice the thickness of currently used electrodes have been folded into the design. State of the art positive electrodes are assumed to have 0.3 A-hr/cm³ of volume and to weigh 9.1 gm/A-hr stored. Both of these changes, combined with the need for relatively large electrode structures, require development prior to implementation.

A gridless positive electrode has the advantages of lower weight and potentially longer life when used in a bipolar cell than those considered for IPV and CPV nickel-hydrogen cells. They may be used in bipolar cells, although unsuitable for IPV and CPV nickel-hydrogen cells because of the importance of lateral current collection needs associated with state of the art and near term cell designs. The lateral electronic conductivity of a gridless electrode is lower than that of an equivalent electrode with a grid, a feature which may help favorably the safety of bipolar batteries during accidental shorts across a separator. Since gridless electrodes have a uniform mechanical structure, cycling induced sinter damage could be

reduced. (2)(3) Therefore, a potential life limiting factor could be mitigated, presenting the possibility of enhanced electrode life. Development requirements associated with the pursuit of gridless electrodes in bipolar cells include characterization of radial expansion during cycling and required mechanical strength for handling and fabrication.

A thick positive electrode is attractive for a bipolar nickel-hydrogen battery because it reduces the cell diameter and can substantially enhance energy density and specific energy. The positive electrode thickness could be doubled from the typical values presently used without severe polarization penalties. For example, a nickel-hydrogen cell with a doubled capacity per unit area of nickel electrodes could be operated at a twofold higher current density. This current density value is not expected to provide any operational problems in view of the high rate (10 C) capability at present IPV cells, or the 20 to 30 C rate capability of a bipolar battery. Dry sinter plaques up to 0.9 mm in thickness were fabricated in the past. Thicker plaque (>3 mm) has been made by using a slurry process but the electrochemical impregnation techniques have not been established to aerospace standards.

A thicker electrode could provide increased mechanical strength which will improve its handling capability without breakage. This is particularly important for gridless electrodes. Areas deserving consideration in future bipolar cell development programs are plaque fabrication, active material loading, and characterization of electrode polarization as a function of thickness. With proper development, each of these technical difficulties could be overcome.

3.3 SEPARATOR

The separator used in the bipolar cell is assumed to be stamped to conform to the electrode and plastic frame geometry shown in Figure 11. Fuel cell grade asbestos paper separators having a nominal thickness of 0.2 mm are good candidates for use in bipolar cells. Their demonstrated low cost, stability in the battery environment, excellent electrolyte retention capability and very high bubble pressure make them the best choice from both weight, volume, cost, electrolyte and oxygen management viewpoints. Since asbestos pore structure is finer than that of Zirconium oxide cloth, separator dryout is not likely to occur since the ZrO_2 reservoir will be resupplying the positive electrode with electrolyte.

3.4 BIPOLAR PLATE

The bipolar plate, illustrated in Figure 12, is a critical cell component. It serves several functions by providing 1) electrical conduction, 2) electrolyte isolation, 3) hydrogen distribution to the negative electrode and oxygen recombination surface located in the vicinity of the positive electrode, and 4) structural coupling between electrode pairs and stack

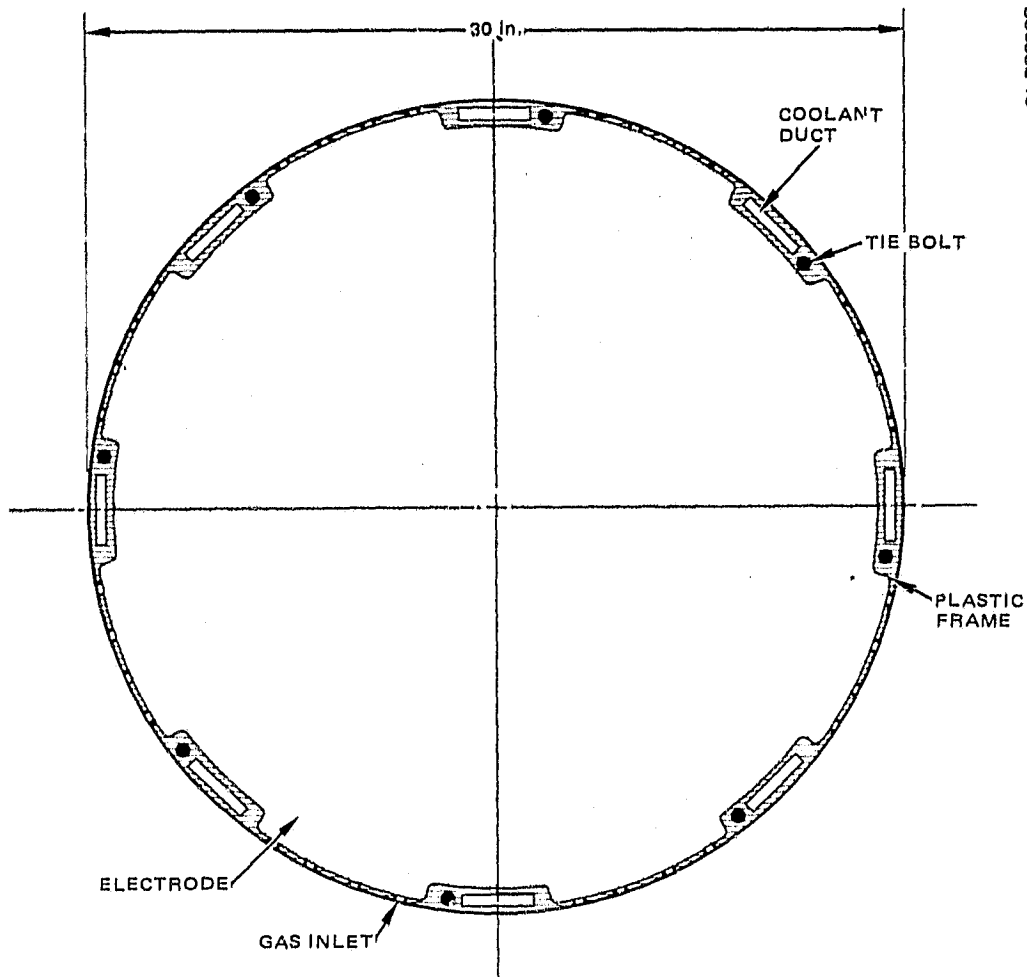


FIGURE 11. ELECTRODE/FRAME GEOMETRY

830552-17

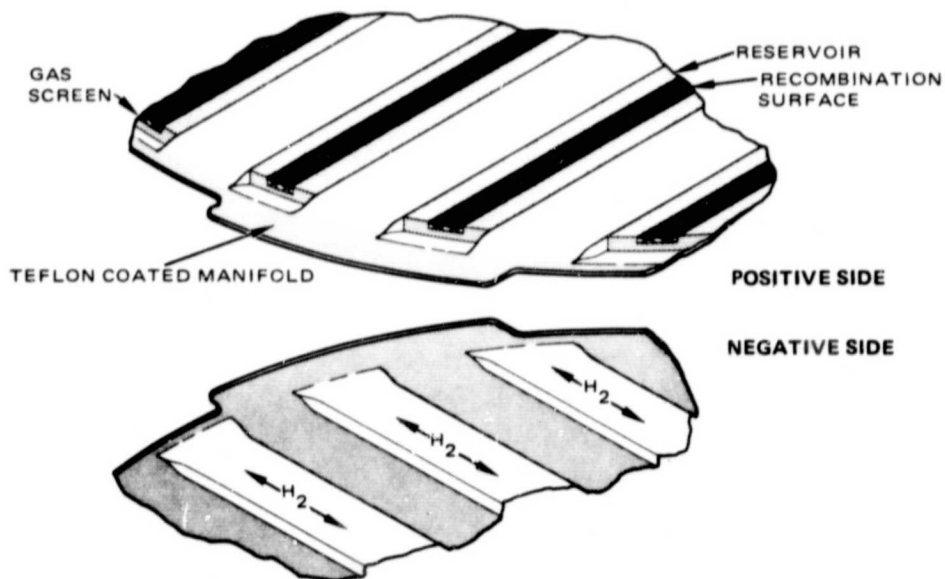
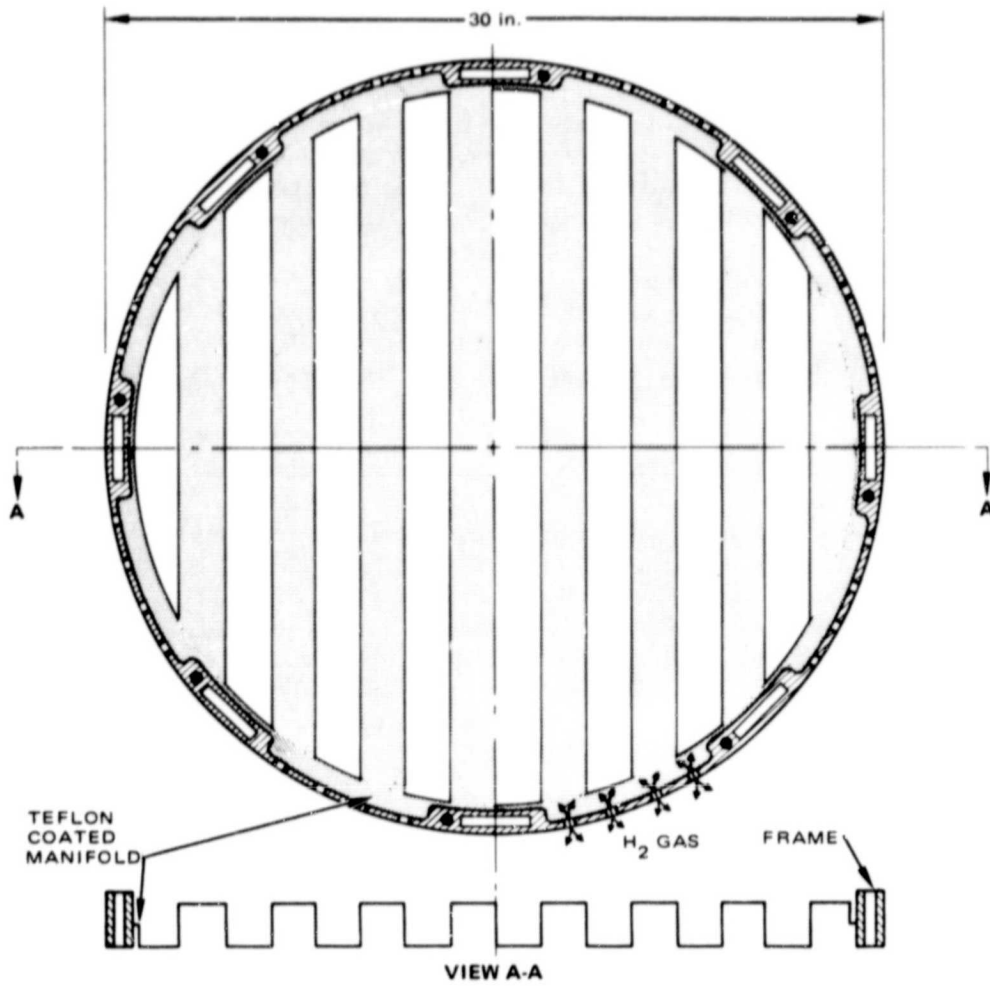


FIGURE 12. BIPOLAR PLATE

subassemblies. This figure shows a schematic view of the plate placed within a stack subassembly frame in a top and cross sectional view and a free standing isometric picture of the positive and negative electrode sides. As shown, the bipolar plate is a corrugated nickel sheet metal structure, having a nominal thickness of 0.2 mm and a corrugation depth of 1.2 mm and width of 2.5 cm. To facilitate hydrogen gas distribution, the bipolar plate has a 2.5 cm wide teflon coated rim located midway in depth. The flat teflon coated clearance acts as a manifold for hydrogen gas distribution to the two electrodes. Teflon coating is added to prevent electrolyte bridging from one electrode pair to the next. Those areas in which contact occurs with the plastic cell stack subassembly frame will be glued partially to it, sealing each electrode pair.

Figure 12 details the location of the electrolyte reservoir, polypropylene gas screen, and associated teflon encapsulated O_2 recombination surface on the positive electrode side. Empty gas flow corrugations are shown on the negative side. Structural loads are transmitted from one electrode pair to the next through the filled areas of the bipolar plate corrugations. Electrical interconnections between cell stack subassemblies occur through the bipolar plates located at each end of the stack subassembly. For best electrical and structural contact between subassemblies, the bipolar plate corrugation shall be rotated 90° out of phase from each other. This rotation will facilitate a more uniform gas flow distribution pattern within the cell stack.

3.5 COOLING PLATES

As indicated in Figures 9 and 13, heat rejection from the cell stack is accomplished through liquid-cooled plates. Manifolding of the coolant to the cooling plates is accomplished through the plastic frames enclosing the cell stack subassembly as shown in Figure 14. Coolant inlet and outlet ports alternate along the periphery of the stack subassembly frame.

To prevent coolant from leaking into the cell stack, gaskets are provided along the periphery of the cooling plate frame interface. As currently envisioned, the coolant most likely to be used is water or 31 percent KOH. To prevent electrolysis, cooling plates are assumed to be injection molded out of polysulfone with proper slots provided at periodic intervals to allow the insertion of electrical conductors. To facilitate heat transfer, the wall thickness of the cooling path has been reduced to 0.2 mm.

3.6 TERMINALS

Coolant inlet and outlet into the cell stack are provided through a coaxial terminal assembly schematically illustrated in Figure 15. The concept, a modified design of a previously patented Hughes concept, relies on the plastic flow of teflon for proper sealing. Other than a considerable extension in size and allowance for separate gas/electrolyte and coolant flow passages, the design is similar to that currently used in $Ni-H_2$ cells.

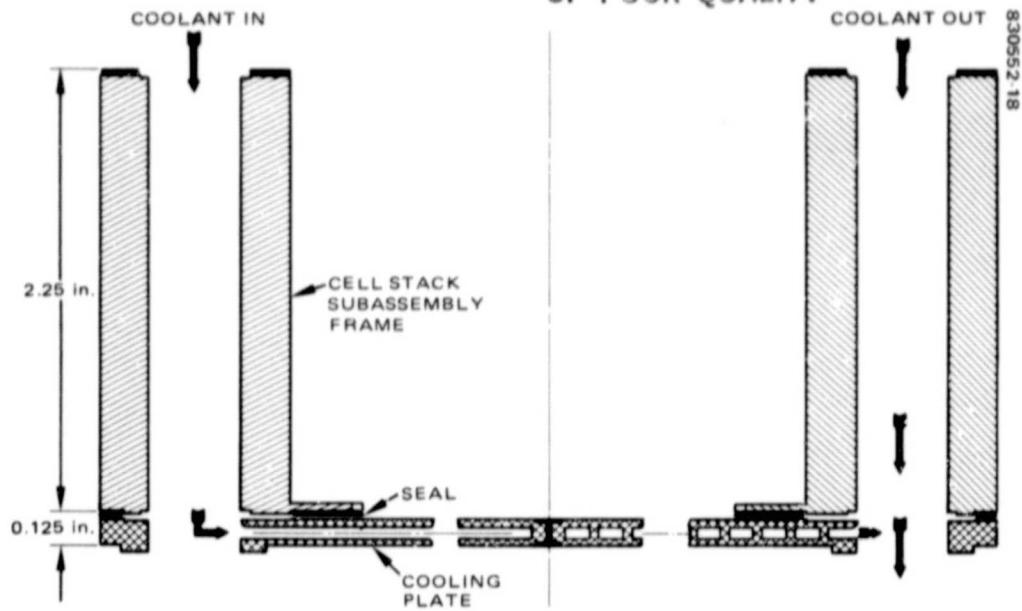


FIGURE 13. COOLING PLATE FRAME ASSEMBLY

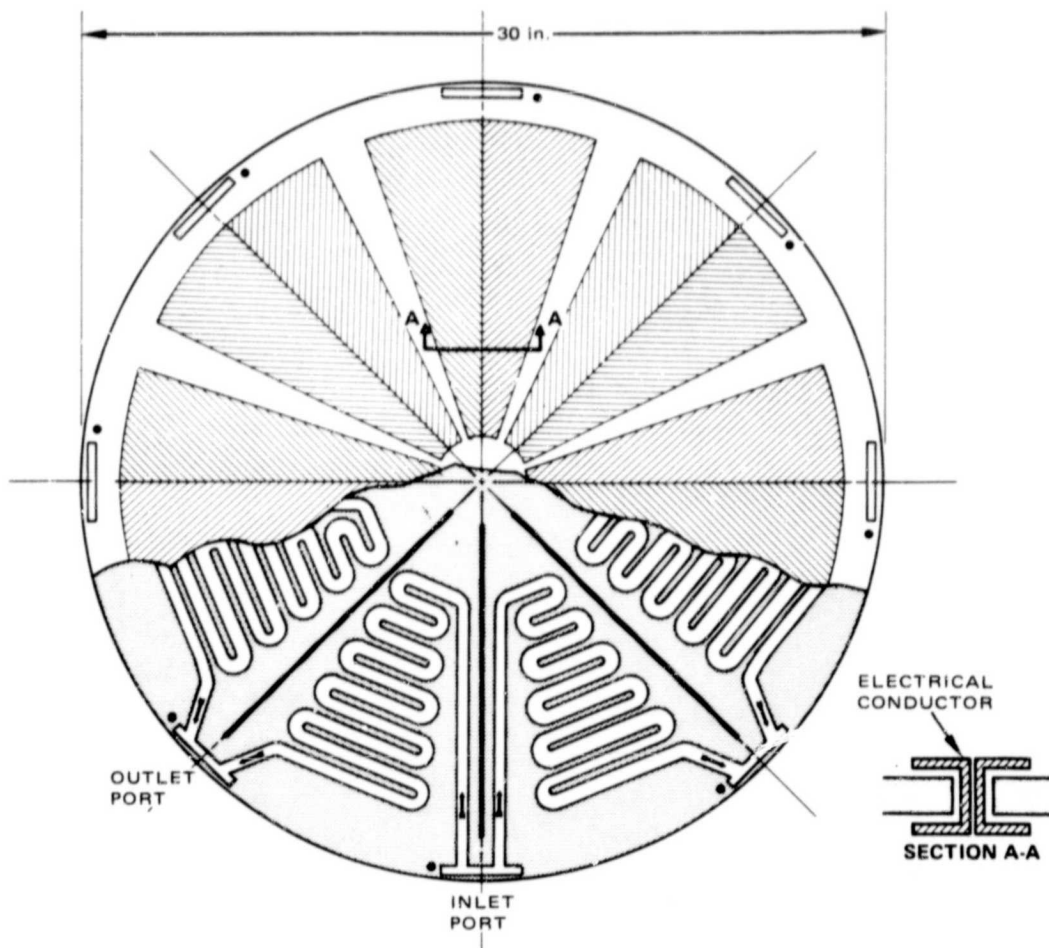


FIGURE 14. COOLING PLATE

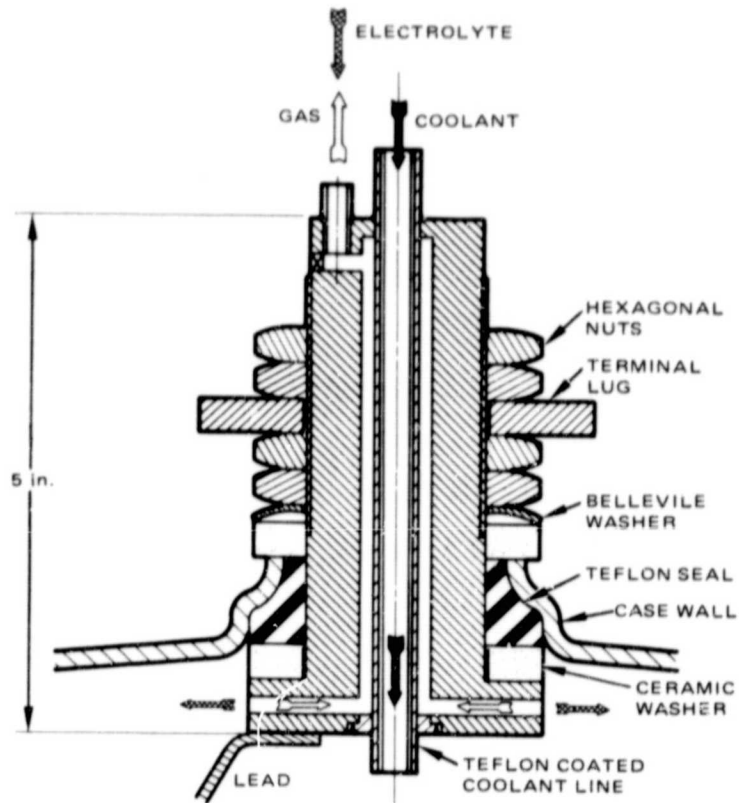


FIGURE 15. TERMINAL

Electrical lead and coolant coupling to the terminals are shown in Figure 2. Electrical leads from the end electrodes are resistance spot welded to a disk located at the bottom of the terminal assembly. Inlet and outlet coolant flow is distributed among four polypropylene tubes by a cross-shaped manifold. From there, coolant lines are connected to the cell stack through the endplate assembly.

3.7 ENDPLATE/WELD RING ASSEMBLY

The function of the endplate shown in Figure 16 is twofold: to maintain a uniform 30 psi preload on the cell stack subassembly and transfer the structural loads from the cell stack to the pressure vessel through the weld ring assembly (shown in Figure 17) without exceeding a 0.2 mm deformation of endplate geometry during anticipated environmental loads.

The load bearing structural components are three inch thick Inconel 718 honeycomb endplates. They have a 1 cm cell size, 1 mm facesheets and a web of 0.1 mm. Cooling passages and eight Inconel 718 tie bolts, 1 cm diameter, penetrate the endplates which have been reinforced with plastic inserts. The resulting structure is sufficiently stiff to allow transfer of 15g loads to the weld ring without any significant loss of preload.

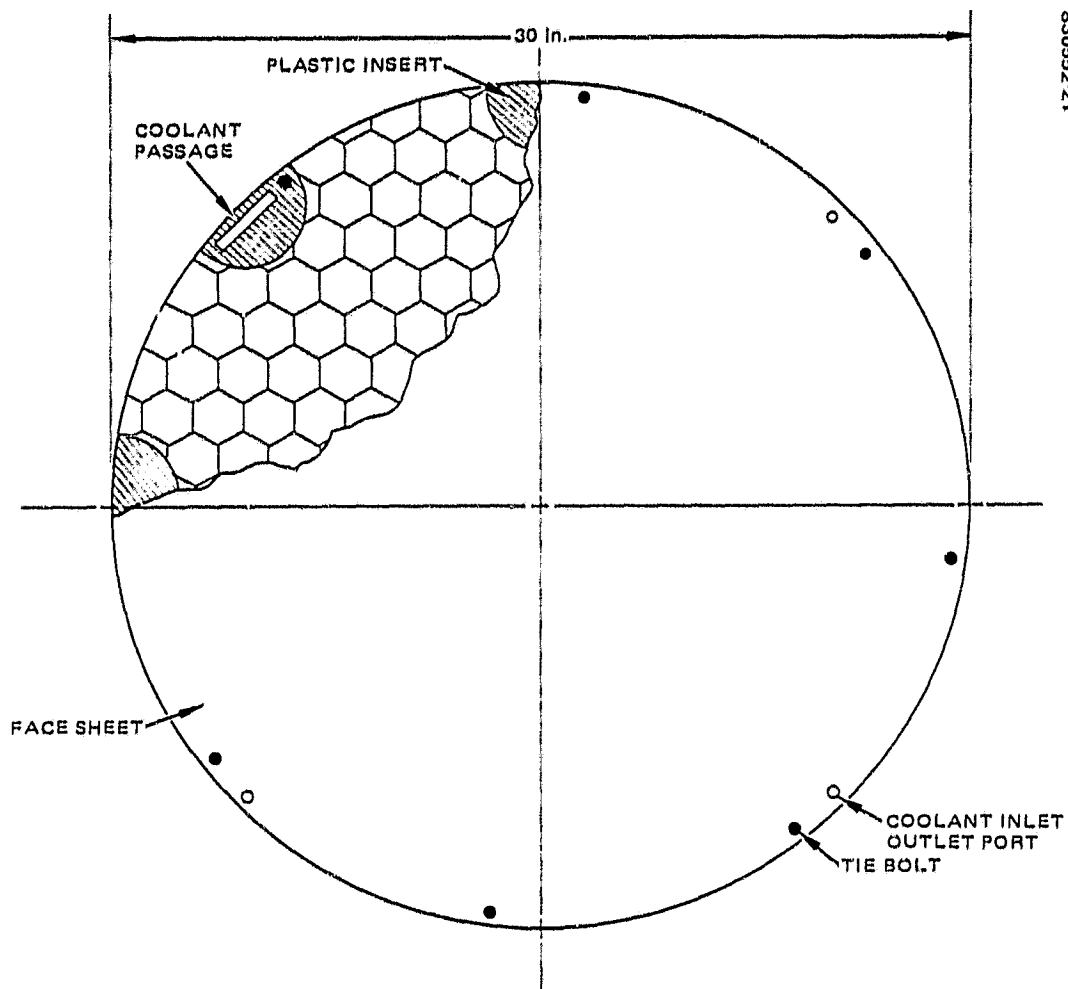
The weld ring design shown conceptually in Figure 17 is assumed to be of a similar configuration to that used currently in nickel-hydrogen cells. Its major function is to structurally couple the cell stack to the pressure vessel.

3.8 PRESSURE VESSEL

The bipolar cell stack is packaged into an Inconel 718 pressure vessel designed to sustain 30,000 pressure cycles in the 3.5 to 7.0 MPA range. It is composed of a cylindrical section attached to hemispheres at each end. Using design allowable stress values of 415 and 345 MPA for the parent and weld metal respectively, the required wall thickness for the cylinder and the domes are 5.3 and 2.5 mm respectively. When in the heat affected area wall, thicknesses are 6.3 mm.

To meet Space Transportation System safety standards, the bipolar battery pressure vessel design must rely on fracture mechanics techniques described in NASA Aerospace Pressure Vessel Safety Standard NASA 1740-1. This is basically a flaw-growth-oriented approach.

A maximum detectable flaw size of 0.01 cm should be selected as the basis for pressure vessel design studies. This goal is to provide a pressure vessel design consistent with a burst to operating pressure ratio of 4:1. To achieve this outcome, pressure vessel compliance with leak-before-burst failure criteria will have to be demonstrated. That is, a crack growth can propagate through the pressure vessel wall without initiating rapid fracture



8305221

FIGURE 16. END PLATE

ORIGINAL PAGE IS
OF POOR QUALITY

830552.22

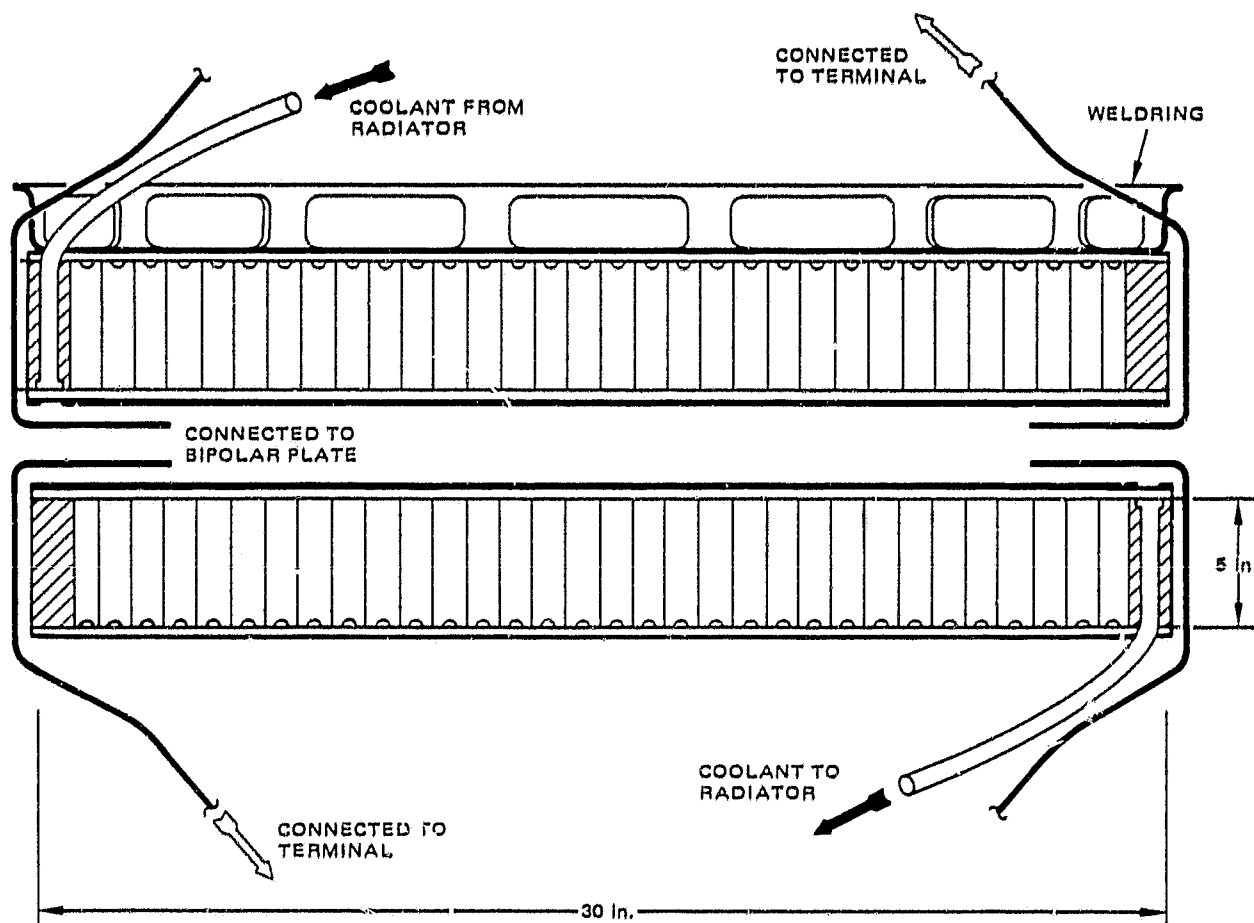


FIGURE 17. END PLATE/WELDRING ASSEMBLY

and fragmentation. Pressure vessel wall and weld thicknesses have been selected to sustain a minimum 120,000 cycles (four times the maximum expected cycle life of 30,000 cycles in 5 year LEO operation) by taking into account Hughes-developed Inconel 718 growth propagation data.

In addition to crack growth, the pressure vessel design addresses manufacturing considerations related to its fabrication and welding. During the program different techniques were considered to make the dome and cylinder in the most cost effective way. The cylindrical section could be made by starting with a cast hollow Inconel 718 cylindrical blank that would be rolled onto the desired configuration using seamless tube rolling techniques. An alternative approach to the design and fabrication of the cylinder would be to roll a 4.5 mm plate into the desired cylindrical shape and then TIG weld it along the inner and outer contact lines.

The two domes could be designed to be made by spinning and then welding numerically machined pressure vessel penetration bosses onto the spun hemispherical sections. After forming, pressure vessel components should be heat treated for full strength and mated with the stack weld ring assembly.

Figure 18 shows schematically the various welds that need to be integrated into the pressure vessel. The use of a K type insert for the seam weld ensures full weld penetration in the rolled cylinder while a root pass with filler wire consumes the insert. Back purging gas is needed at that time to prevent oxide formation.

The two-part weld design required for the seal boss doubler to the dome attachment is shown in the same figure. After tacking the doubler in place, a circular weld joins a weld land to the doubler. Subsequent fill passes complete the first step. The assembly is then indexed, and a fillet weld joins the outside edge of the doubler to the dome.

The final pressure vessel closure weld, as shown in the figure is laser welded after the mating dome and cylinder/stack/dome subassembly have been tack welded. An alignment fixture is used to maintain exact positioning and centering of the closure weld. Tacking secures the components prior to final closure weld, and a root and one or two fill passes complete the weld. An X-ray may be required after the initial root pass to ensure complete penetration of the weld. The finished weld, as well as all others previously mentioned, is X-rayed and dye penetrant inspected to aerospace quality standards prior to the buyoff of each weld.

The weld design of the battery to spacecraft structural attachment interface rings to the cylindrical portion of the pressure vessel requires three weld steps. One will provide the butt weld for the rolled rings, and another will result in tacking of the ring assembly to the cylinder. Finally, fillet welding will be used to attach the mounting ring to the pressure vessel.

ORIGINAL 10-81-82
OF POOR QUALITY

830552 23

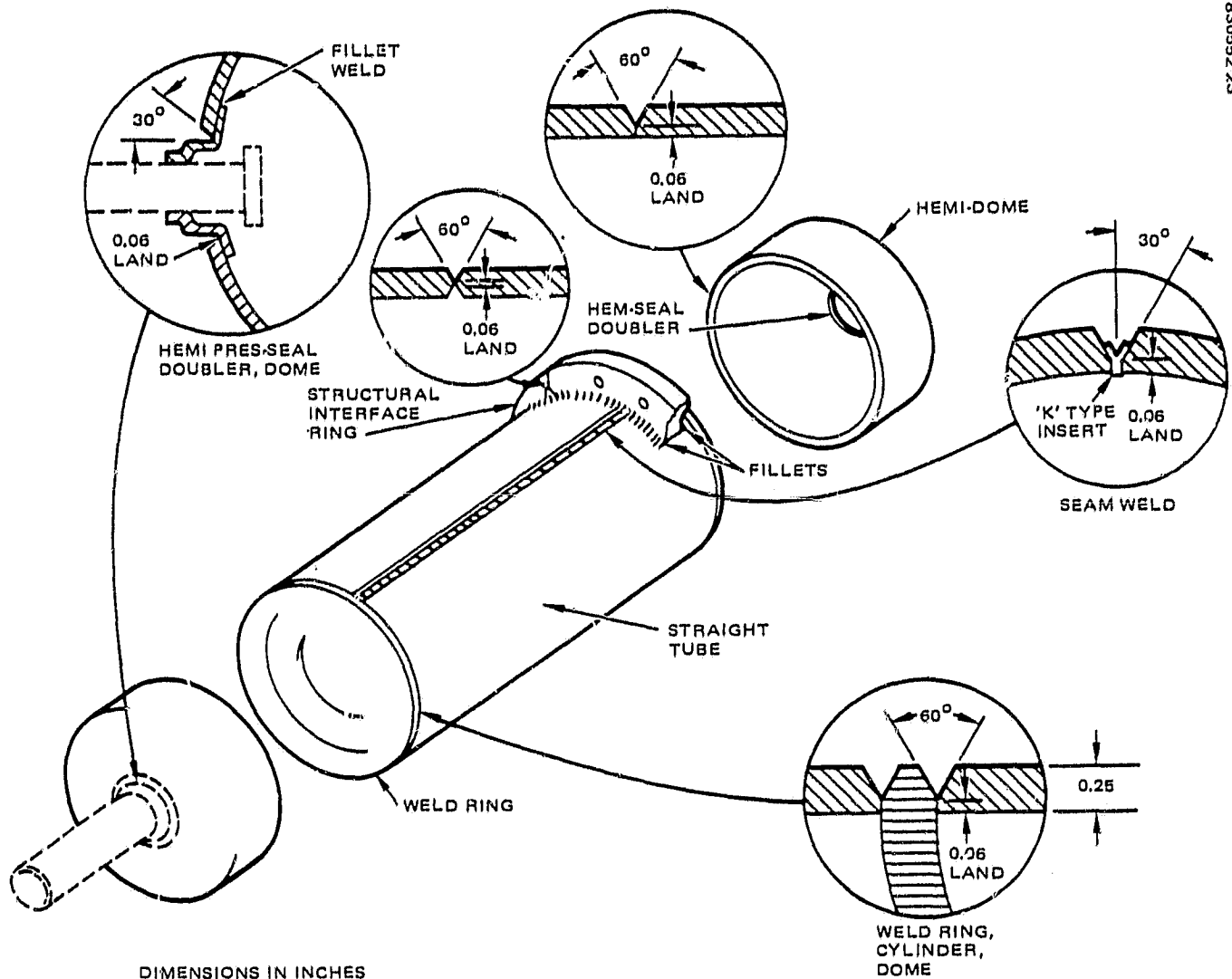


FIGURE 18. PRESSURE VESSEL WELD DESIGN

3.9 INSTRUMENTATION

The purpose of the bipolar battery instrumentation package is to provide information to the battery control system to maintain the battery-stack temperatures within their specified limits and to manage the electrolyte distribution in the stack. Instruments to measure the following quantities are required:

- 1) H_2 gas pressure
- 2) Stack and coolant temperatures
- 3) Coolant flow rate
- 4) Electric current and voltage

3.9.1 Pressure

Several pressure-measurement instruments are available commercially. Transducers are good for this application because they provide an electrical output which can be employed to initiate a control function. For example, Validyne Engineering Corporation, Chatsworth, California, manufactures a variety of diaphragm-type variable-magnetic reluctance transducers with ac or dc output, along with associated electronics. Its P300A absolute pressure transducer has a line pressure range of 0 to 3200 psia, is compatible with measures 1-3/8 by 1-5/8 by 4-1/2 inches, and weighs 16 ounces.

3.9.2 Temperature

Several temperature measurement instruments are available commercially. Thermocouples, thermistors, or RTDs are desired for this application because they provide an electrical output which can be employed to initiate a control function. The required temperature range is nominal room ambient, so that commercially available flight instruments should suffice. For example, Omega Engineering, Inc., Stamford, Connecticut, distributes a thermocouple and thermistor equipment consistent with this application. Fine spatial resolution and fast response are required for accurate temperature measurements.

3.9.3 Flow Rate

For liquids, such as water and KOH, a turbine flow meter, which measures the flow rate through the angular speed of this turbine, is the best choice for accurate flow control. As an alternative, instead of using a flow meter with the liquid-cooled scheme, it might be advantageous to calibrate the flow system in a laboratory and use this laboratory calibration to deduce the flow rate in space flight. For example, the mass flow rate can be deduced by measuring the velocity at constant density. The velocity in turn can be measured with a hot wire probe. Alternatively, because the flow rate through the cooling plate is a monotonic function of the coolant pressure drop across

the cooling place, the flow rate can be deduced by a measurement of the difference between the cooling plate outlet and inlet pressures. Such flow indirect measurements are done routinely at Hughes for actively cooled flight systems.

3.9.4 Electronic Current and Voltage

To monitor bipolar battery performance flight qualified high voltage and current systems could be used.

3.10 ELECTROLYTE AND OXYGEN MANAGEMENT

3.10.1 Shunt Currents Through Electrolyte Bridges

A universal problem of series connected CPV or bipolar stack designs is the presence of shunt currents through electrolyte bridges connecting unit cells. A voltage applied across such a bridge will most likely be well over the electrolyte decomposition voltage in a nickel-hydrogen cell. Therefore, a shunt current always flows through the bridge until the cells connected by the bridge are totally discharged. This shunt current can create a number of technical difficulties in a bipolar cell depending on the magnitude of the current:

- 1) Unbalanced charge distribution among bipolar repeating units that could result in reversal or overcharge of some unit
- 2) Uneven distribution of KOH concentration and amount of electrolyte among unit cells due to K⁺ ion migration
- 3) Uneven distribution of water vapor pressure and oxygen evolution due to unbalanced KOH concentration
- 4) Uneven heat generation caused by oxygen evolution

These issues are similar to those identified in common pressure vessel nickel-hydrogen cells. ⁽⁴⁾

Ion migration, which could play a key role in bipolar battery degradation in the presence of electrolyte bridges, occurs because of the difference in the transference number of K⁺ ion (0.22) and OH⁻ ion (0.78). It means that 78 percent of the total current through the electrolyte bridge is carried by OH⁻ ions 22 percent of the current is carried by K⁺ ion migration. The next long term result of these processes is the creation of uneven electrolyte conditions in the cell stack and an unacceptable self-discharge rate.

Because of these potential problems, prevention of the shunt current through electrolyte films is an important consideration for the design of a long life bipolar nickel-hydrogen battery. Although these difficulties need to be investigated in conjunction with large bipolar battery design efforts, it appears that a satisfactory design solution is feasible in view of positive

test results obtained from smaller CPV nickel-hydrogen modules⁽⁵⁾ which demonstrated 5000 cycles without exhibiting shunt currents in multistack configurations.

3.10.2 Electrolyte Dryout and Reservoirs

A potential difficulty associated with the operation of bipolar nickel-hydrogen batteries is electrolyte dryout. It will be encountered in cells with an insufficient amount of electrolyte for normal performance of a cell over its useful life. This situation can develop as a result of the following factors:

- 1) Nickel electrode expansion
- 2) Electrolyte transfer outside of a unit cell by mechanical means, e. g. , by entrainment in H_2 gas
- 3) Electrolyte dryout by evaporation due to localized heating
- 4) Poor oxygen management

Mechanically induced electrolyte dryout depends on stack design and can be prevented easily. The success that CPV modules had,⁽⁵⁾ indicates that a bipolar battery could be operated for long periods without such problems.

The most serious of the previously outlined factors contributing to dryout, however, is believed to be the nickel electrode expansion. Electrode expansion in excess of 50 percent has been observed after 6100 cycles of an accelerated LEO cycle at 80 percent depth-of-discharge at 40°C. Possible solutions could control expansion by additives and by reduced loading. An alternative approach could provide an extra electrolyte reservoir in the individual unit cells as it has been done in state of the art nickel-hydrogen cells.

The structure of reservoir should be such that it retains excess electrolyte during launch, but gives it up easily when the positive electrode needs it. Such a condition can be achieved by selecting a reservoir material such as Zirconium oxide cloth or porous nickel which has pores larger than those of the positive electrode. The long term interactions between the electrodes and the reservoir, specifically as they are being applied in bipolar cells, deserve further study in future nickel-hydrogen battery development programs.

3.10.3 Electrolyte Maldistribution

Maldistribution of electrolyte among individual unit cells of series connected stacks can be developed by several different mechanisms. These include shunt currents, entrainment by hydrogen and oxygen gas, evaporation and condensation of water vapor, and uneven recombination of oxygen. All of these can be prevented by adequate mechanical design and appropriate thermal management. However, these phenomena require sophisticated and accurate modeling in conjunction with the oxygen management system of any future bipolar cell design.

3.11 OXYGEN MANAGEMENT

Potential oxygen mismanagement difficulties in series connected bipolar cells are caused by oxygen which is evolved in one cell and migrates to the other through the common gas space to be recombined in an unbalanced manner in another cell. This problem could cause preferential dryout of one cell and flooding of the other. This imbalance in turn could lead to capacity and voltage performance imbalances among individual cells resulting in a positive feedback loop which in time will lead to cell failure. A solution to this problem, demonstrated at NASA's Lewis Research Center, confines oxygen inside individual cells by recombining it with hydrogen before it leaves the cell. Such a recombination device is provided in the bipolar cell design concept described in this report. However, the evaporation of water from the recombination strips to the electrode requires further study of transport mechanisms beyond the scope of this effort before accurate life predictions can be made for bipolar cells or batteries using this oxygen management system.

The analytical considerations which will need to be addressed during future design efforts are outlined in Tables 3 and 4. They include the following:

- 1) Cyclic variation in hydrogen and oxygen concentrations in the gap surrounding each recombination wire
- 2) Cyclic temperature variation of the adjacent electrode and bipolar plate surfaces
- 3) Characteristics of the heterogeneous reaction at the platinum surface (for example, influence of pressure and temperature on the chemical rate constant)
- 4) Influence of temperature and pressure on diffusion factors, heat of reaction, and thermal properties of teflon.
- 5) Specification of thermal and fluid boundary conditions at the outer surface of the teflon coating (conduction diffusion in stagnant volume, convection, and radiation)

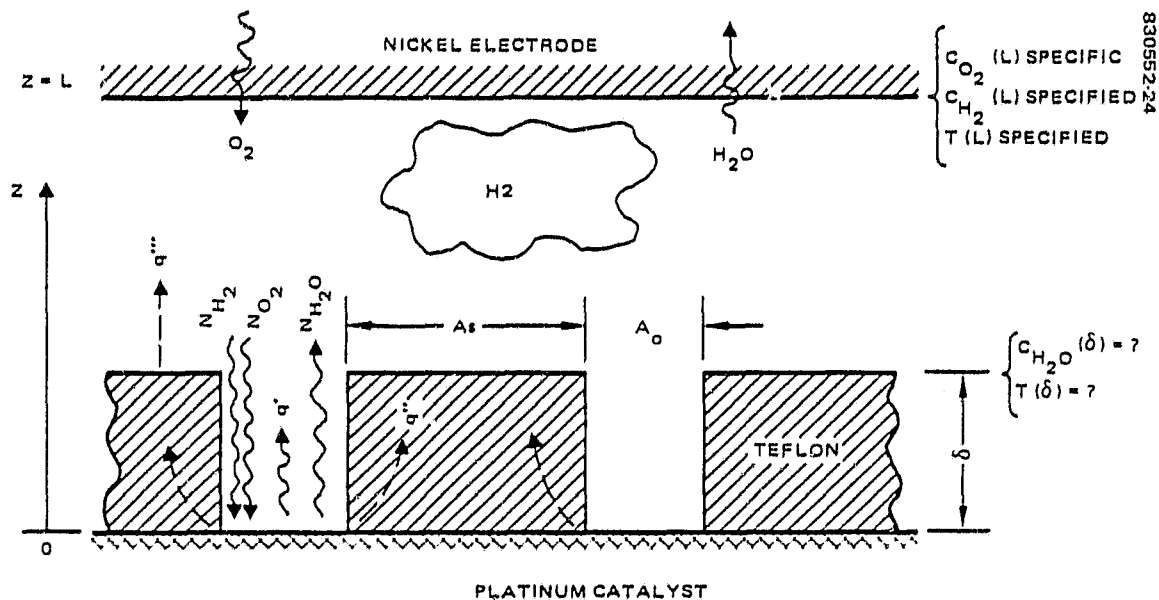
As shown in Figure 19 the thermal boundary condition at the porous teflon/platinum interface may be represented as an energy balance between the heat of reaction based on the exposed platinum area and heat losses by conduction through the nonporous teflon and by combined gas conduction and mass transfer through the pores. The governing equations of coupled heat and mass transfer appropriate to the proposed geometry may be formulated for a one dimensional, radial coordinate system. These equations with proper boundary conditions should be solved using teflon coating porosity and thickness as parameters. The solution may be found in closed form if nonlinearities and mass/energy coupling are not critical or by simple numerical integration if greater realism is required.

TABLE 3. RECOMBINATION STRIP MODELLING ASSUMPTIONS

Dilute concentrations of O_2 and H_2O in H_2
 Diffusivities, $D(O_2, \text{mix})$, and $D(H_2O, \text{mix})$ known
 Reaction rate coefficient, k_n'' ($O_2:H_2O$), known
 Fick's law diffusion of O_2 and H_2O species through stagnant layer of H_2
 Heat of reaction, $\Delta h(O_2:H_2O)$, known
 Energy released by reaction at catalyst surface transported through solid TFE by conduction and through gas mixture by combined conduction and mass/enthalpy transfer
 Isothermal catalyst surface and adiabatic pore walls
 Specified concentrations and temperature at surface of nickel electrode

TABLE 4. RECOMBINATION STRIP DESIGN MODELLING PROCEDURE

<u>Step</u>	<u>Action</u>
1	Calculate molar flux N_{O_2} of O_2 recombining at catalyst surface, A_o
2	Heat balance at catalyst surface: $A_o N_{O_2} \Delta h = A_o q' + A_s q''$
3	Calculate concentration $C(H_2O, \delta)$ and temperature, $T(H_2O, \delta)$ of H_2O at open end of pore
4	Calculate temperature, $T(TFE, \delta)$, of teflon at gas-solid interface
5	Find partial pressure and corresponding saturation temperature of H_2O at open end of pore: $P_{H_2O}(\delta)$, $T_{sat}(H_2O, \delta)$
6	Verify condensation occurs at the TFE surface if $T(TFE, \delta) < T_{sat}(H_2O, \delta)$
7	Control $T(TFE, \delta)$ by proper design of A_o , A_s , and δ



NOMENCLATURE

A_o	OPEN AREA IN TFE COATING
A_s	SOLID (NON-POROUS) AREA IN TFE COATING
$C_{O_2}(Z)$	MOLAR CONCENTRATION OF O_2 AT LOCATION Z
$C_{H_2O}(Z)$	MOLAR CONCENTRATION OF H_2O AT LOCATION Z
L	GAS DISTANCE BETWEEN CATALYTIC SURFACE AND ELECTRODE SURFACE
N_{H_2}	MOLAR FLUX OF H_2
N_{O_2}	MOLAR FLUX OF O_2
N_{H_2O}	MOLAR FLUX OF H_2O
q'	HEAT TRANSFERRED BY GAS CONDUCTION AND MASS TRANSFER THROUGH A_o
q''	HEAT TRANSFERRED BY SOLID CONDUCTION THROUGH A_s
q'''	HEAT TRANSFERRED BY GAS CONDUCTION ABOVE A_s
$T(Z)$	TEMPERATURE A LOCATION Z
δ	THICKNESS OF TFE COATING
Z	COORDINATE MEASURED FROM CATALYTIC SURFACE

FIGURE 19. OXYGEN RECOMBINATION SITE MODEL

An analysis along these lines could be instrumental in determining a design with suitable O_2 recombination conditions in the bipolar cell stack and establishing whether anomalous conditions created during cell operation could cause localized flooding of the recombination sites.

3.12 THERMAL MANAGEMENT

Inefficiencies associated with bipolar battery operation will generate a substantial amount of heat within the stack. For example, during charge and discharge to 80 percent DOD in a low earth orbit, instantaneous heat generation varies in a 75 A-hr, 275 volt bipolar battery system from approximately 18 kW (60,000 Btu/hr) at the end of discharge to zero during more than half of the charge required and approximately 52 kW (180,000 Btu/hr) by the end of charge. The orbital average of heat release is approximately 10 kW (36,000 Btu/hr). The thermal management system, shown schematically in Figure 20, removes this heat in a controlled way by minimizing the temperature swing to an optimum 0 to 30°C range. Complete failure of the system could result in an overheating-caused temperature rise of 70°C/cycle.

The removal of waste heat can be accomplished directly through the spacecraft radiator to which the bipolar battery could be coupled either directly, i.e., by circulating the same coolant through the battery and radiator, or indirectly by coupling an independent spacecraft cooling system to the battery through an interface heat exchanger. Both of these approaches require the implementation of an independent, fluctuating, pressurized liquid circulation and battery heat rejection system or the structural reinforcement of the cooling passages within the stack to withstand the instantaneous pressure differential between the spacecraft coolant and hydrogen gas environment. The use of an interface heat exchanger could allow easier control and integration of the battery design into the spacecraft.

To allow accurate temperature projections within the bipolar battery stack, the battery stack and coolant flow concept were modelled as a transient, lumped-parameter thermal network using proprietary Hughes software. A transient model is required to account for the time variant battery power dissipation profile and to avoid excessive system weight inherent in a steady state design. The symmetry of the stack/coolant passage geometry allows the use of approximately 50 nodes in the thermal network to calculate stack and coolant temperatures at approximately 20 locations each. The required inputs to the thermal analyzer code are heat capacity (product of mass and specific heat), conductances (solid-to-solid and solid-to-fluid), coolant inlet temperature, coolant flow rate, and transient nodal power dissipation. The outputs are transient nodal temperatures. Changes in type of coolant, geometry, flow rate, etc, are accomplished by appropriate changes of conductances, capacities, and boundary conditions.

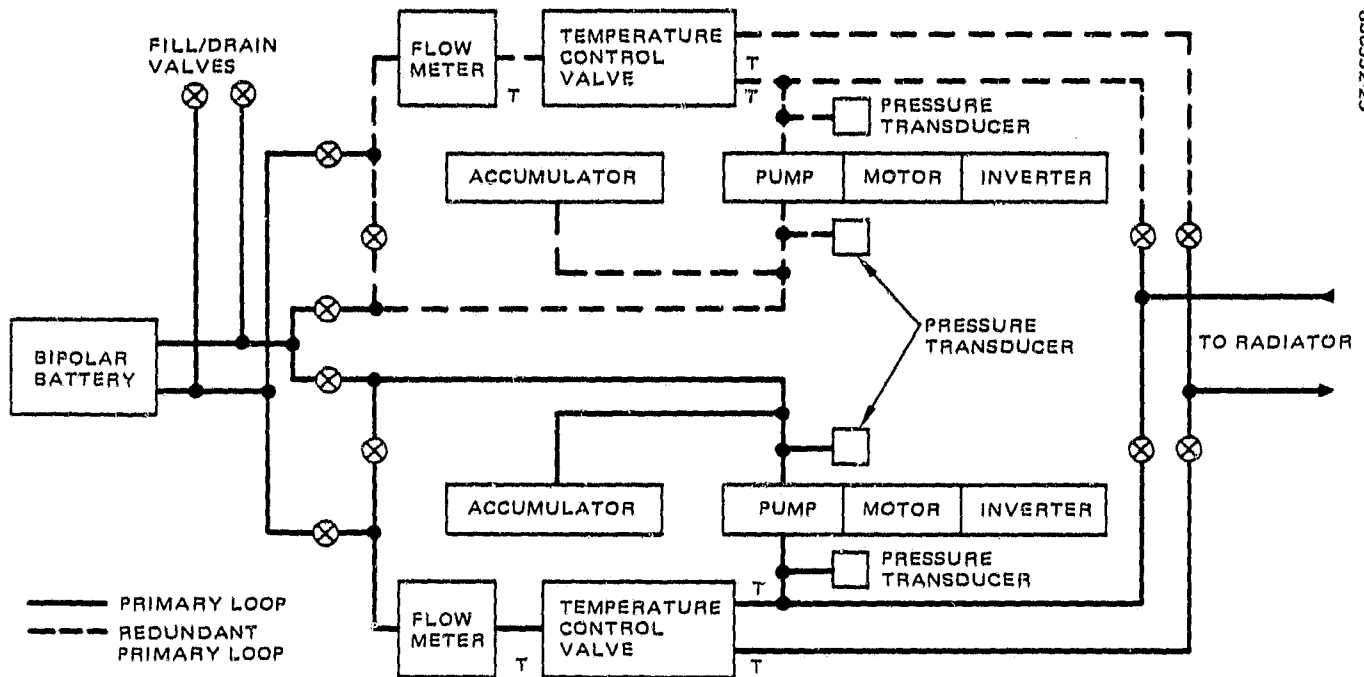


FIGURE 20. FULLY REDUNDANT LIQUID-COOLED THERMAL MANAGEMENT SYSTEM

The thermal network used to model the design relied on a 23-node transient TAP-3 network stack subassembly (Figure 21). Because of symmetry, only a 90° sector of the stack subassembly has to be modelled. The stack was modelled by two 11-node layers and simulated the cooling plate and coolant film coefficient corresponding to the anticipated coolant flow rate. The battery stack properties were modelled as an equivalent uniform, but nonisotropic medium having parallel and perpendicular thermal conductivities of 0.934 and 0.0868 Btu/hr/ft/°F respectively and a specific heat of 0.183 Btu/lb/°F. A larger thermal conductivity is being used for the thermal connectors in the plane of the cooling plate than for those in the direction perpendicular to the cooling plate. The dissipation per unit volume is assumed to be uniform at any instant.

Figure 22 shows the temperature distribution in the stack as a function of time was calculated for a typical 80 percent DOD low earth orbit heat-generation profile. As shown in this example, in which the coolant flow rate is constant, the difference between the maximum and minimum temperatures continues to increase after the dissipation ceases. This occurs because of the close proximity of the minimum temperature point to the cooling plate which causes the minimum temperature to decrease faster after the heat generation ceases than does the maximum temperature. In view of this result, it might be advantageous to vary the coolant flow rate as a function of time.

Preliminary evaluation of the liquid cooled bipolar battery design indicates that sufficiently uniform temperature distributions can be maintained within a bipolar stack to assure nominal operating conditions in a low earth orbit.

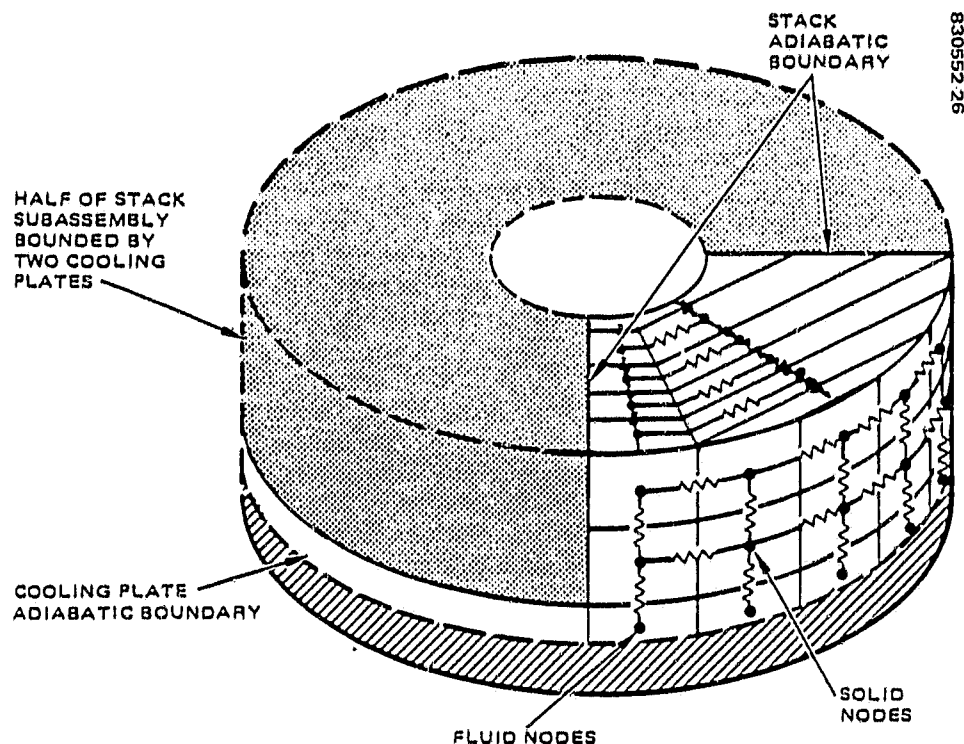


FIGURE 21. LIQUID-COOLED STACK THERMAL NETWORK MODEL

3.13 PERFORMANCE PROJECTIONS

The bipolar nickel-hydrogen battery configuration evolved as a result of intensive computerized optimization studies conducted on this contract. This subsection describes the proprietary bipolar battery optimization computer software developed to accommodate the design evolution. The computer model deals primarily with the relationships between 85 compatible independent physical parameters and 123 dependent battery design and performance parameters. Examples of these are weight, volume, watt-hours per unit weight, etc. The program incorporates factors related to the electrochemical performance of the stack, such as capacity versus plate density and utilization and compressibility of hydrogen gas related to free volume for both low earth and geosynchronous orbit battery operation.

The thermal performance of each battery design in a given orbit is calculated within the program, and the results are used to calculate flow rates and distribution pressure drops for a liquid-cooled system. To maintain the maximum degree of simplicity, each section uses only results obtained in a prior section, and there is no looping of logic. Therefore, it is relatively simple to update any stage so that the most current method of analysis or configuration may be used. The design optimization process is broken into ten sections addressing specific areas of battery design.

830552-27

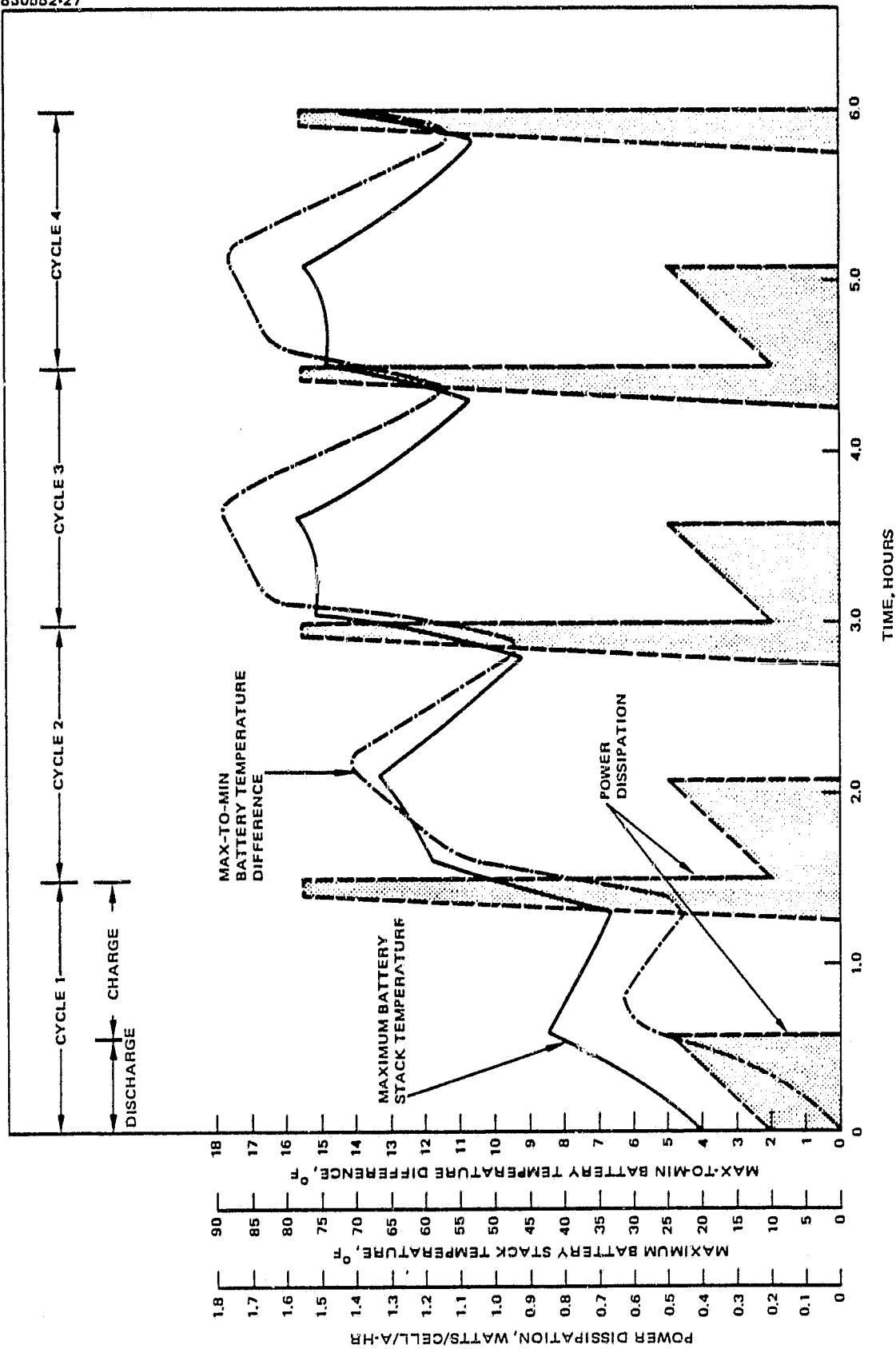


FIGURE 22. PRELIMINARY THERMAL ANALYSIS RESULTS OF LIQUID-COOLED STACK SUBASSEMBLY

The input to the program is via keyboard in a conversational mode with only the changes from the baseline to be typed. The program allows for any two of the input variables to be varied from a lower limit to an upper limit in specified increments, and the result is plotted as a function of any one of the output variables. The values of the selected input parameter and all output parameters for each case are printed out for later reference. In its present form, this program can be a valuable design tool.

By using this computer program the battery designer can ensure the development of an optimized bipolar battery design. Specific energy and energy density can thus be optimized in relation to component geometry and specifications, voltage, and operating pressure. This battery optimization software package was exercised during the design effort. Figures 23 and 24 show the dependence of bipolar battery specific energy on battery voltage capacity and positive electrode thickness. Figure 25 shows the effect of battery operating pressure on energy density. Required cooling system flow rates, pressure drop, and pumping power as a function of battery voltage and capacity are shown in Figure 26.

3.14 DEVELOPMENT REQUIREMENTS

This preliminary engineering effort shows that a viable high voltage high capacity bipolar nickel-hydrogen cell could be configured with proper development for use in large power systems. The optimization studies indicate, as described in Section 4, that such a system could offer potential weight savings vis-a-vis the state of the art nickel-hydrogen technology.

The bulk of the development effort associated with future implementation of this concept is going to be related to the scale-up of established nickel-hydrogen and fuel cell components to the specific requirements of bipolar cells. In addition to enabling the large scale demonstration of bipolar battery technology, these developments will substantially enhance the performance of state of the art IPV nickel-hydrogen cells and CPV modules.

To facilitate the successful development of a bipolar battery, future efforts should emphasize the following aspects of battery and nickel electrode design:

- 1) Battery Design
 - a) Electrolyte bridging elimination
 - b) Electrolyte entrainment reduction
 - c) Optimization of electrolyte reservoir designs for reservoir capacity, pore size distribution, electronic conduction, and accommodation of nickel electrode expansion
 - d) Reduction or elimination of oxygen migration from the individual cell units

2) Positive Electrode Design

- a) Sinter structure optimization in terms of pore size and mechanical strength
- b) Active material loading optimization for the best cycle life
- c) Development and evaluation of gridless nickel electrodes
- d) Development and evaluation of thicker nickel electrodes for improved energy density and reduced cost which include plaque fabrication techniques and active material impregnation methods

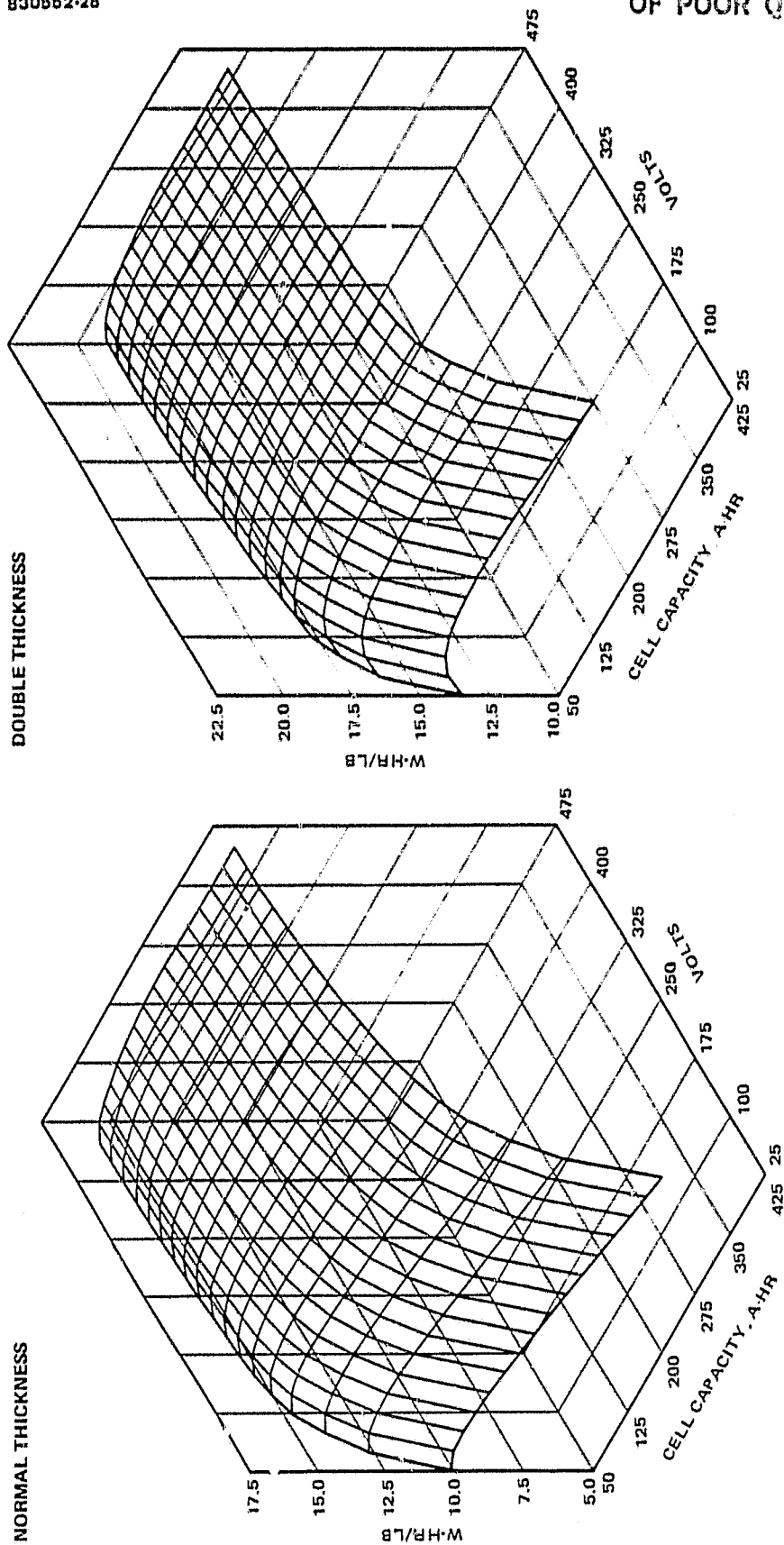


FIGURE 23. BIPOLAR BATTERY SPECIFIC ENERGY VERSUS CELL CAPACITY VOLTAGE AND POSITIVE ELECTRODE THICKNESS

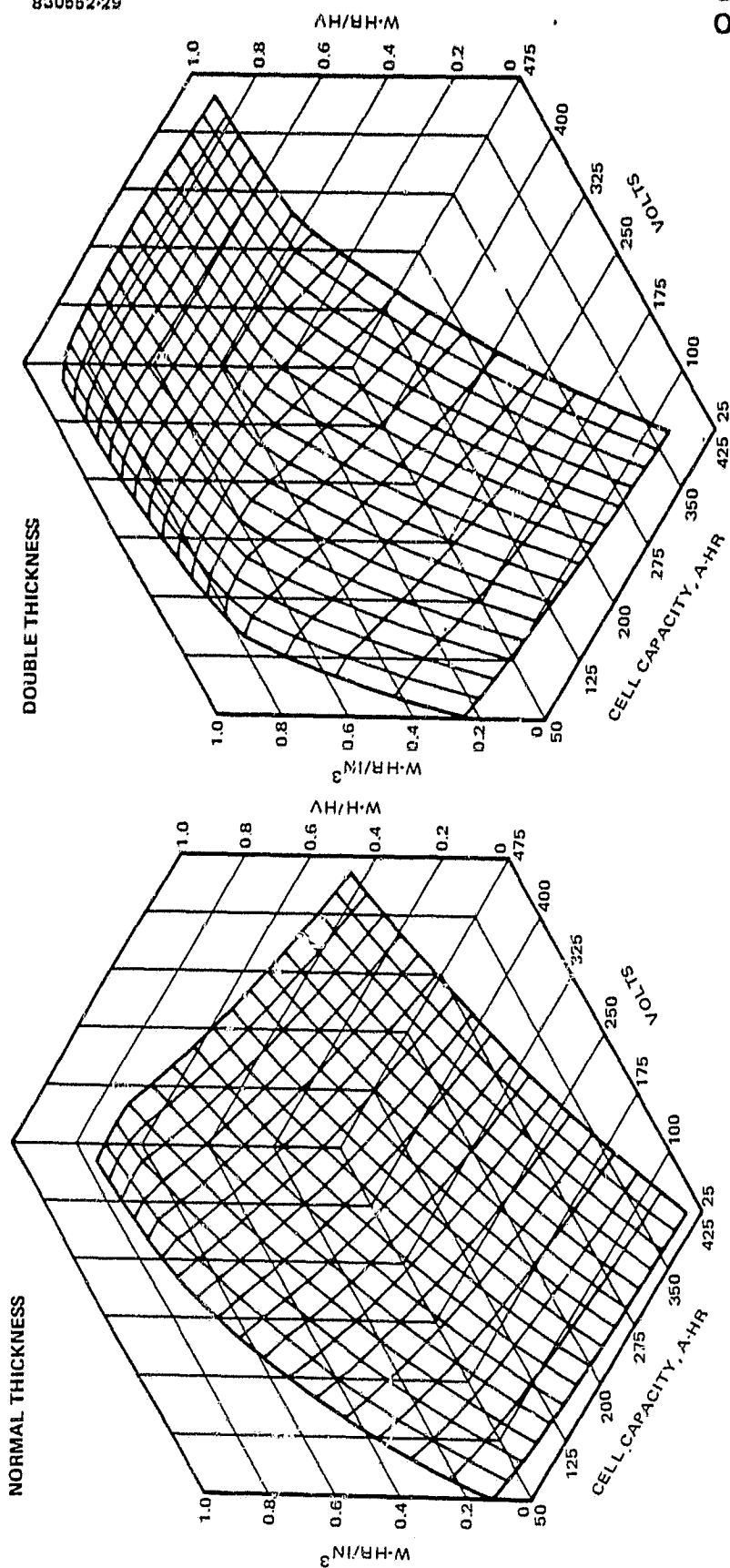


FIGURE 24. BIPOLAR BATTERY ENERGY DENSITY VERSUS CELL CAPACITY VOLTAGE AND POSITIVE ELECTRODE THICKNESS

830552-30

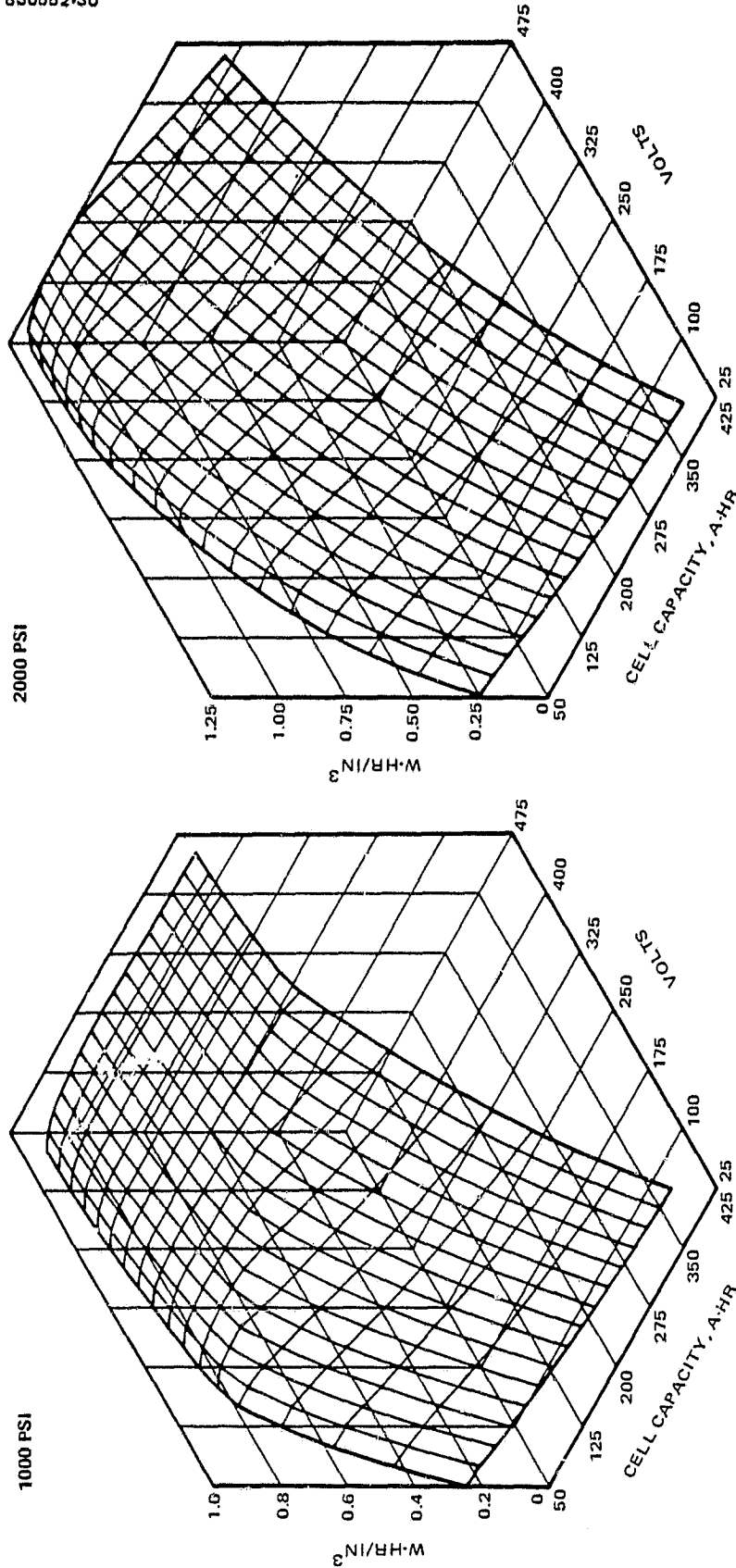
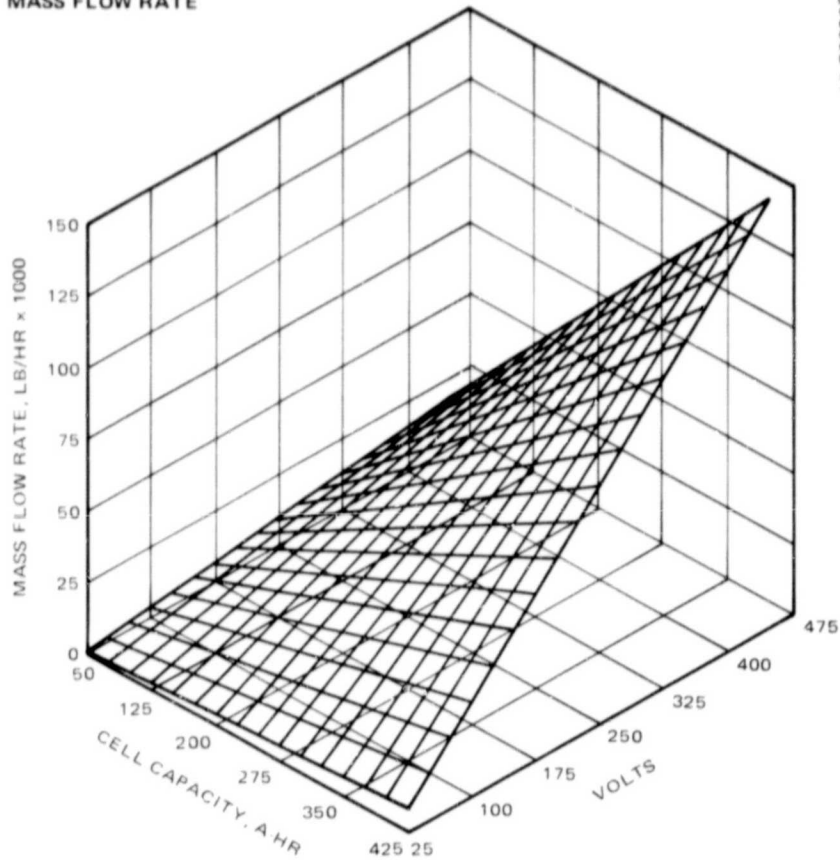


FIGURE 25. EFFECT OF OPERATING PRESSURE ON ENERGY DENSITY

MASS FLOW RATE



830552-31

LAMINAR PRESSURE DROP

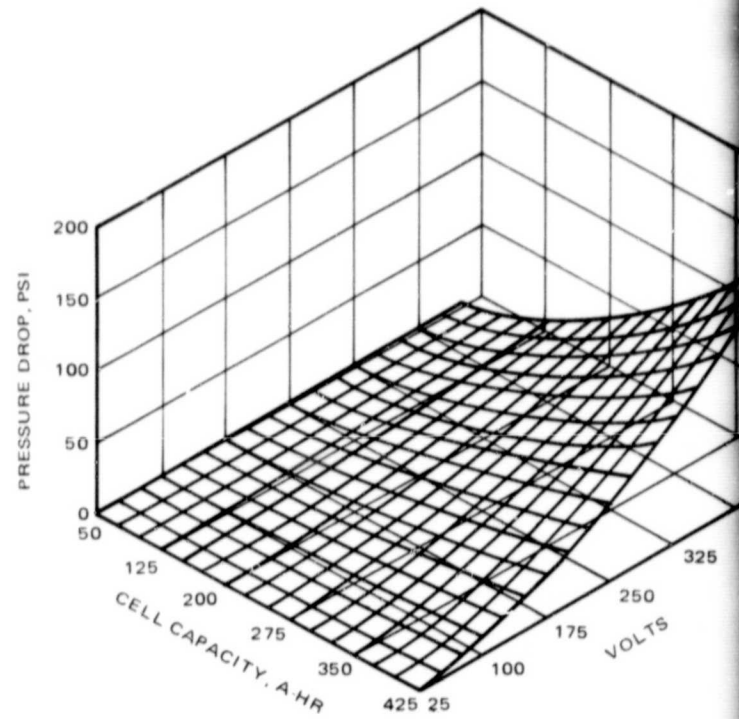


FIGURE 26. PROJECTED BIPOLAR BATTERY COOLING SYSTEM CHARACTERISTICS

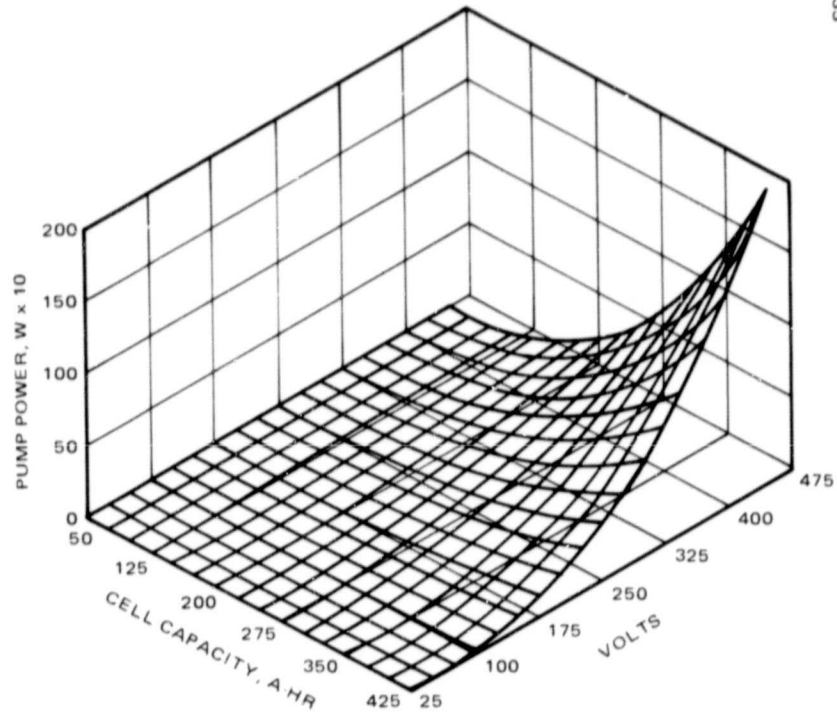
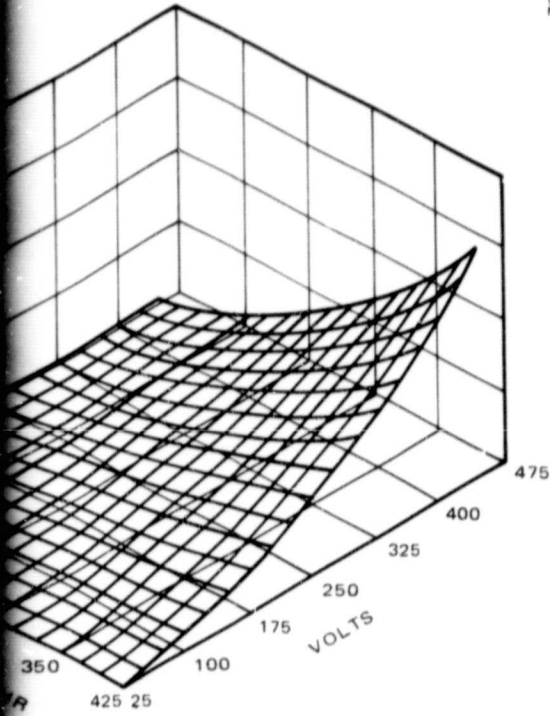
FOLDOUT FRAME

ORIGINAL PAGE IS
OF POOR QUALITY

LAMINAR PUMPING POWER

830552-32

830552-33



FOLDOUT FRAME

4. SPACECRAFT INTEGRATION

Battery system weight and launch vehicle limitations have been a principal deterrent to the implementation of high power output aerospace electrical power systems. However, with the advent of Space Transportation System (STS), larger spacecraft are under development for NASA and military use. One of these missions and the potential benefits it could accrue from the utilization of bipolar nickel-hydrogen batteries is described below.

4.1 BASELINE MISSION

In one of its configurations, the selected baseline Air Force mission is designed for solar array/battery-load-sharing during peak loads occurring during either daylight or eclipse. To do this, the spacecraft relies on eight sodium-sulfur batteries of 84 cells, each rated at 80 A-hr. The battery terminal voltage during discharge varies from 135 to 174 volts dc. A discharge regulator processes the variable voltage battery power to a constant 180 ± 3 volts dc for the radar load, and a battery charger reduces the solar array voltage to the battery level. These two power processors allow the battery to operate at a lower voltage than the distribution bus. Additionally, two 16-cell, 50 A-hr nickel-cadmium batteries are utilized for a 28-volt spacecraft housekeeping loads that are at a distance of 350 feet from the payload batteries. A block diagram of the electrical system is shown in Figure 27.

The satellite operates in a 5600 n.mi., 6-hour orbit and its solar array/battery system is sized to meet a 55 kW peak load with 31 kW, provided by the solar array and the remainder from the batteries. Payload operation occurs during only half the orbit, so almost the full solar array is available for 3 hours of battery charging. The stored electrical energy delivered to the load is approximately 52 kW/hr.

The bipolar nickel-hydrogen battery cannot compete on a weight and cost basis with the predicted performance of the sodium-sulfur energy storage system. However, before the sodium-sulfur technology is available for spacecraft use, several technical problems will have to be solved. The long term resolution of these problems, if possible, may require considerable time in view of the current pace of the development effort. Therefore, a nickel-hydrogen battery could be an attractive near term possibility for lower resolution radar satellites.

PRECEDING PAGE BLANK, NOT FILMED

ORIGINAL FIGURE 19
OF POOR QUALITY

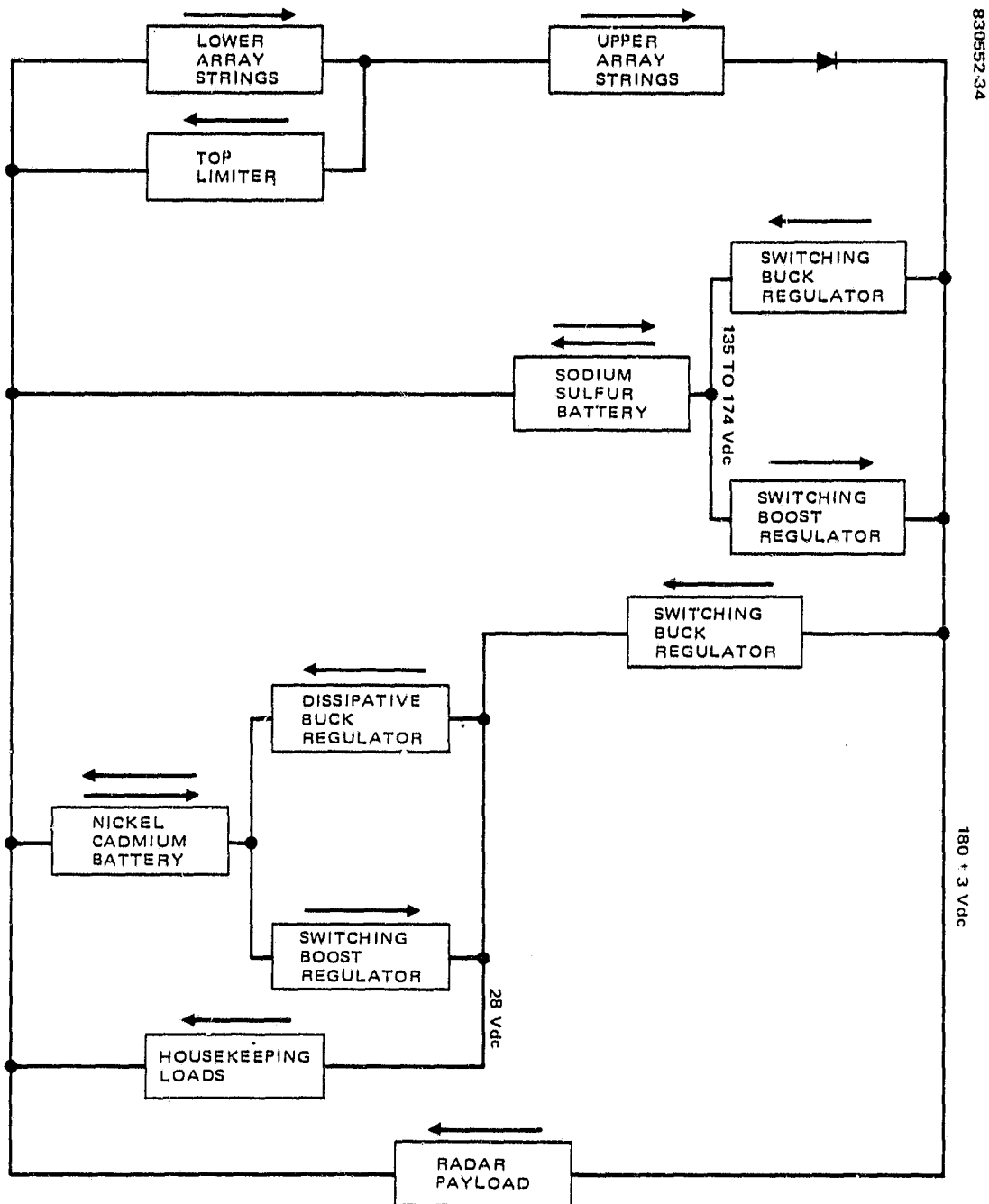


FIGURE 27. BASELINE SATELLITE POWER SYSTEM

Table 5 presents a comparison between the system level characteristics associated with candidate Ni-H₂ battery designs shown in Figure 1. Four bipolar batteries would replace 100 CPV modules or 600 IPV cells having similar functional capabilities.

4.2 INDIVIDUAL PRESSURE VESSEL CELL INTEGRATION

The integration of IPV cells into a battery relies on a pack concept shown in Figure 28. Twenty IPV cells are mounted to a 2.5 cm thick aluminum honeycomb assembly to form a battery pack. Five battery packs make up one annular shelf; six shelves are needed to satisfy baseline mission requirements.

Thermal control could be provided by a redundant pumped two phase ammonia system. Figure 29 presents a schematic diagram of such a system. This system requires an operating pressure of about 10 atmospheres to maintain the nominal battery temperature at 20°C. The 1.25 cm I.D. aluminum pipes are bonded to each battery array in a circuitous manner (Figure 30), with the redundant pipe path staggered relative to the previous coolant loop. Each evaporator pipe traverses every shelf twice in a serpentine path.

In this concept, the radiator is integrated into the spacecraft skin. The 1.25 cm I.D. aluminum pipes are bonded to the inner surface of the spacecraft skin in a helical configuration with a pitch of 15.2 cm. The required length of each fluid loop condenser pipe is estimated as 100 m (15 kg wet weight). Each fluid loop thermal control system therefore requires 300m of pipe and a pump package with approximately 3.1 watts of pump power at 25 percent efficiency.

TABLE 5. BASELINE SATELLITE NICKEL-HYDROGEN BATTERY DESIGN CHARACTERISTICS

Design Characteristics	IPV	CPV	Bipolar
Energy to load, kWh	52	52	52
Nominal voltage, V	170	170	170
Nominal DOD, %	60	60	60
Max DOD, %	80	80	80
Installed capacity, A-hr	500	500	500
Number of batteries*	4	4	4
Number of cells/battery**	150	150	150
Number of modules/battery	—	25	1

*Meets mission requirements with a failed battery.

**10 percent provided for redundancy.

830552-35

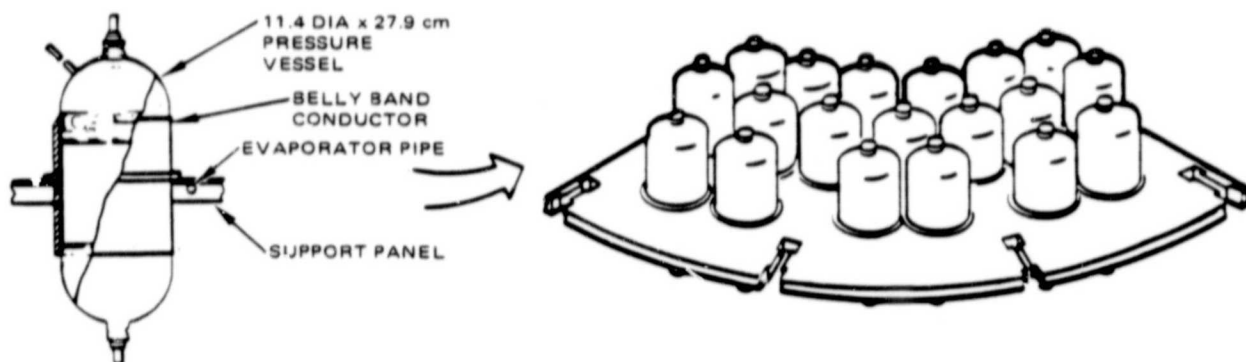


FIGURE 28. INDIVIDUAL PRESSURE VESSEL CELL AND BATTERY PACK CONCEPT

830552-36

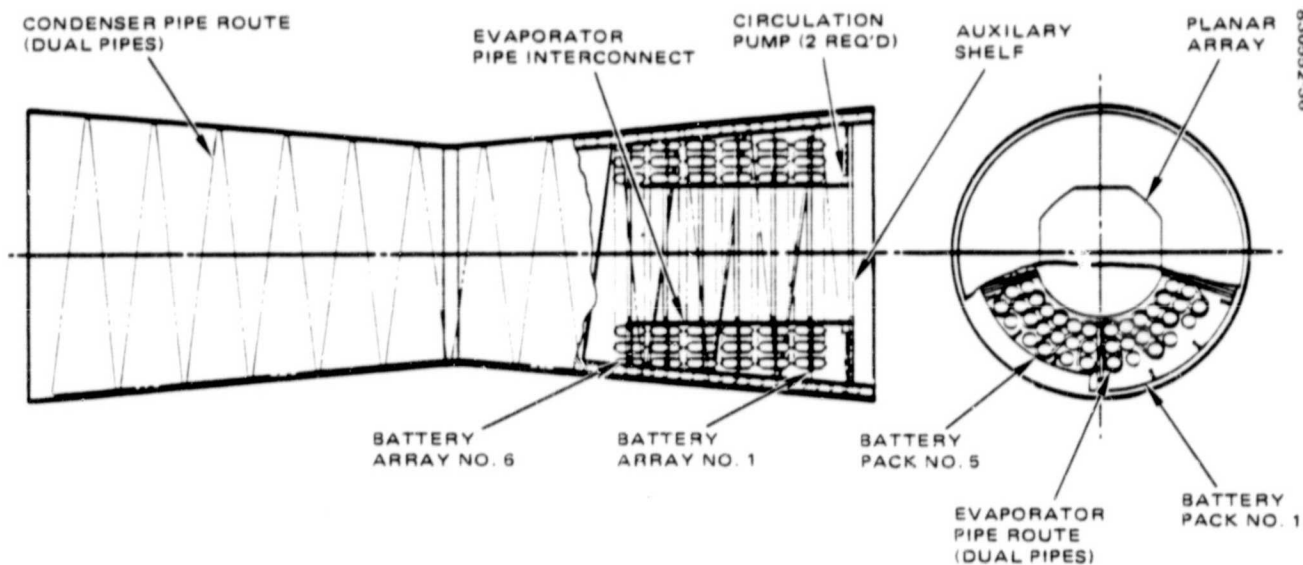


FIGURE 29. TWO-PHASE FLUID LOOP INSTALLATION

830552-37

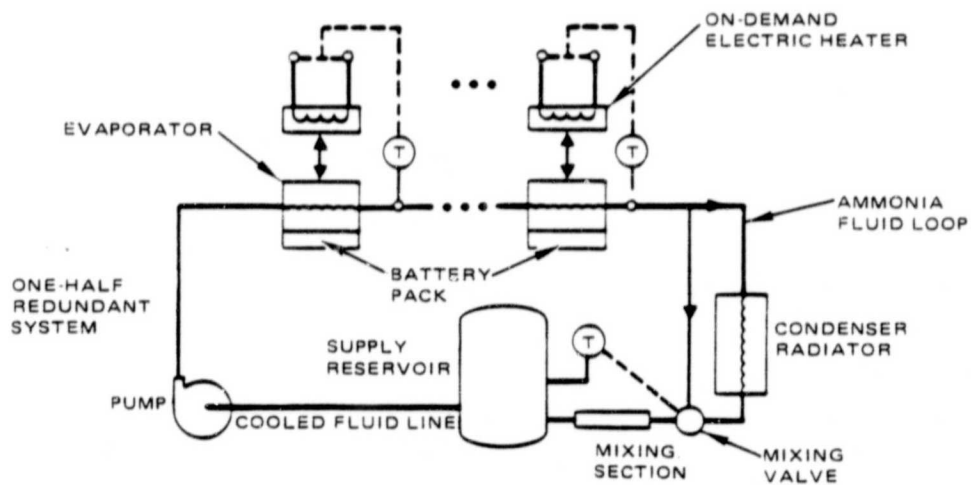


FIGURE 30. TWO-PHASE FLUID LOOP SCHEMATIC

4.3 COMMON PRESSURE VESSEL MODULE INTEGRATION

CPV module integration into the battery pack shown in Figure 31 was designed so that the thermal loads on each shelf match those using IPV cells. Each pack includes four or five CPV modules horizontally mounted on an aluminum honeycomb/facesheet structure to provide more uniform heat conduction along the axial direction. Four packs make up one annular shelf, and six shelves are needed for the three-battery system. The battery shelves are contained in the spacecraft body in a manner similar to that shown in Figure 29 for the IPV design. The horizontal mounting configuration permits closer spacing of the shelves in the CPV design for more efficient use of spacecraft volume. Thermal control is provided by a redundant pumped two-phase ammonia system similar to that shown in Figure 30.

4.4 BIPOLAR BATTERY INTEGRATION

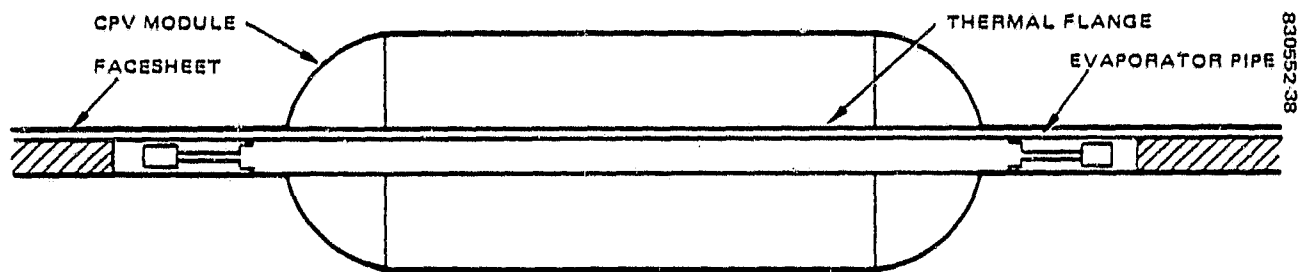
Four bipolar batteries placed along the spacecraft axis could replace the pack/shelf/battery arrays required to support the integration of IPV cells and/or CPV modules into the spacecraft. Due to weight, structures at the spacecraft bipolar battery interface must be designed to sustain and transmit the critical design loads from spacecraft to the battery. The stiffness supplied by the interface structure must be sufficient to maintain a minimum mounting frequency to satisfy the environmental requirements.

The interface structures selected to attach the bipolar battery to the spacecraft consist of rings attached to the spacecraft at two stations (Figure 32). Their cross section can be determined only with knowledge of spacecraft mounting definition. The aft ring, welded to the pressure vessel as described in 3.8, reacts to axial and radial loads; the forward ring, by allowing sliding in relation to the pressure vessel, reacts to radial loads only. This accommodates the changes in pressure vessel dimensions caused by thermal and pressure fluctuations.

The relationship between the bipolar battery and its dedicated radiator system is shown schematically in Figure 33. A preliminary weight estimate of dedicated radiator weight associated with a bipolar battery is shown in Figure 34. Secondary thermal interfaces occur at the surface of the pressure vessel, the structural mounting points, and the electrical terminals, but heat exchanges between the battery and the spacecraft at these locations can be minimized by passive means (e.g., multifoil vacuum thermal insulation). The radiator design considered in Figure 34 is assumed to consist of a helical aluminum tube bonded to the 12-mil aluminum skin of a cylinder. Tube diameters were adjusted to provide turbulent flow heat transfer to the coolant undergoing at 20 °C (45 °F) temperature drop.

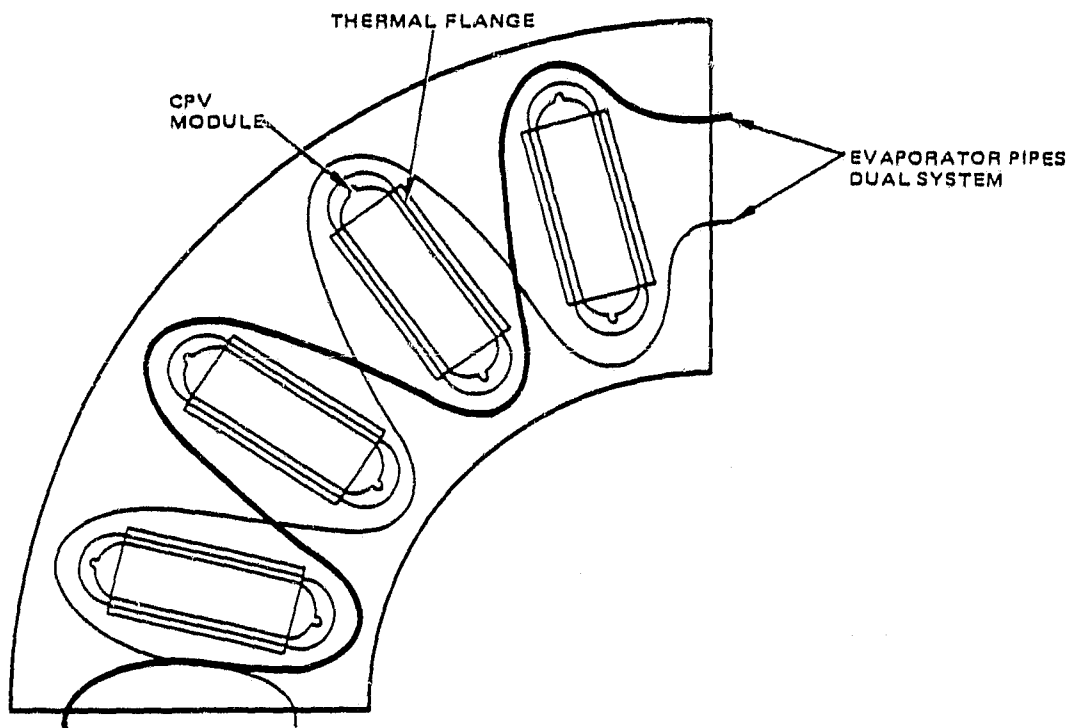
In practice, a radiator system for bipolar batteries would be designed to operate with several cooling loops in parallel by considering tradeoffs between allowable pressure drops and radiator weight control system complexity and reliability, all beyond the scope of this development program.

ORIGINAL PAGE 17
OF POOR QUALITY



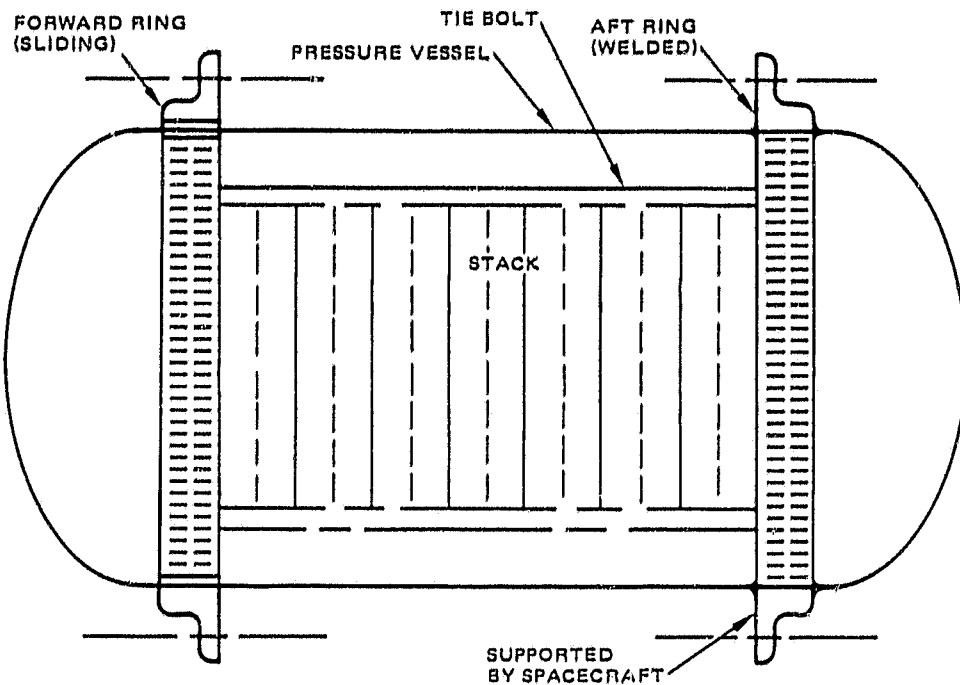
830552-38

a) SIDE VIEW OF CPV MODULE IN PACK



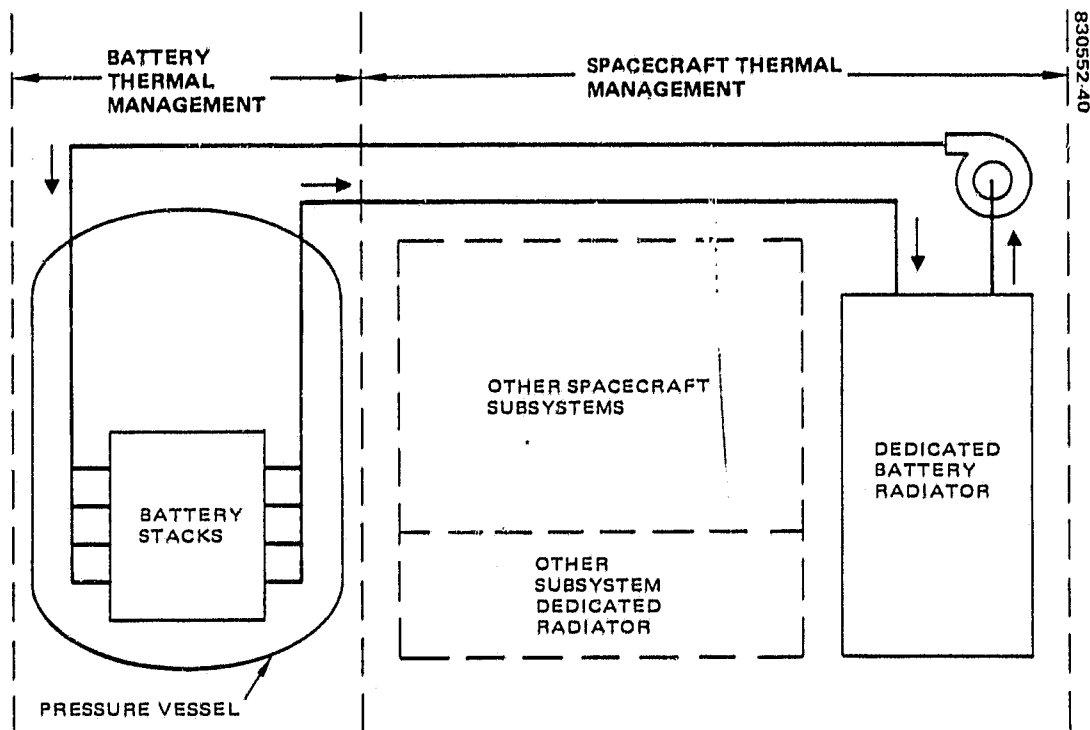
b) TOP VIEW OF PACK

FIGURE 31. COMMON PRESSURE VESSEL BATTERY PACK



830552.39

FIGURE 32. SPACECRAFT BIPOLAR BATTERY INTERFACE RINGS



830552.40

FIGURE 33. THERMAL INTERFACE BETWEEN BIPOLAR BATTERY AND SPACECRAFT HEAT REJECTION SYSTEMS

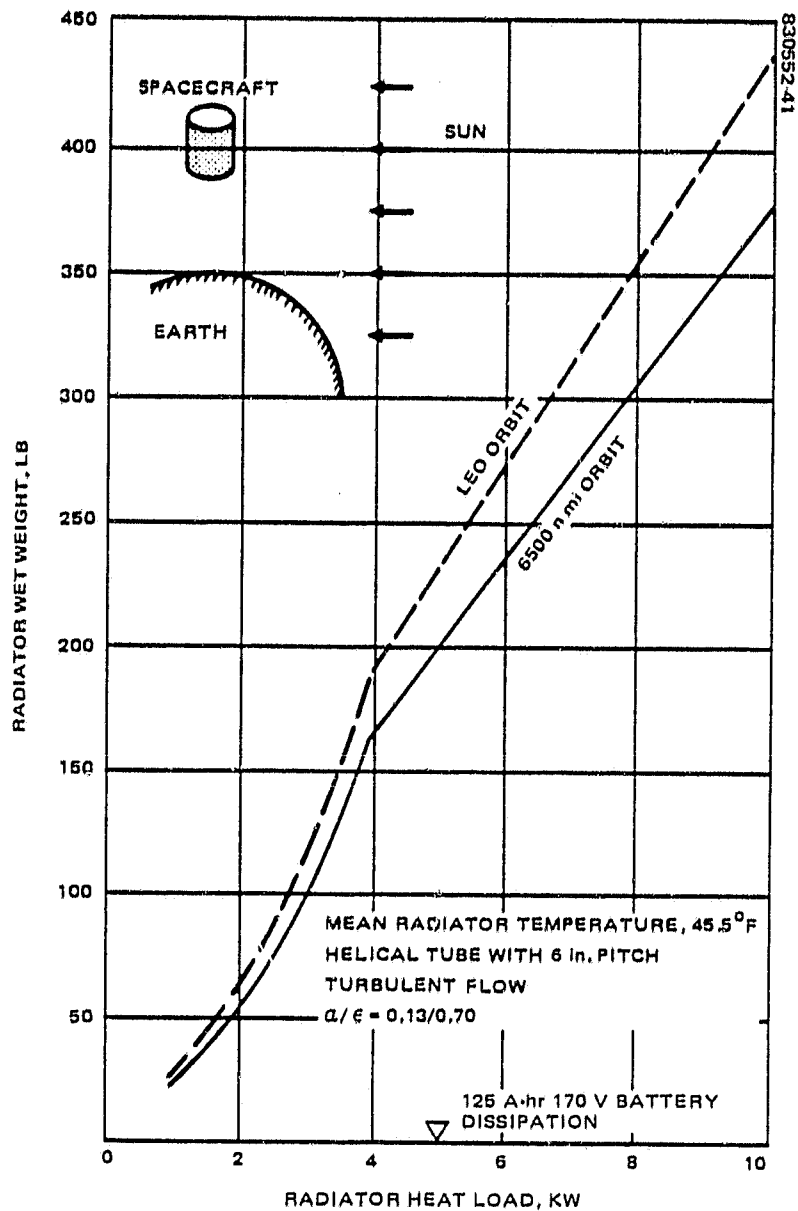


FIGURE 34. CYLINDRICAL SPACECRAFT RADIATOR WEIGHT
VERSUS DISSIPATED POWER

4.5 SYSTEMS COMPARISON

Based on the outcome of the optimization and system integration efforts, bipolar batteries utilizing advanced positive electrode technologies offer potential weight savings of 850 kg and 400 kg at the battery system level when compared to equivalent IPV and CPV nickel-hydrogen systems utilizing state of the art electrode technologies. As shown in Table 6, more than two-thirds of the 15 to 25 percent weight savings are credited to the elimination of auxiliary components, such as relays, wiring, and structures needed to support the integration of IPV or CPV nickel-hydrogen systems.

TABLE 6. RADAR SATELLITE NICKEL-HYDROGEN BATTERY WEIGHT COMPARISON

Components	Projected Weight, Kg (lb)					
	IPV		CPV		Bipolar	
Cells	2400	(5280)	2200	(4840)	2127	(4680)*
Bypass	100	(222)	17	(37)		
Wiring	78	(172)	13	(29)		
Attachments	64	(140)	11	(24)		
Instrumentation	48	(105)	8	(18)		
Mounting plate	92	(202)	82	(180)		
Thermal control	93	(205)	93	(205)		
Thermal management	343	(756)*	344	(756)**	240	(528)***
	3218	(7082)	2768	(6089)	2367	(5208)

*Includes heat exchanger/pump interface.

**Includes pump and radiator.

***Includes radiation only.

5. CONCLUSIONS

This design study has identified the potential weight savings associated with packaging several hundred cells into a single pressure vessel to provide a self-contained high voltage bipolar battery. The cost of such a system could be lower than equivalent IPV or CPV energy storage systems of equivalent total capacity because one pressure vessel, even though it is larger, will replace several hundred, and a set of several hundred electrodes will replace thousands. Although the technical challenges associated with the development of a large bipolar Ni-H₂ battery design are considerable, our preliminary evaluation indicates that by proper application of state of the art technology, a battery meeting all of NASA's requirements could be produced.

Toward the end of this study, the design team was asked to identify several alternative component design concepts that could considerably reduce the substantial technical risks associated with the development, manufacturing, and integration of bipolar batteries into large spacecraft. Due to the limited resources of this program, no detailed evaluation of these concepts could be made. However, they are outlined below for sake of completeness and for future consideration.

As previously described, the bipolar battery system baselined in this study was predicated on the premise that an independent external heat management system would be used for heat rejection. This, in turn, required the selection of a pressurized liquid-cooled system to preclude the irreversible accumulation of water vapor that would occur in a lightweight gas-cooled space radiation and also to reduce the heat management system weight. However, the implementation of a reliable dedicated pressurized fluid loop control system exposed to 30,000 pressure cycles is not practical with state of the art lightweight hardware.

Bipolar battery cooling system reliability and safety can be enhanced considerably by integrating coolant flow regulation within the pressure vessel boundary and by eliminating the exposure of external coolant circulation and space-radiator-related hardware to the large fluctuating pressure differentials

PRECEDING PAGE BLANK NOT FILMED

associated with battery operation. Spacecraft integration is thus simplified by relying on a single expanded spacecraft payload radiator and thermal control system rather than on two separate radiator and thermal control systems for the battery system and the rest of the spacecraft. A similar design philosophy has been adopted by NASA on both the Apollo and STS programs.

Coupling the bipolar battery to the spacecraft cooling system could result in additional safety benefits by making practical the utilization of a gas-cooled cooling system in which water vapor transport between the heat exchanger and the stack can be eliminated during normal operating conditions and which provides uniform hydrogen/oxygen gas mixing within the pressure vessel. In addition to the thermal management system, several areas critical to stack design could benefit from reconsideration prior to the full scale development of the bipolar stack.

In the baseline bipolar battery design outlined above several cells were assumed to be contained within a frame which provided liquid flow to cooling plates placed on either side of the cell stack subassembly. The implementation of such a design is highly complex because of the unique requirements placed on the frame which must be inert to potassium hydroxide, electrically nonconductive, hydrophobic, manifesting low creep characteristics under load, easy to bond with, having electrode-compatible thermal and structural expansion characteristics, and manufacturable in large diameters with minimum distortion. Materials that have the potential of meeting such requirements, such as ETFE (fluorocarbon polymers) would require reinforcement with potassium titanate, asbestos crysolite, or graphite fibers and considerable materials development effort.

To prevent these difficulties, it is believed that an alternative approach to stack design could have considerable weight and cost benefits if it will rely on edge treatment of selected components to render them hydrophobic. Substantial improvement in overall battery system reliability can be achieved this way since the liquid manifold-to-cooling-plate interface seals can be isolated from cell stack preload changes associated with positive electrode expansion during cycling or from the creep inherent in most loaded ETFE structures.

Additional changes in cell stack layout could reduce battery system weight. For example, the corrugated bipolar plate weight considered in this study could be as much as 10 to 15 percent of the overall battery system weight. The most practical approach to reducing bipolar plate weight is to rely on a very thin, flat, nickel sheet. To implement, the electrolyte reservoir function has to be provided by other components, i. e., negative or positive electrode, and the recombination strips have to be embedded in the positive electrodes. The combined effect of these two changes could allow the utilization of a thin flat bipolar sheet and provide a reduction of the overall bipolar plate weight contribution to the battery system from the 10 to 15 percent to the 2 to 3 percent range. Additionally, increasing the positive electrode thickness will reduce the cell diameter, thus reducing the associated weights of negatives, separators, and bipolar plates. With these additional concepts incorporated into advanced bipolar battery design, weight and cost advantages over state of the art technologies would be enhanced.

6. REFERENCES

1. R.L. Cataldo and J.J. Smithrick, Proceedings 17th Intersociety Energy Conversion Engineering Conference, Los Angeles, California, August 1982, p. 780.
2. D.H. Fritts, J. Power Sources, 6, 323 (1981).
3. D.H. Fritts, J. Electrochem. Soc. 129, 118 (1982).
4. G.L. Holleck, Proceedings 15th Intersociety Energy Conversion Engineering Conference, Seattle, Washington, August 1980, p. 1908.
5. AFWAL-TR-81-2097 (1981) and AFWAL-TR-80-2109 (1980), "Common Pressure Vessel Nickel-Hydrogen Battery," by EIC Laboratories, Inc.

APPENDIX

DEVELOPMENT OF A LARGE SCALE BIPOLAR NiH_2 BATTERY

E. Adler, F. Perez

Hughes Aircraft Company

ABSTRACT

Bipolar battery design concepts developed by Hughes and NASA's Lewis Research Center have been described in previous publications (1). In the Hughes version of the design, shown schematically in Figure 1, electrolyte is contained inside each unit cell by integrating cell components in an insulated hydrophobic frame. Oxygen recombination sites are provided behind each nickel electrode to reduce oxygen migration outside the stack and to prevent recombination on the adjoining negative electrodes. This paper outlines an approach to bipolar battery design, describes key issues related to the development of suitable electrodes, oxygen, and electrolyte management systems, and presents a preliminary assessment of battery performance. Although some of these technical issues are similar to related items encountered in fuel cells and CPV modules, their resolution will require innovative design and new fabrication technologies.

INTRODUCTION

Long-term trends in the evolution of space power technology point in the direction of increased payload power demand, which in turn requires both higher battery system charge storage capability and higher operating voltages. State-of-the-art nickel-hydrogen cells of the 50-60Wh size can meet the required cycle life for a wide range of anticipated operating conditions but present several drawbacks to battery system integration efforts. Because of their size, high voltage/high power systems would require the integration of hundreds of cells into the operating system. Packaging related weight and volume inefficiencies will substantially degrade the energy density and specific energy of individual cells currently at 30Wh/dm³ and 40Wh/kg respectively. Also, the increased parts count and associated handling will significantly affect overall battery related costs. Spacecraft battery systems designers within industry and government have realized that a reduction in battery weight, volume, and cost will require increases in nickel-hydrogen cell capacity.

The bipolar battery concept shown in Figure 2 described below extends the advantages realized by the near-term IPV and CPV cell technology by packaging the equivalent several hundred cells into a single pressure vessel. The following paragraphs outline the projected performance, development requirements, and a possible approach to bipolar battery design. Other design variations are possible without significantly affecting the technical feasibility of the concept.

BIPOLAR BATTERY DESIGN

The bipolar stack configuration illustrated in Figure 3 packages electrode pairs within a common hydrophobic plastic frame. Cells are connected in series by a corrugated, conductive bipolar plate. Movement of hydrogen (H_2) gas to and from the negative electrode is provided through corrugations built into the bipolar plate. Recombination of evolved O_2 takes place behind the positive electrode on a teflon enclosed platinum catalyst strip embedded in the bipolar plate corrugation facing the positive electrode. Recombination strips are in turn supported by a layer of zirconium oxide (ZrO_2) cloth that acts as an electrolyte reservoir for the positive electrode, and a piece of

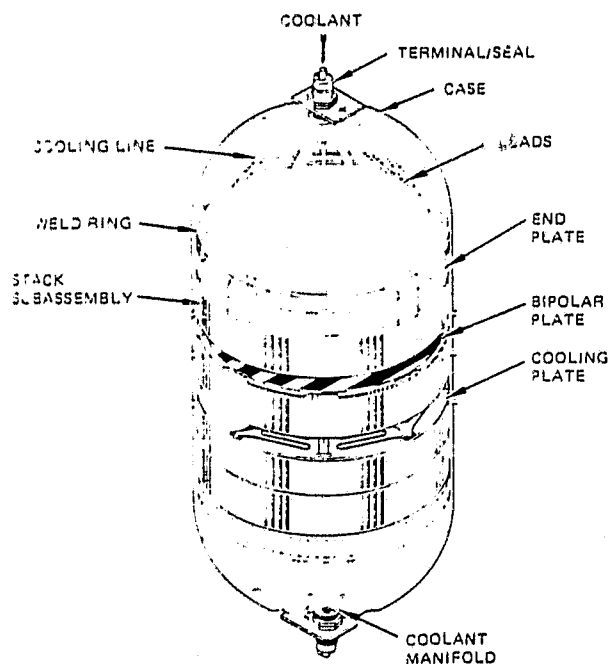


FIGURE 1. BIPOLAR BATTERY

polypropylene gas screen that allows access of hydrogen gas to the back of the platinum coated recombination strip. A high bubble pressure fuel cell grade asbestos separator is used between the

positive and negative electrode to prevent the bulk of evolved O_2 from recombining at the negative electrode.

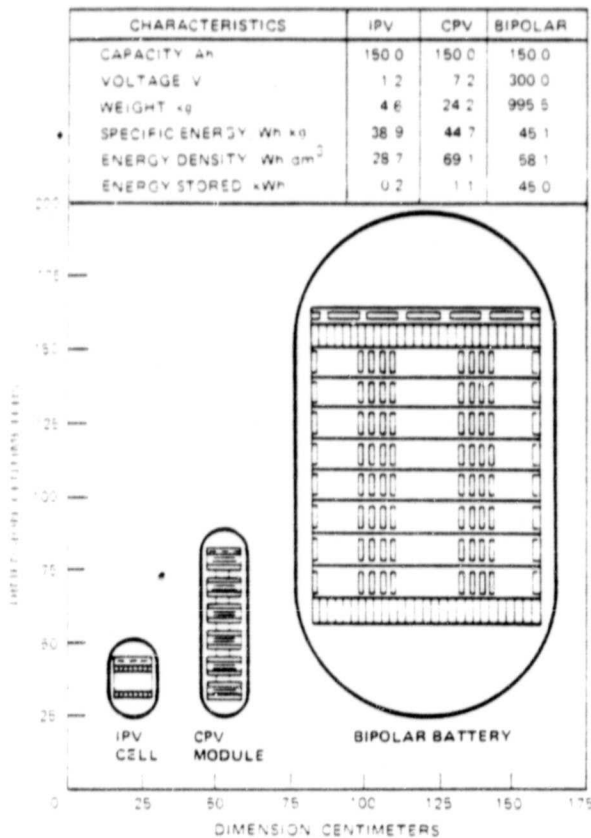


FIGURE 2. COMPARISON OF 150 AH IPV, CPV, AND BIPOLAR SYSTEMS

This stacking concept provides both O_2 and electrolyte management within the cell stacks, as discussed below. As shown in Figure 4, thermal management is provided for a group of 25 series connected electrode pairs through mechanical contact at both ends of the group with liquid-cooled plates. The ratio of cooling plates to electrodes is primarily a function of capacity and cell operating regime, i.e., low earth orbit (LEO) geosynchronous orbit (GEO) or peaking, and the allowable maximum temperature difference within the electrode stack, assumed at $10^\circ C$ in this study to minimize intercell water vapor transfer.

To complete the cell stack, several cooling plate cell stack subassembly pairs are connected in series as shown in Figure 1 to build up the required voltage. They are held together by compression between two rigid honeycomb endplates. Electrical connections and cooling lines brought out from the cell stack are connected to the sealed coaxial terminals. The whole assembly is contained within an Inconel 718 pressure vessel.

Negative Electrodes

The electrode technology selected for our study is similar to the one currently used in state-of-the-art NiH_2 cells. As currently envisioned, it relies on a photochemically etched 0.1mm thick nickel substrate coated with a 10 mg/cm^2 mixture of platinum powder and TFE30. With the use of fuel-cell based electrode technology, in which a carbon based electrode or screen substrate is coated with platinum/carbon particles, loading could probably be reduced to the 1 mg/cm^2 level, resulting in substantial cost savings in materials. To prevent dryout of the electrode by

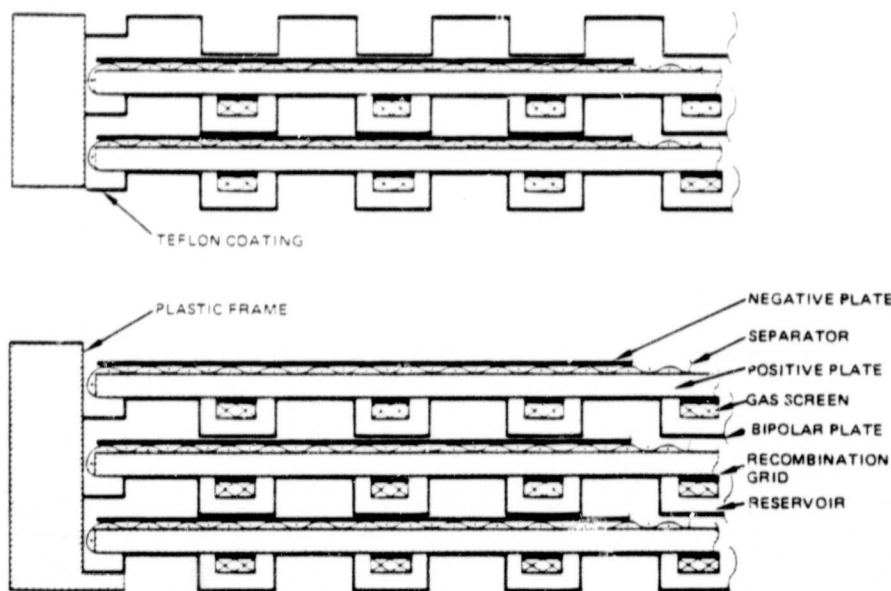


FIGURE 3. BIPOLAR CELL STACK ASSEMBLY

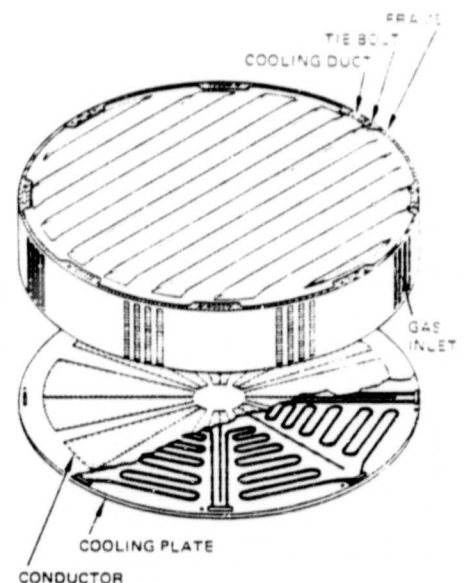


FIGURE 4. STACK SUBASSEMBLY

H₂ gas entrainment, active portions of the electrode can have a 2 mil thick Goretex backing that is permeable to gas flow but impervious to liquid transport. The resulting nominal electrode thickness will be approximately 0.2mm.

Positive Electrodes

As a critical part of NiH₂ cell operation, positive electrodes have received considerable attention in the literature. The bipolar battery configuration permits several changes in electrode design, most importantly elimination of the screen and doubling of the electrode thickness from the currently used 0.8mm while retaining the same active material loading of 1.6-1.8gm/cm³ and the same overall sinter and electrode porosities of 80 percent and 45 percent, respectively. As shown in Figure 5, these changes can result in a 15 percent increase in bipolar cell specific energy. In this figure, electrodes twice as thick as currently used have been folded into the design.

When used in the bipolar cell, a gridless positive electrode has the advantages of lower weight and potentially longer life than those considered for IPV and CPV NiH₂ cells. The gridless electrode may be used in bipolar cells, whereas it is unsuitable for IPV and CPV nickel-hydrogen cells because of the importance of lateral current collection needs associated with state-of-the-art cell designs. The uniform mechanical structure of gridless electrodes permits reduction of cycling induced sinter damage (2)(3). Their development for bipolar cells will require characterization of radial expansion during cycling and required mechanical strength for handling and fabrication.

Increases in positive electrode capacity can be accommodated by the H₂ electrodes, which have low polarization over a wide range of current densities. The positive electrode thickness could be doubled from the typical values presently used without severe polarization penalties in view of the high rate (10C) capability of present IPV cells. Positive electrode related areas deserving consideration in future bipolar cell development programs are plaque fabrication, active material loading, and characterization of electrode polarization as a function of thickness. With proper development, each of these technical difficulties could be overcome.

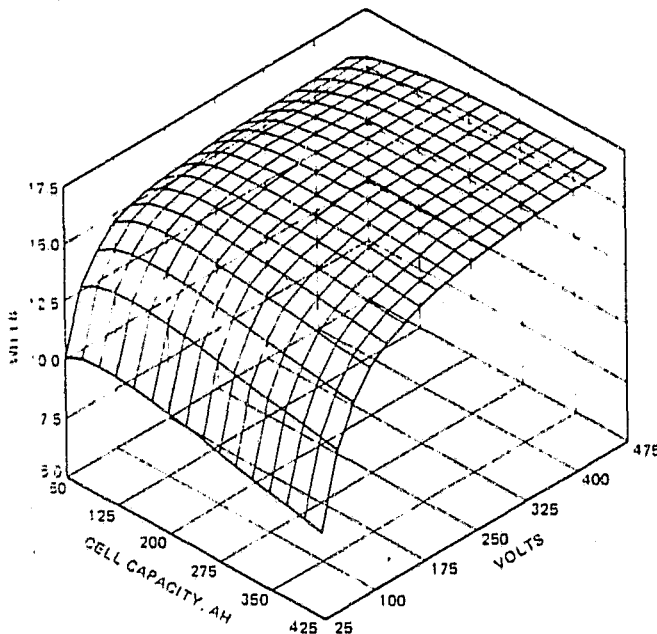
Separator

The separator will be stamped to conform to the electrode and plastic frame geometry shown in Figure 4. Fuel cell grade asbestos paper separators having a nominal thickness of 0.2mm are the best choice for a bipolar cell. Asbestos paper offers demonstrated low cost, stability in the battery environment, excellent electrolyte retention capability, and extremely high bubble pressure. Its pore structure, which is finer than that of ZrO₂, tends to prevent separator dryout because the ZrO₂ cloth reservoir will resupply the positive electrode with electrolyte.

Bipolar Plate

The bipolar plate illustrated in Figures 3 and 4 serves several functions by providing 1) electrical conduction, 2) electrolyte management and isolation, 3) hydrogen distribution to the negative electrode and positive electrode recombination surface, and 4) structural coupling

NORMAL THICKNESS



DOUBLE THICKNESS

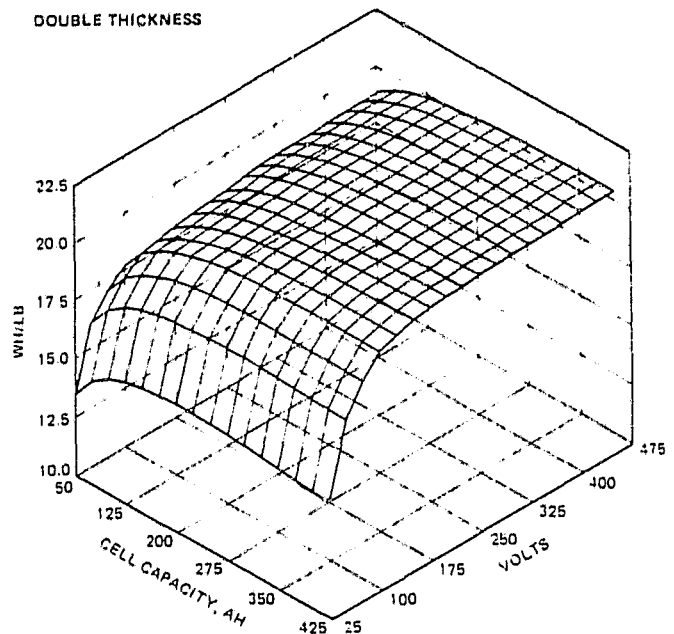


FIGURE 5. BIPOLAR BATTERY SPECIFIC ENERGY VERSUS CELL CAPACITY VOLTAGE AND POSITIVE ELECTRODE THICKNESS

between electrode pairs and stack sub-assemblies. Figure 3 shows a schematic view of the plate placed within the stack subassembly frame in a cross sectional view. As shown in Figure 3, the bipolar plate is a corrugated nickel sheet metal structure with a nominal thickness of 0.2mm and a corrugation depth of 1.2mm and width of 2.5cm. To facilitate hydrogen gas distribution, a 2.5cm wide teflon coated rim is located midway in depth. The flat teflon coated rim acts as a manifold for hydrogen gas distribution to the two electrodes, and prevents electrolyte bridging from one electrode pair to the next.

Figure 3 details the location of the electrolyte reservoir, polypropylene gas screen, and associated teflon encapsulated O_2 recombination surface on the positive electrode side. Empty gas flow corrugations are shown on the negative side. Structural loads are transmitted from one electrode pair to the next through the filled areas of the bipolar plate corrugations. Electrical interconnections between cell stack subassemblies occur through the bipolar plates located at each end of the stack subassembly. For optimal electrical and structural contact between subassemblies and facilitation of uniform gas flow distribution pattern within the cell stack, the bipolar plate corrugations could be rotated 90° out of phase from each other.

Cooling Plates

As indicated in Figures 1 and 4, heat rejection from the cell stack is accomplished through liquid-cooled plates. Manifolding of the coolant to the cooling plates is accomplished through the plastic frames enclosing the cell stack subassembly. To prevent coolant from leaking into the cell stack, gaskets are provided along the periphery of the cooling plate frame interface. As currently envisioned, the coolant most likely to be used is water or 31 percent KOH. To prevent electrolysis, cooling plates are assumed to be injection molded out of polysulfone with proper slots provided at periodic intervals to allow the insertion of electrical conductors. To facilitate heat transfer, cooling plate wall thickness has been reduced to 0.2mm.

Terminals

As previously pointed out, coolant inlet and outlet into the cell stack is provided through a coaxial terminal assembly. The design is similar to that currently used in NiH_2 cells, except that it relies on the plastic flow of teflon for proper sealing and is considerably enlarged to allow for separate gas/electrolyte and coolant flow passages. Electrical lead and coolant coupling to the terminals is shown in Figure 4. Electrical leads from the end electrodes are resistance spot welded to a disc located at the bottom of the terminal assembly. Inlet and outlet coolant flow is distributed among four polypropylene tubes by a cross-shaped manifold. From there, coolant lines are connected to the cell stack through the endplate assembly.

Endplate/Weldring Assembly

The function of the endplate presented in Figure 1 is twofold: 1) to maintain a uniform 30 psi preload on the cell stack subassembly, and 2) to transfer the structural loads from the cell stack to the pressure vessel through the welding assembly shown in Figure 1 without exceeding a 0.2mm deformation of endplate geometry during anticipated environmental loads. The load bearing structural components are 3 inch thick Inconel 718 honeycomb endplates. They have a 1 cm cell size, 1mm face sheets, and a web of 0.1mm. Cooling passages and eight Inconel 718 tie bolts 1 cm in diameter penetrate the endplates, which are reinforced with plastic inserts. The resulting structure is sufficiently stiff to allow transfer of 15g loads to the welding without any significant loss of preload.

Pressure Vessel

The bipolar cell stack is packaged in an Inconel 718 pressure vessel designed to sustain 30,000 pressure cycles in the 3.5 to 7.0 MPA range. The vessel is composed of a cylindrical section attached to hemispheres at each end. Using allowable stress values of 415 MPA and 345 MPA for the parent and weld metal respectively, the required wall thicknesses for the cylinder and the domes are 5.3mm and 2.5mm, respectively. In the heat affected area, wall thicknesses are 6.3mm. Electrolyte film buildup on the pressure vessel is prevented by teflon coating pressure vessel components outside the heat affected zone.

THERMAL MANAGEMENT

To assure proper electrochemical performance, cell stack operating temperatures must be restricted to the -5°C to $+20^\circ\text{C}$ range. In this range, the charge efficiency of the positive electrodes is adequate to maintain a stable state of charge with a 105 percent charge return over a wide range of orbital operating conditions. Stack heat rejection is accomplished by relying on a liquid-cooled system coupled to a space radiator. Integration of cell heat rejection into the spacecraft could also be accomplished through a cross-flow heat exchanger connected to the spacecraft cooling system.

ELECTROLYTE AND OXYGEN MANAGEMENT

Shunt Currents Through Electrolyte Bridges

A universal problem of series connected cell designs is the presence of shunt currents through electrolyte bridges connecting unit cells. A voltage applied across such a bridge will most likely be well over the electrolyte decomposition voltage in a NiH_2 cell. Therefore, a shunt current always flows through the bridge until the cells connected by the bridge are totally discharged. Depending on the magnitude of this current, it can create a number of technical difficulties in a bipolar cell: 1) unbalanced charge distribution among bipolar repeating units, 2) uneven distribution of KOH

ORIGINAL PAGE IS OF POOR QUALITY

concentration and amount of electrolyte among unit cells because of K⁺ ion migration, 3) uneven distribution of water vapor pressure and oxygen evolution resulting from unbalanced KOH concentration, or 4) uneven heat generation caused by oxygen evolution.

These issues are similar to those identified in common pressure vessel (CPV) NiH₂ cells (4). Their prevention is an important consideration for the design of a long-life bipolar NiH₂ battery. Although these difficulties must be investigated in conjunction with large bipolar battery design efforts, a satisfactory design solution seems feasible in view of positive test results obtained from CPV NiH₂ cells (5), which demonstrated 5,000 cycles without exhibiting shunt currents in multi-stack configurations.

Electrolyte Dryout and Reservoirs

A potential difficulty associated with the operation of bipolar NiH₂ batteries is "electrolyte dryout," a phenomenon encountered in cells with an insufficient amount of electrolyte. This situation can develop as a result of the following factors: 1) nickel electrode expansion, 2) electrolyte transfer outside of a unit cell by mechanical means; for example, by entrainment in H₂ gas, 3) electrolyte dryout by evaporation due to localized heating, or 4) poor O₂ management.

Mechanically induced electrolyte dryout depends on stack design and can easily be prevented. The most serious of the previously outlined factors contributing to dryout, however, is believed to be the nickel electrode expansion. An electrolyte reservoir placed in the individual unit cell will prevent dryout if the structure of the reservoir holds electrolyte but gives it up easily when the positive electrode needs it. Such a structure can be achieved by selecting a reservoir material such as ZrO₂ cloth or porous nickel that has pores larger than those of the positive electrode. The long term interactions between the electrodes and the reservoir, specifically as they are being applied in bipolar cells, deserve further study in future NiH₂ battery development programs.

Electrolyte Maldistribution

Maldistribution of electrolyte among individual cells of series connected stacks can be developed by several different mechanisms. These mechanisms, which include shunt currents as discussed above, entrainment by H₂ and O₂ gas, evaporation and condensation of water vapor, and uneven recombination of O₂, can all be prevented by adequate mechanical design and appropriate thermal management. However, these phenomena require accurate modeling in conjunction with the O₂ management system of any future bipolar cell design.

Oxygen Management

Potential O₂ mismanagement difficulties in series connected bipolar cells are caused by O₂

that is evolved in one cell and migrates to the other through the common gas space to be recombined in an unbalanced manner. Because this is equivalent to water transport from one cell to another, which leads to an electrolyte imbalance, it could cause preferential dryout of one unit and flooding of the other. This imbalance in turn could lead to a performance imbalance among individual cells, resulting in a positive feedback loop that in time will lead to cell failure.

A solution to this problem demonstrated at NASA Lewis confines O₂ inside individual unit cells by recombining it before it leaves the unit cell. Such a recombination device is provided in the bipolar cell design concept described here. However, the understanding of water transport mechanisms from the recombination strips to the electrode requires further study before accurate life predictions can be made for cells using this O₂ management system.

PERFORMANCE

The bipolar NiH₂ battery configuration described above evolved as a result of intensive computerized optimization studies conducted on NAS3-22249. Our computer model deals primarily with the relationships between 85 compatible independent physical parameters and 123 dependent battery design and performance parameters. Examples of these are weight, volume, watt-hours per unit weight, etc. The thermal performance of each battery design in a given orbit is calculated within the program, and the results are used to calculate flow rates and distribution pressure drops for a liquid-cooled system.

By using this computer program, the battery designer can ensure the development of an optimized bipolar battery design. Specific energy and energy density can thus be optimized in relation to component geometry and specifications, voltage, and operating pressure. This battery optimization software package was exercised during the design effort. Figure 5 shows the dependence of bipolar battery specific energy on battery voltage and capacity.

The outputs of the program can be used to compare the performance of various NiH₂ batteries in large spacecraft systems. A preliminary system integration trade-off study has been conducted for a 52 kWh USAF satellite with the intent of providing a system level comparison between various NiH₂ battery systems. State-of-the-art IPV technology has thus been compared to advanced bipolar and CPV batteries. Tables 1 and 2 present a comparison between the system level characteristics associated with candidate NiH₂ battery designs. As shown there, four bipolar batteries could replace 100 CPV modules or 600 IPV cells having similar functional capabilities. The overall weight advantages of the bipolar system compared to the other two options is evident. Its major advantage is the reduced number of electrical thermal and structural auxiliary components needed to support its operation.

ORIGINAL PAGE IS OF POOR QUALITY

TABLE 1. RADAR SATELLITE NiH_2 BATTERY
DESIGN CHARACTERISTICS

Design Characteristics	IPV	CPV	Bipolar
Energy to load (kWh)	52	52	52
Nominal voltage (V)	170	170	170
Nominal DOD (%)	60	60	60
Max DOD* (%)	80	80	80
Installed capacity (Ah)	500	500	500
Number of batteries*	4	4	4
Number of cells/battery**	150	150	150
Number of modules/battery	-	25	1

*Meets mission requirements with a failed battery.

**10% provided for redundancy.

TABLE 2. RADAR SATELLITE NiH_2 BATTERY WEIGHT COMPARISON

Components	Projected Weight, Kg (lb)		
	IPV	CPV	Bipolar
Cells	2400 (5280)	2200 (4840)	212 (4680***)
Bypass	100 (222)	17 (37)	
Wiring	78 (172)	13 (29)	
Attachments	64 (140)	11 (24)	
Instrumentation	48 (105)	8 (18)	
Mounting plate	92 (202)	82 (180)	
Thermal control	93 (205)	93 (205)	
Thermal management	343 (756*)	344 (756*)	240 (526**)
	3218 (7082)	2768 (6089)	2367 (5206)

*Includes pump and radiator

**Radiator only

***Includes heat exchanger/pump interface at 400 lb.

CONCLUSIONS

The outcome of this preliminary engineering effort indicates that a viable high voltage, high capacity, bipolar NiH_2 cell can be configured with proper development for use in large power systems. Such a system offers substantial weight savings over state-of-the-art NiH_2 technology. The bulk of the development effort associated with future implementation of this concept will be related to the scale-up of established NiH_2 and fuel cell components to the specific requirements of bipolar cells. These developments will enhance the performance of state-of-the-art NiH_2 cells. To facilitate the successful development of a bipolar battery design, future development efforts should emphasize the following aspects of battery and nickel electrode design:

- Development and evaluation of thicker nickel electrodes for improved energy density and reduced cost.
 - Plaque fabrication techniques
 - Active material impregnation methods

ACKNOWLEDGMENTS

The authors wish to acknowledge the technical guidance provided by Bob Cataldo of NASA's Lewis Research Center and the financial support of the Center on Contract NAS3-22249 and the valuable contributions of Dr. H.S. Lim of Hughes Research Labs, whose work was helpful in the definition of development requirements.

References

1. R. L. Cataldo and J. J. Smithrick, "Design of a 35 kW Bipolar Nickel-Hydrogen Battery for Low Earth Orbit Applications," Proc. 17th Intersociety Energy Conversion Engineering Conference, Los Angeles, CA, August 1982, p. 780.
2. D. H. Fritts, "A Discussion of Causes for Blistering of Sintered Nickel Hydroxide Electrodes," J. Power Sources, 6, 323 (1981).
3. D. H. Fritts, "Mechanics of Electrochemically Coprecipitated Cobalt Hydroxide and Nickel Hydroxide Electrodes," J. Electrochem. Soc., 129, 118 (1982).
4. G. L. Holleck, "Common Pressure Vessel Nickel Hydrogen Battery Design," Proc. 15th Intersociety Energy Conversion Engineering Conference, Seattle, WA, August 1980, p. 1908.
5. EIC Laboratories, Inc., "Common Pressure Vessel Nickel-Hydrogen Battery," AFWAL-TR-81-2097 and AFWAL-TR-80-2109.

Battery Design

- Electrolyte bridging elimination.
- Electrolyte entrainment reduction.
- Optimization of electrolyte reservoir designs for:
 - Reservoir capacity
 - Pore size distribution
 - Electronic conduction
 - Accommodation of nickel electrode expansion
- Reduction or elimination of O_2 migration from the individual cell units.

Electrode Design

- Sinter structure optimization in terms of pore size and mechanical strength.
- Active material loading optimization for the best cycle life.
- Development and evaluation of gridless nickel electrodes.